

Aus dem Bereich  
Klinische Medizin  
der Medizinischen Fakultät der Universität des Saarlandes,  
Homburg/Saar

**Investigation of the association between  
receptor-interacting serine/threonine protein  
kinase 3 expression and the outcome of  
photodynamic therapy in vivo and in an HPV8-  
positive organotypic 3D cell culture model**

Dissertation

zur Erlangung des Grades eines Doktors der Medizinwissenschaften  
(Dr. med.)

der Medizinischen Fakultät der  
UNIVERSITÄT DES SAARLANDES

January 2024

Submitted by  
Juliane Anna Kütten  
born 06.09.1990  
in Kaiserslautern

The experimental work presented in this thesis has been carried out at the Institute of Virology at Saarland University, Germany.

Date of doctorate: 05.07.2024

Dean: Prof. Dr. M.D. Menger

Reviewer:

Prof. Dr. Sigrun Smola

Prof. Dr. N. Szentmáry

**“There are only two ways to live your life. One is as though nothing is a miracle.  
The other is as though everything is a miracle.”**

Albert Einstein

# Table of Contents

TABLE OF FIGURES .....	VII
LIST OF TABLES.....	VIII
LIST OF ABBREVIATIONS .....	IX
SUMMARY .....	1
ZUSAMMENFASSUNG .....	3
<b>1 INTRODUCTION .....</b>	<b>5</b>
1.1 HUMAN PAPILLOMA VIRUS .....	5
1.1.1 <i>Cutaneous Papillomaviruses</i> .....	9
1.2 PRECANCEROUS LESIONS OF THE SKIN AND THE VULVAR .....	11
1.2.1 <i>Actinic keratosis</i> .....	11
1.2.2 <i>Vulvar intraepithelial neoplasia</i> .....	14
1.3 PHOTODYNAMIC THERAPY .....	16
1.4 NECROPTOSIS AND RIPK3 .....	18
1.5 AIM OF THE STUDY .....	23
<b>2 MATERIAL.....</b>	<b>24</b>
2.1 CELL LINES .....	24
2.2 CELL CULTURING .....	24
2.2.1 <i>Media used for cell culture</i> .....	24
2.2.2 <i>Reagents used for cell culture</i> .....	25
2.2.3 <i>Complex medium used for cell culturing of keratinocytes and fibroblasts</i> .....	25
2.2.4 <i>Complex medium used for cell culturing of siRNA transfected keratinocytes</i> .....	25
2.2.5 <i>Complex medium used for 3D-cultures</i> .....	25
2.3 ANTIBODIES FOR IMMUNOHISTOCHEMICAL STAINING .....	26
2.3.1 <i>Primary antibodies</i> .....	26
2.3.2 <i>Secondary antibodies</i> .....	26
2.4 CHEMICALS AND REAGENTS .....	26
2.5 BUFFER AND SOLUTIONS.....	27
2.5.1 <i>10x Phosphate buffered saline (PBS)</i> .....	27
2.5.2 <i>1x PBS</i> .....	27
2.5.3 <i>0.25% trypan blue solution</i> .....	27
2.5.4 <i>10x Tris-buffered saline (TBS)</i> .....	28
2.5.5 <i>1x TBS</i> .....	28
2.5.6 <i>Sodium-citrate-buffer</i> .....	28

2.5.7	2.5.7. 4% formaldehyde-solution.....	28
2.6	EQUIPMENT .....	28
2.7	SOFTWARE.....	29
<b>3</b>	<b>METHODS.....</b>	<b>30</b>
3.1	ETHICAL EVALUATION .....	30
3.2	SAMPLE COLLECTION .....	30
3.3	CULTURING OF EUKARYOTIC CELLS.....	30
3.4	CELL COUNTING .....	31
3.5	PRODUCTION OF 3D-CULTURES .....	31
3.5.1	<i>Preparation of fibroblast-collagen-matrixes</i> .....	31
3.5.2	<i>Preparation of keratinocytes</i> .....	32
3.5.3	<i>Transfer of the 3D cell cultures onto the lattice work</i> .....	32
3.6	PRODUCTION OF siRNA-TRANSFECTED 3D CULTURES .....	33
3.6.1	<i>Seeding</i> .....	33
3.6.2	<i>Transfection</i> .....	34
3.6.3	<i>Production of 3D cultures</i> .....	34
3.6.4	<i>Transfer of the 3D-cell cultures onto the latticework</i> .....	34
3.7	PHOTODYNAMIC RADIATION OF 3D-CULTURES.....	35
3.8	FIXATION AND EMBEDDING .....	35
3.9	PRODUCTION OF PARAFFIN SECTIONS.....	36
3.10	IMMUNOHISTOCHEMICAL STAINING.....	36
3.11	EVALUATION OF IMMUNOHISTOCHEMICAL STAINING INTENSITY .....	37
3.12	TREATMENT RESPONSE TO PHOTODYNAMIC THERAPY.....	37
3.13	TESTING OF PATIENT SAMPLES FOR HPV.....	38
3.14	STATISTICAL ANALYSIS.....	38
<b>4</b>	<b>RESULTS .....</b>	<b>40</b>
4.1	RIPK3 EXPRESSION VARIES IN LESIONS OF ACTINIC KERATOSIS AND IS CORRELATED TO PDT RESPONSE.....	40
4.2	IMMUNOHISTOCHEMICAL RIPK3-STAINING OF 3D CULTURES .....	44
4.2.1	<i>RIPK3 expression in vitro does not change under PDT</i> .....	44
4.2.2	<i>HPV8 E6 alters RPK3 expression in 3D cultures</i> .....	46
4.3	IMPACT OF PDT ON CELL DAMAGE AND PROLIFERATION .....	48
4.3.1	<i>Double strand breaks occur especially in superficial cell layers after PDT</i> .....	48
4.3.2	<i>PDT leads to higher Ki67 expression in 3D cell cultures</i> .....	52
4.4	IMPACT OF THE ONCOPROTEIN HPV 8E6 ON THE SUSCEPTIBILITY TO PDT.....	56
4.4.1	<i>HPV 8E6-transduced keratinocytes express less <math>\gamma</math>-H2AX when exposed to PDT</i> .....	57
4.4.2	<i>HPV 8E6-transduced cells show higher Ki67 expression after PDT</i> .....	59
4.5	IMPACT OF THE REPRESSION OF RIPK3 ON SUSCEPTIBILITY TO PDT IN KERATINOCYTES. ....	61
4.5.1	<i><math>\gamma</math>-H2AX-expression does not change after RIPK3 knock-down</i> .....	62

4.5.2	<i>Repression of RIPK3 reduces Ki67 expression in PDT-treated cells</i> .....	64
4.6	RIPK3 EXPRESSION NEGATIVELY CORRELATES WITH GRADE OF VIN LESION .....	66
<b>5</b>	<b>DISCUSSION</b> .....	<b>70</b>
5.1	RIPK3 CORRELATES WITH PDT SUSCEPTIBILITY OF ACTINIC KERATOSIS.....	70
5.2	PDT DOES NOT ALTER RIPK3 EXPRESSION IN 3D CULTURES .....	71
5.3	HPV 8E6 NEGATIVELY INFLUENCES THE EXPRESSION OF RIPK3 IN PDT-TREATED 3D CULTURES .....	72
5.4	PDT HAS OPPOSITE EFFECTS IN 3D CULTURES DEPENDENT ON THE EPITHELIAL LAYER.....	73
5.4.1	<i>PDT induces DNA damage in the superficial but favours cell growth in the lower cell layers of the 3D cultures</i> .....	73
5.5	HPV 8E6-TRANSDUCED 3D CULTURES SHOW AN ALTERED RESPONSE TO PDT .....	75
5.5.1	<i>HPV 8E6-transduced cells show less DNA damage and higher proliferation rates in response to PDT</i> 75	
5.6	REPRESSION OF RIPK3 HAS NO SIGNIFICANT IMPACT ON PDT-INDUCED DNA DAMAGE OR POST-PDT-PROLIFERATION IN 3D CULTURES.....	76
5.7	RIPK3 EXPRESSION CORRELATES WITH VIN GRADE .....	78
<b>6</b>	<b>ACKNOWLEDGMENTS</b> .....	<b>81</b>
<b>7</b>	<b>DECLARATION</b> .....	<b>82</b>
<b>8</b>	<b>CURRICULUM VITAE</b> .....	<b>83</b>
<b>9</b>	<b>REFERENCES</b> .....	<b>85</b>

# Table of Figures

Figure 1: Phylogenetic tree of HPV.....	6
Figure 2: HPV genome organisation of alpha and beta HPV types.....	7
Figure 3: Interaction of HPV E6 and HPV E7 with host cell tumour suppressors p53 and Rb.....	8
Figure 4: Pathobiology of the development of actinic keratosis upon ultraviolet radiation.....	12
Figure 5: Schematic illustration of the development of normal tissue into an invasive vulvar carcinoma.....	15
Figure 6: Illustration of the cell-damaging photochemical effect during photodynamic therapy..	17
Figure 7: Simplified schematic illustration of TNF- $\alpha$ induced signaling pathways.....	20
Figure 8: Schematic process of 3D cell culture production.....	33
Figure 9: Absorption-check with the black-light-lamp.....	35
Figure 10: Correlation between RIPK3 staining intensity and PDT response to patients' age and sex.....	43
Figure 11: $\gamma$ -H2AX-positive stained nuclei in PDT- and control cell cultures over time.....	50
Figure 12: Schematic illustration of the $\gamma$ -H2AX staining profile in PDT-treated cultures.....	51
Figure 13: Ki67-positive stained nuclei in PDT- and control cell cultures over time.....	55
Figure 14: Schematic illustration of the expression profile of $\gamma$ -H2AX and Ki67 in PDT-treated cultures.....	56
Figure 15: $\gamma$ -H2AX-positive stained nuclei in PDT- and control cell cultures in HPV 8E6- and pLXSN-transduced cells.....	58
Figure 16: Ki67-positive stained nuclei in PDT- and control cell cultures in HPV 8E6- and pLXSN-transduced cells.....	61
Figure 17: $\gamma$ -H2AX-positive stained nuclei in PDT- and control cell cultures transfected with either siRIPK3, non-coding siRNA or no siRNA.....	63
Figure 18: Ki67-positive stained nuclei in PDT- and control cell cultures transfected with either siRIPK3, non-coding siRNA or no siRNA.....	65
Figure 19: Correlation between VIN grade and RIPK3- staining intensity.....	68
Figure 20: Difference in RIPK3 staining intensity depending on HPV status in VINs.....	69

## List of tables

<i>Table 1: Cell lines used</i> .....	24
<i>Table 2: Media used for cell culture</i> .....	24
<i>Table 3: Reagents used for cell culture</i> .....	25
<i>Table 4: Primary antibodies used for immunohistochemical staining</i> .....	26
<i>Table 5: Secondary antibodies used for immunohistochemical staining</i> .....	26
<i>Table 6: Chemicals and reagents used</i> .....	27
<i>Table 7: Equipment used</i> .....	28
<i>Table 8: Software used</i> .....	29
<i>Table 9: Required quantity of components to produce 5 or 10 ml of collagen</i> .....	32
<i>Table 10: Ingredients for siRNA transfection of keratinocytes with non-coding siRNA or siRIPK3</i> .....	34
<i>Table 11: Evaluation of immunohistochemical staining shown for RIPK3 staining of actinic keratosis lesions</i> .....	37
<i>Table 12: Treatment response groups of patients with actinic keratosis to PDT</i> .....	38
<i>Table 13: Frequency distribution off RIPK3 staining patterns in actinic keratosis samples</i> .....	40
<i>Table 14: Immunohistochemical RIPK3 staining of actinic keratosis lesions</i> .....	41
<i>Table 15: Immunohistochemical RIPK3 staining of 3D cultures</i> .....	45
<i>Table 16: Immunohistochemical RIPK3 staining of 3D cultures transduced with HPV 8E6 and pLXSN</i> .....	47
<i>Table 17: Immunohistochemical <math>\gamma</math>-H2AX staining of 3D cultures over time</i> .....	49
<i>Table 18: Immunohistochemical Ki67 staining of 3D cultures over time</i> .....	53
<i>Table 19: Immunohistochemical <math>\gamma</math>-H2AX-staining of 3D-cultures transduced with HPV 8E6 and pLXSN</i> .....	57
<i>Table 20: Immunohistochemical Ki67-staining of 3D cultures transduced with HPV 8E6 and pLXSN</i> .....	60
<i>Table 21: Immunohistochemical <math>\gamma</math>-H2AX-staining of 3D-cultures transfected with either siRIPK3, non-coding siRNA or no siRNA</i> .....	62
<i>Table 22: Immunohistochemical Ki67-staining of 3D cultures transfected with either siRIPK3, non- coding siRNA or no siRNA</i> .....	64
<i>Table 23: Frequency distribution of RIPK3 staining patterns in vulva intraepithelial neoplasia samples</i> .....	66
<i>Table 24: Immunohistochemical RIPK3 staining of VIN lesions</i> .....	67



## List of Abbreviations

3D	Three-dimensional
5-FU	5-fluorouracil
µg	Microgram
µl	Microliter
ALA	Aminolevulinic acid
ATR	Ataxia telangiectasia and Rad3-related protein
Bak	Bcl-2 homologous antagonist/killer
BSA	Bovine serum albumine
C/EBPα	CCAAT/enhancer-binding protein alpha
CYLD	Cylindromatosis
d	Days
dl	Deciliter
dH <sub>2</sub> O	Distilled water
DMEM	Dulbecco's Modified Eagle Medium
DPBS	Dulbacco's Balanced Salt Solution
DNA	Deoxyribonucleic acid
EBV	Epstein-Barr virus
EGF	Epidermal growth factor
EV	Epidermodysplasia verruciformis
FCS	Fetal calf serum
g	Gram
h	Hours
HIPK2	Homeodomain-interacting protein kinase 2
HNSCC	Head and neck squamous cell carcinoma
HPV	Human papillomavirus
HSIL	High-grade squamous intraepithelial lesions
IRS	Immunoreactive score
ISSVD	International society or the study of vulvar disease

LSIL	Low-grade squamous intraepithelial lesions
L	Litre
MAL	Methyl aminolevulinate
MAML1	Mastermind-like protein 1
Mg	Milligram
ml	Millilitre
MLKL	Mixed lineage kinase domain like pseudokinase
M	Molar
mM	Millimolar
MT1 MMP	Membrane-bound matrix-metalloproteinase
NOS2	Nitric oxide synthase
NO	Nitric oxide
No.	Number of
ORF	Open reading frame
PBS	Phosphate buffered saline
PCR	Polymerase chain reaction
PDT	Photodynamic therapy
Poly-IC	Polyinosinic-polycytidylic acid
PUVA	Psoralens and Ultraviolet A Radiation
Rb	Retinoblastoma
RIPK1	Receptor-interacting serine/threonine-protein kinase 1
RIPK3	Receptor-interacting serine/threonine-protein kinase 3
RNA	Ribonucleic acid
ROS	Reactive oxygen species
SCC	Squamous cell carcinoma
siRNA	Small interfering ribonucleic acid
SIRS	Systemic inflammatory response syndrome
TBS	Tris-buffered saline
TNF $\alpha$	Tumour necrosis factor alpha

TRAIL	Tumour Necrosis Factor Related Apoptosis Inducing Ligand
URR	Upstream regulatory region
VIN	Vulvar intraepithelial neoplasia

## Summary

Human Papillomaviruses (HPV), particularly the high-risk HPV types 16 and 18, are pivotal in the development of cervical carcinoma and other tumorous entities in the anogenital tract, such as the vulva, as well as in the oropharyngeal region. Also, certain cutaneous beta-HPVs, such as HPV5 and 8, are thought to play a cofactor role of in the development of non-melanocytic skin cancer in epidermodysplasia verruciformis (EV) patients. HPV-associated cancers develop via precancerous lesions, such as mucosal intraepithelial neoplasia, or cutaneous actinic keratoses, respectively.

In addition to cutaneous non-melanoma skin cancers, precursor skin lesions such as actinic keratosis or vulvar intraepithelial neoplasia (VIN) are presently addressed through photodynamic therapy (PDT). PDT induces necroptosis, a form of cell death that combines criteria of necrosis and apoptosis and involves the factor "receptor-interacting serine/threonine-protein kinase 3" (RIPK3). Our group had recently shown that RIPK3-dependent necroptosis in HPV-positive tumour cells, induced by dsRNA, strongly activates the immune system. Thus, in contrast to apoptosis, RIPK3-dependent necroptosis represents a form of immunogenic cell death.

In this work, we now aimed to investigate the involvement of RIPK3 expression in the response to PDT in skin cancer precursors in vivo or HPV-positive cells in vitro. First, RIPK3 expression in actinic keratoses was analysed. Significant differences in the expression patterns were found. RIPK3 expression in actinic keratoses correlated with the success of PDT in vivo. In VINs, RIPK3 expression decreased significantly with severity. Thus, less RIPK3 was detected in less differentiated tumour tissue. Standard therapy for VINs and vulvar carcinoma is currently radical excision, which is often associated with dramatic physical but also psychological consequences for the affected patients. Whether or not RIPK3 expression in VIN is associated with responsiveness to PDT warrants further investigation.

A cutaneous 3D cell culture model was used to study the effects of PDT in vitro. To investigate the role of HPV8 and its influence on RIPK3 expression and effects on PDT treatment outcome, the HPV8 E6 oncogene was expressed in keratinocytes by retroviral gene transfer, which were then subjected to PDT. Keratinocytes transduced with HPV8 E6 exhibited diminished RIPK3 expression after PDT, particularly within the superficial cell layers, in comparison to non-irradiated cultures, despite RIPK3 being suppressed in both conditions. The detection of PDT-dependent DNA double-strand damage by  $\gamma$ -H2AX was limited to the suprabasal cell layers. HPV8 E6-transduced cells exhibited less PDT-dependent DNA damage and were more resistant to PDT overall. Interestingly,

## Summary

---

basal cell layers were more likely to be stimulated to proliferate in this model. Whether this observation also applies to the in vivo situation remains unclear at present and would need further investigation in the future.

## Zusammenfassung

Humane Papillomviren (HPV), insbesondere die sogenannten Hochrisiko-HPV Typen 16 und 18, spielen eine entscheidende Rolle für die Entstehung des Zervixkarzinoms und weiterer Tumorentitäten im Anogenitaltrakt, wie beispielsweise der Vulva, sowie im Oropharynxbereich. Auch wird eine Kofaktor-Rolle bestimmter kutaner beta-HPV, wie HPV5 und 8, bei der Entstehung des nicht-melanozytären Hautkrebses vermutet. Die Entwicklung dieser Krebsarten erfolgt über Krebsvorstufen, mukosale intraepitheliale Neoplasien bzw. kutane aktinische Keratosen.

In Ergänzung zu nicht-melanozytären Hautkrebsarten werden derzeit auch Krebsvorstufen wie die aktinische Keratose oder die vulväre intraepitheliale Neoplasie (VIN) mittels photodynamischer Therapie (PDT) behandelt. PDT induziert Nekroptose, eine Form des Zelltods, der Kriterien der Nekrose und der Apoptose vereinigt und den Faktor „Receptor-interacting serine/threonine-protein Kinase 3“ (RIPK3) involviert. Unsere Arbeitsgruppe hatte kürzlich gezeigt, dass HPV-positive Tumorzellen, die durch dsRNA in die RIPK3-abhängige Nekroptose getrieben werden, das Immunsystem stark aktivieren. Im Gegensatz zur Apoptose, stellt die RIPK3-abhängige Nekroptose demnach eine immunogene Zelltodform dar.

In dieser Arbeit sollte nun überprüft werden, inwieweit auch das Ansprechen auf eine PDT bei Hautkrebsvorstufen in vivo oder HPV-positiver Zellen in vitro von der RIPK3 Expressionsstärke abhängt. Zunächst wurde die RIPK3 Expression in aktinischen Keratosen untersucht. Es fanden sich erhebliche Unterschiede im Expressionsmuster. In der Tat korrelierte die RIPK3 Expression in aktinischen Keratosen mit dem Erfolg einer PDT in vivo. Bei VINs nahm die RIPK3-Expression mit dem Schweregrad deutlich ab. So wurde in weniger differenziertem Tumorgewebe weniger RIPK3 nachgewiesen. Standardtherapie der VIN und des Vulvakarzinoms ist derzeit die radikale Exzision, was für die betroffenen Patientinnen oftmals mit dramatischen physischen aber auch psychischen Folgen einhergeht. Auf Grundlage dieser Daten wäre es sinnvoll zukünftig zu untersuchen, ob über die Bestimmung der RIPK3 Expression vor Therapiebeginn Patientinnen selektiert werden könnten, deren VINs besonders gut auf PDT ansprechen, um ihnen eine radikale Exzisionstherapie zu ersparen.

Mit Hilfe eines kutanen 3D-Zellkulturmodells wurden die Auswirkungen der PDT auch in vitro untersucht. Um die Rolle von HPV8 und dessen Einfluss auf die RIPK3 Expression und Auswirkungen einer PDT-Behandlung zu untersuchen, wurden das HPV8 E6 Onkogen mittels retroviralem Gentransfer in Keratinozyten zur Expression gebracht und einer PDT unterzogen. Die RIPK3 Expression in HPV8 E6-transduzierten Zellen nach

einer PDT-Behandlung fiel niedriger aus, verglichen mit der Kontrollgruppe, wobei auch hier eine Reduktion zu verzeichnen war. Vor allen in den oberflächlichen Schichten ließ sich kaum RIPK3 nachweisen.

Der Nachweis PDT-abhängiger DNA-Doppelstrang-Schäden mittels  $\gamma$ -H2AX begrenzte sich allerdings auf die suprabasalen Zellschichten. HPV8 E6-transduzierte Zellen wiesen weniger PDT-abhängige DNA-Schäden auf und waren insgesamt resistenter gegen eine PDT. Interessanterweise wurden basale Zellschichten in diesem Modell eher zur Proliferation angeregt. Ob diese Beobachtung auch auf die in vivo Situation übertragbar ist, bleibt derzeit unklar und müsste in Zukunft weiter untersucht werden.

# 1 Introduction

## 1.1 Human Papilloma Virus

Human papillomaviruses (HPV) belong to the family of papillomaviridae and are non-enveloped, double-stranded DNA viruses. To date, over 200 different types of HPV have been identified, with the number constantly growing. These viruses infect the skin or mucous membranes, giving rise to the formation of both benign and malignant lesions. HPV is primarily transmitted through microlesions in the epithelium via skin-to-skin contact or sexual intercourse, including anal-, oral and vaginal sex. Consequently, it is considered the most frequently transmitted sexually transmitted infection worldwide. However, not every transmission or contact automatically results in a persistent infection. Risk factors for a persistent infection with HPV have been evaluate, including early age of first sexual intercourse, smoking and immunodepression (WHO 2021).

Interestingly, the number of malignant tumours linked to HPV infection, particularly those derived from high-risk HPV types such as HPV 16 and 18, is higher in women, with 6250 new cases per year in Germany, and 1600 in men (WHO 2021). Cervical carcinoma is the fourth most frequent malignant tumour in women and nearly 100% of cervical carcinoma are HPV associated. HPV infection is a widespread issue, especially amongst sexually active and younger individuals. Early detection of HPV infection itself or histopathological abnormal tissue is crucial to prevent the malignant transformation into invasive carcinoma. Therefore, annual gynaecological physical and cytological examinations are highly recommended (Robert Koch Institut 2021).

Overall, it is evident that HPV and the risk of cancer development due to an HPV infection remain a concern for patients' health and, consequently, the healthcare system. Further research is indispensable to understand the virus, its biology and pathobiology on promoting cancer development as well as finding effective strategies in early detection and therapy are indispensable.

The classification of HPV subtypes primarily relies on analysing the nucleotide sequence of the open reading frame (ORF) responsible for encoding the capsid protein L1. This classification is illustrated in figure 1, which depicts a phylogenetic tree. According to Bernard et al. (2010), there are five major HPV genera:  $\alpha$ -papillomavirus,  $\beta$ -papillomavirus,  $\gamma$ -papillomavirus,  $\mu$ -papillomavirus, and  $\nu$ -papillomavirus.

Of particular interest is the  $\alpha$ -genera as it encompasses predominantly oncogenic HPV types that are responsible for the development of various types of carcinoma, including cervical, penile, oral, vaginal and vulvar carcinoma (Curado, et al. 2008, Walboomers, et



al. 1999). From an oncogenic perspective HPV can be further classified into low-risk HPV and high-risk HPV. Persistent infections with high-risk viruses significantly enhance the potential for malignant transformation, as the viral genome integrates into the host DNA, leading to modification in the cellular regulatory machinery, promoting cellular immortality. On the other hand, low-risk HPV type contribute, for example, for the development of genital warts.

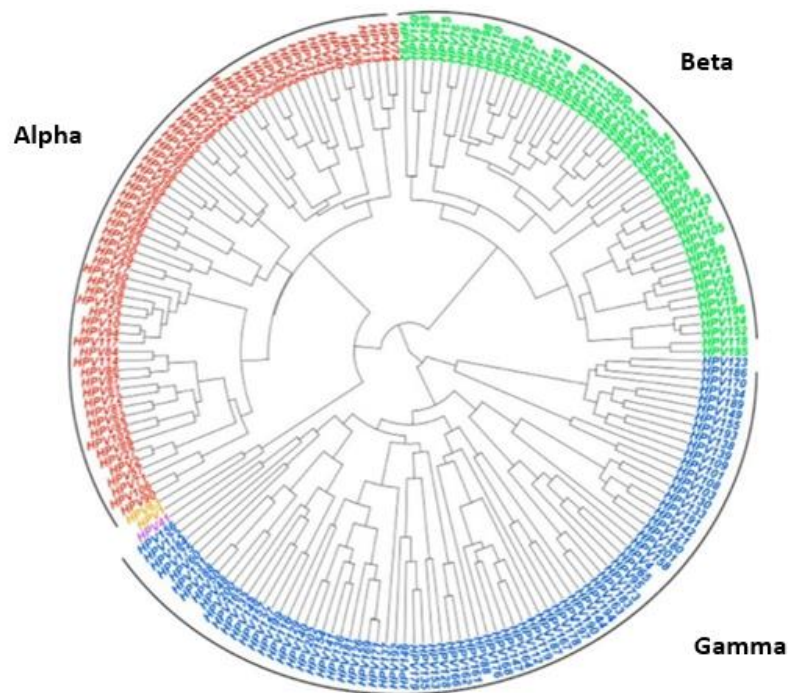


Figure 1: Phylogenetic tree of HPV

The classification HPV subtypes is primarily based on the nucleotide sequences of the open reading frame (ORF) encoding the capsid protein L1. Five major HPV genera can be distinguished, ( $\alpha$ -papillomavirus,  $\beta$ -papillomavirus,  $\gamma$ -papillomavirus,  $\mu$ -papillomavirus and  $\nu$ -papillomavirus),  $\alpha$ -,  $\beta$ -,  $\gamma$ -HPV genera being the greatest representatives (Bernard, et al. 2010, modified from Bzhalava, Eklund and Dillner 2015).

Across all papillomaviruses, highly conserved protein-coding sequences are present in the viral genome. These coding sequences provide information for the transcription of viral proteins, which subsequently determine the specific characteristics of the papillomavirus type, including host and tissue preferences, as well as the potential clinicopathological manifestations of an infection (Reid and Campion 1988). The viral genome can be divided into three main regions: the upstream regulatory region (URR), the early (E) region, and the late (L) region (figure 2). The URR primarily contains promoters and enhancers that regulate the transcription of viral proteins. The early

sequences are essential for the production of viral proteins that play a role in modifying the cellular environment of the host, favouring viral replication and DNA replication. The late proteins are necessary for viral assembly and vegetative viral replication. Figure 2 illustrates the gene organization of alpha-, and beta-papillomaviruses, including the coding sequences for viral proteins.

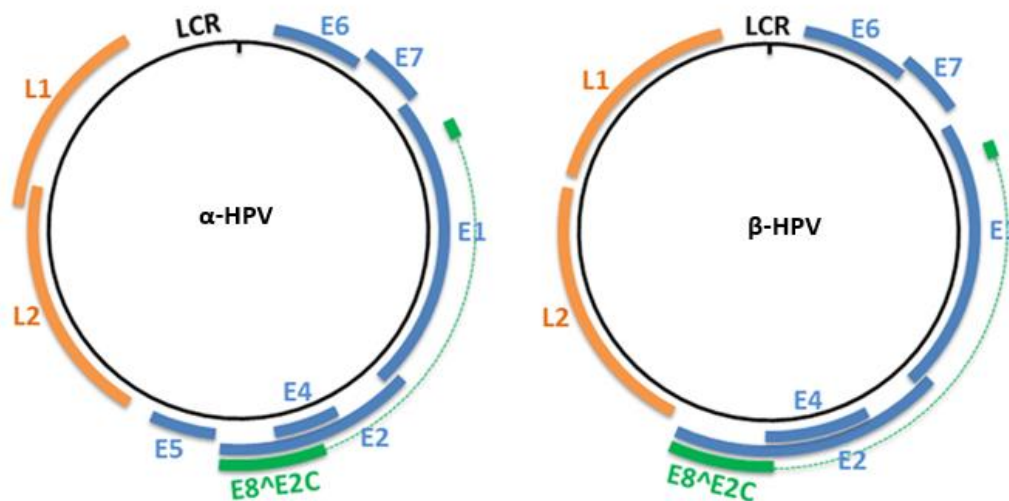


Figure 2: HPV genome organisation of alpha and beta HPV types

The genome of alpha and beta HPV with its circular double stand DNA (black line) is illustrated. The early genes, including the sequences for the oncogenic proteins E6 and E7 are showed in blue, the lates genes in orange (modified from Gheit 2019).

Of particular interest are the oncogenic proteins E6 and E7, encoded by high-risk HPV types such as HPV 16 and HPV 18. E6 forms a complex with the tumour suppressor protein p53 in the host cell, leading to its degradation. The p53 protein functions as a crucial regulator of the cell cycle, inducing cell cycle arrest and potentially triggering cell death in response to DNA damage. By inactivating p53, E6 promotes unlimited cell proliferation, facilitating the development and growth of malignant tumours.

On the other hand, E7 interacts with the retinoblastoma (Rb) protein, another tumour suppressor protein in the host cell. Rb normally interferes with transcription factors, repressing cell replication. However, the binding of E7 to the retinoblastoma protein leads to the release of these transcription factors, resulting in unrestricted stimulation of the cell cycle and cell division (Yim and Park 2005). The interaction between E6 and E7 with the tumour suppressors p53 and Rb is illustrated in figure 3.

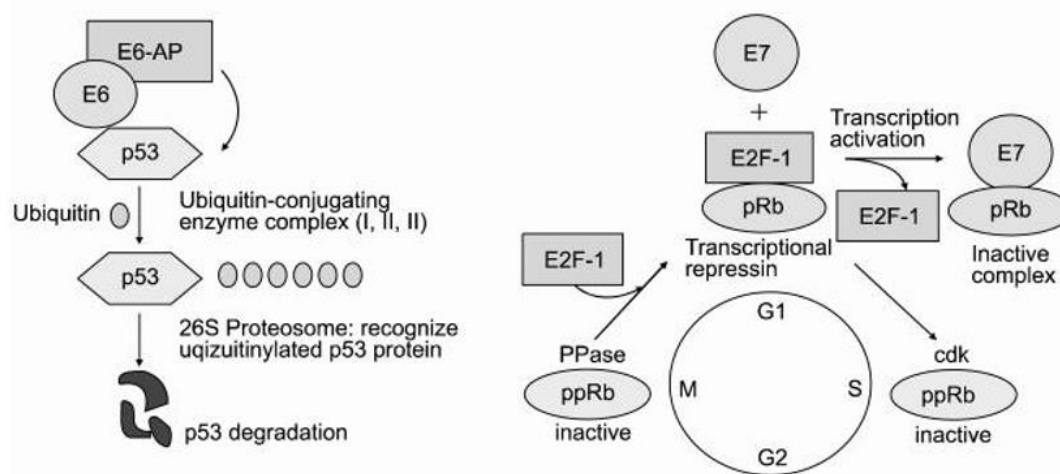


Figure 3: Interaction of HPV E6 and HPV E7 with host cell tumour suppressors p53 and Rb

The oncogenic proteins E6 and E7 of HPV interfere with crucial host cell tumour suppressor proteins, namely p53 and retinoblastoma protein (Rb), respectively. E6 binds to p53, causing its degradation and facilitating cell cycle progression. Similarly, E7 binding to Rb leads to the formation of an inactive complex, promoting cell proliferation (modified from Yim and Park, 2005).

The role of HPV E6 and HPV E7 in the potential malignant transformation of cells has been extensively studied, and these oncogenic proteins have been shown to play a crucial role in the development of HPV-associated tumours. However, the mechanisms underlying the induction, persistence, and eventual malignant transformation of host cells in HPV infection are far more complex. Ma et al. (2016) demonstrated that HPV employs sophisticated mechanisms to evade the host cells' attempt at immunological clearance of an HPV infection. They found that the downregulation of RIPK3 and its downstream effectors, such as MLKL, reduces TNF $\alpha$ -induced necroptosis of infected keratinocytes. Additionally, Schmidt et al. (2015) revealed the critical role of RIPK3 expression in cervical cancer for antitumor immune stimulation by the dsRNA analogue PolyIC, which mimics infection with a dsRNA virus. RIPK3 not only induces necroptosis but also promotes the release of interleukin 1 $\alpha$ , stimulating dendritic cells to produce interleukin-12, which is critical for an effective antitumor response. Furthermore, they observed significant variations in RIPK3 expression in cervical cancer tissue through in-situ analysis. These findings are of great importance for understanding HPV-driven cancer, its mechanisms of immune evasion, and potential treatment options.

The marker Ki67 can be used to identify replicating cells, as it is rarely expressed in resting cells. Ki67 is commonly utilized as a marker for cell proliferation in immunohistochemistry. The fraction of Ki67-positive cells in tumour tissue often correlates with the patient's clinical outcome (Scholzen and Gerdes 2000). Cancer immunotherapy shows promise as a therapeutic approach but requires further

investigation. However, the therapeutic efficacy may be limited by the dependence on the presence of RIPK3. Therefore, the expression level of RIPK3 in cancer tissue could potentially serve as a predictive factor for a patient's treatment outcome before therapy is initiated.

### 1.1.1 Cutaneous Papillomaviruses

Cutaneous human papillomaviruses (HPVs) of the  $\beta$ -generation are present in both the normal skin microbiota of individuals and cutaneous (pre-) cancerous lesions, including actinic keratosis and squamous cell carcinoma (Pfister, 2003). The high prevalence of cutaneous HPVs in infants and young children suggests early exposure during childhood (Antonsson et al., 2003). Despite their existence as commensal pathogens on the skin, the involvement of cutaneous HPVs in the initiation and perpetuation of tumorigenesis has long remained unclear.

The data presented by Pfister (2003) and Orth (2006) indicated a significant presence of  $\beta$ -HPVs, specifically HPV 5 and 8, in both benign and malignant lesions in long-term immunosuppressed patients and those affected by the rare autosomal recessive disorder epidermodysplasia verruciformis (EV). This finding suggests a strong correlation between immunosuppression and heightened vulnerability to viral infection, and an oncogenic potential of  $\beta$ -HPVs. Consequently, HPV 5 and HPV 8 have been categorized as "possibly carcinogenic" in individuals with epidermodysplasia verruciformis (Bouvard et al., 2009).

Since  $\beta$ -HPVs are predominantly found in the early stages of skin carcinogenesis and are less described transcribed or even missing in skin carcinomas (Weissenborn et al., 2005; Arron et al., 2011, Neale, et al. 2013), a "hit and run" hypothesis has been proposed (Hasche, Vinzón, & Rösl, 2018). Hence, there is the suggestion that  $\beta$ -HPVs might have a critical co-factorial role in the initiation of carcinogenesis rather than its perpetuation. Potential underlying mechanisms how  $\beta$ -HPVs might promote tumorigenesis following cutaneous infection are a focus of latest research.

The interaction between the oncogenic protein E6 of mucosal high-risk HPVs, specifically HPV 16 and 18, and the checkpoint inhibitor p53 serves as a crucial catalyst in the process of carcinogenesis and has been intensively investigated within the last decade. This interaction leads to the binding of p53 and subsequent degradation, thereby facilitating unrestricted cell cycle progression and the potential for malignant cell growth. However, it appears that in the majority of  $\beta$ -HPVs, the E6 protein does not directly interfere with p53 (Steger and Pfister 1992, White, et al. 2012, Elbel, et al. 1997), but has

found alternative elaborated strategies to alter host cell communication and integrity. In fact, some  $\beta$ -HPV E6 proteins indirectly modify p53 function by inhibiting for example the transcription of p53-induced proapoptotic genes (Giampieri and Storey 2004) or by altering homeodomain-interacting protein kinase 2 (HIPK2) -mediated phosphorylation of p53 (Muschik, et al. 2011).

Furthermore, there are evidence that the oncoprotein E6 of  $\beta$ -HPVs promote tumour progression by interacting, amongst others, with CCAAT/enhancer-binding protein alpha (C/EBP $\alpha$ ) and Mastermind-like protein 1 (MAML1), both involved in the differentiation of keratinocytes, encouraging tumorigenesis (Marthaler, et al. 2017, Tan, et al. 2012). Furthermore, apoptosis, induced upon UV-mediated DNA-damage seems to be avoided by interaction with the proapoptotic protein Bcl-2 homologous antagonist/killer (Bak) following an infection with HPV 8 for example (Jackson, et al. 2000, Underbrink, et al. 2008). In addition, HPV8 E6 seems to enhance the activation of EGFR-signalling upon UV exposure, resulting in an increased proliferation rate and cell growth, favouring the development of squamous cell carcinoma (Taute, Pfister and Steger 2017).

Both the  $\beta$ -HPV E6 and the oncogenic protein E7 appear to play a role in tumour development. In high-risk mucosal HPVs, E7 interacts with the tumour suppressor protein, the retinoblastoma protein (Rb), resulting in its degradation. This interaction bypasses cell cycle arrest and facilitates viral genome replication. It has been demonstrated that  $\beta$ -HPV E7 also binds to Rb (Schmitt et al., 1994). However, E7-induced alterations in the epithelial microenvironment, by interfering with membrane-bound matrix metalloproteinase (MT1 MMP) or C/EBP $\beta$ , also favour epithelial proliferation and tumorigenesis (Smola-Hess et al., 2005; Sternlicht and Werb, 2001, Sperling, et al. 2018).

Along with these findings, several *in vivo* studies, including animal models, have demonstrated a compelling association between infection with cutaneous  $\beta$ -HPVs, specifically HPV8, and an elevated incidence of skin tumours. For instance, Schaper et al. (2005) conducted experiments utilizing transgenic mice and found that the expression of early genes of HPV8 led to a spontaneous augmentation in skin tumours, even in the absence of additional exogenous carcinogens. Furthermore, the oncoprotein E6 of HPV8 has been identified as a pivotal factor in tumorigenesis in a mouse model (Marcuzzi et al., 2009).

In conclusion, comprehensive *in vitro* and *in vivo* investigations have indicated that HPV8, along with other cutaneous  $\beta$ -HPVs, may serve as significant co-factor in tumour initiation, albeit employing different mechanisms than mucosal HPVs. These  $\beta$ -HPVs predominantly exert their influence by modifying the tissue microenvironment and

altering the expression of proteins involved in UV damage repair, such as p300 or ataxia telangiectasia and Rad3-related protein (ATR). This substantially contributes to an increased susceptibility to UV-induced DNA damage and consequent skin carcinogenesis (Wallace et al., 2012; Marcuzzi et al., 2009).

## 1.2 Precancerous lesions of the skin and the vulvar

HPV appears to have a pivotal role in the carcinogenesis of both cutaneous and mucosal lesions, being present in precancerous skin lesions as well as vulvar intraepithelial neoplasia. Actinic keratosis and vulvar intraepithelial neoplasia are considered precancerous lesions that are associated with HPV infections (Weissenborn, et al. 2005, Campion and Singer 1987, M. Campion 1987). Photodynamic therapy has emerged as a minimally invasive treatment option for both conditions, offering a low incidence of side effects (Tosti, et al. 2018, Arenberger and Arenbergerova 2017, Reinehr, Bakos and al. 2019). In the following two precancerous lesions of the skin and the vulvar, actinic keratosis and vulvar intraepithelial neoplasia, both treatable with PDT are presented.

### 1.2.1 Actinic keratosis

Actinic keratosis, also known as keratosis solaris, is a precancerous dermal lesion characterized by the proliferation of atypical epidermal keratinocytes. It has the potential to progress into non-melanoma skin cancer, particularly squamous cell carcinoma. These lesions predominantly occur in sun-exposed areas of the skin, such as the scalp (in individuals with thinning hair), décolleté, nose, and dorsal surface of the hands. Consequently, ultraviolet radiation has been identified as the primary factor contributing to the development of actinic keratosis. However, individual factors such as genetic predisposition, sex, age, and previous history of cutaneous neoplasms also play a role (Berman, Cockerell and al. 2013).

Although actinic keratosis is primarily considered a precancerous lesion, cytological analysis reveals distinct changes than can also be found in manifest neoplasia. These alterations include an increased rate of mitosis and mutations in the cell cycle regulatory gene p53. Given the fluid threshold between precancerous lesions and definitive carcinomas, early diagnosis and treatment are crucial.

Epidemiologically, actinic keratosis holds significant importance worldwide. In Australia, for instance, actinic keratosis is diagnosed in approximately 40% to 60% of the Caucasian population over 45 years of age (Reinehr, Bakos and al. 2019). This high

prevalence can be partially attributed to the intense solar radiation in the country. However, actinic keratosis can also be found in 10% to 30% of individuals over 40 years old in Europe and the United States of America. It is widely recognized that the prevalence of actinic keratosis significantly increases with age. While individuals under 30 years old are rarely affected, the prevalence rises to over 80% in people between 60 and 70 years old (Green, et al. 1988). Considering the demographic changes and the associated increase in actinic keratosis incidence, medical treatment of actinic keratosis is becoming increasingly important. Moreover, men appear to be more susceptible to developing actinic keratosis than women, which can be explained by the assumption that men experience higher levels of solar radiation exposure throughout their lives, particularly in outdoor occupations such as roofing or road construction (DGUV 2023). Additionally, skin type plays a significant role, with individuals of lighter complexion being more prone to developing actinic keratosis compared to those with darker skin tones.

As previously mentioned, exposure to ultraviolet radiation is the primary factor contributing to the development of actinic keratosis. The pathogenesis behind the initiation and manifestation of actinic keratosis is complex and often involves a cascade of molecular changes in the cells. Figure 4 illustrates the intricate pathogenesis of how UV radiation contributes to the development of actinic keratosis.

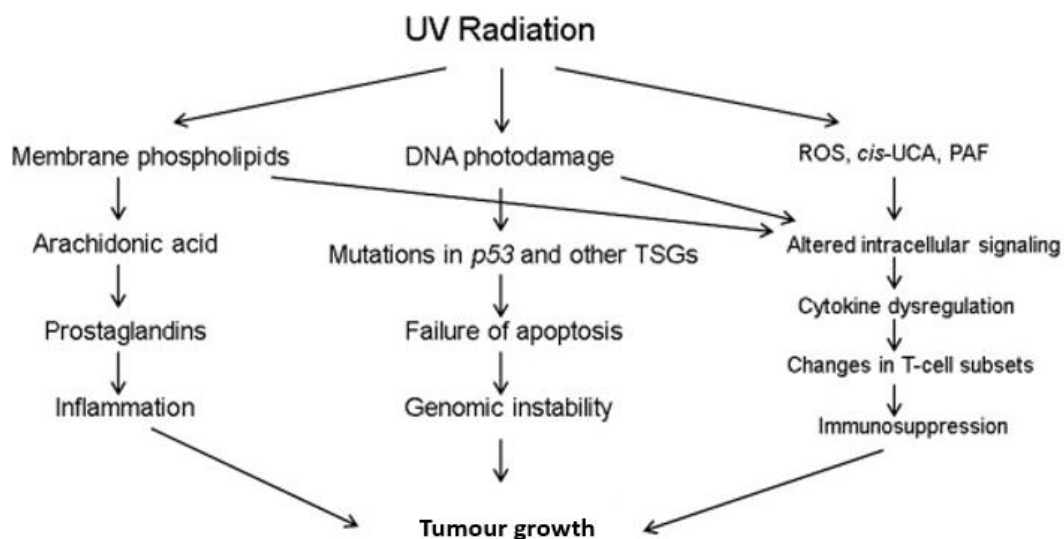


Figure 4: Pathobiology of the development of actinic keratosis upon ultraviolet radiation

UV radiation induces cellular damage that promotes the formation of precancerous skin lesions through various mechanisms. On one hand, UV exposure can result in photodamage to the genome, leading to cell growth following mutations. On the other hand, it can also trigger tissue inflammation and provoke alterations in immune response (modified from Berman, Cockerell et al., 2013).

The image illustrates three primary pathways that contribute to the enhanced proliferation of keratinocytes. Firstly, UV radiation interacts with membrane components, leading to the production of proinflammatory cytokines, including prostaglandins, which induce an inflammatory response. Secondly, direct exposure to UV radiation causes mutations in the cell's DNA, including mutations in the p53 tumour suppressor gene or other tumour suppressor genes. P53 serves as a regulator of the cell cycle, responsible for inducing apoptosis in cells that do not meet the criteria for proliferation due to DNA damage, for example. If this control pathway is ineffective, cells with damaged genetic information can replicate, resulting in the proliferation of abnormal cells. Lastly, UV radiation induces an increase in reactive oxygen species, which further causes DNA damage and collectively contributes to alterations in intracellular signalling pathways. These changes initiate an impaired immune response that is ineffective in recognizing and eliminating genetically modified abnormal cells. The impact of immunosuppression on the development of actinic keratosis is evident from the higher prevalence of actinic keratosis in patients receiving systemic immunosuppressive drugs (Ulrich, et al. 2009).

Clinical inspection and palpation are the primary methods for diagnosing actinic keratosis. The condition typically presents as an erythematous base with yellow-brownish vulnerable keratoses that can be felt as irregular, rough surfaces. Dermoscopy is regularly employed for more accurate identification. In addition to clinical examination and dermoscopy, other diagnostic options include optical coherence tomography, histopathological examination, and immunohistochemical examination of the lesion. Actinic keratosis is histopathologically characterized by the presence of parakeratosis and hyperkeratosis in the stratum corneum. Additionally, the epidermis exhibits atypical keratinocytes with large, pleomorphic, and hyperchromatic nuclei. There is defective cell differentiation and maturation, and the keratinocytes lose their polarity. The number of mitoses is significantly increased, and infiltration of immune cells due to inflammatory reactions is often observed (Roewert-Huber, et al. 2007). Immunohistochemical examination is primarily performed in cases where a definite diagnosis of actinic keratosis is otherwise uncertain. The proteins commonly stained for identification include cytokeratins, such as cytokeratin 5, 8, 15, and 19 (Aslan, et al. 2006).

As actinic keratosis has the potential to progress to a malignant lesion, early and effective treatment is crucial. Various treatment options are available. A fundamental aspect of therapy should always be patient education regarding the disease, the risk factors contributing to its occurrence, and prevention strategies. Additionally, regular skin examinations conducted by a dermatologist, as well as self-examinations by the patient,



are essential (Reinehr, Bakos and al. 2019, Ceilley and Jorizzo 2013). Treatment options can be broadly classified into topical treatments, such as the application of 5-fluorouracil (5-FU), Imiquimod, or photodynamic therapy, and ablative surgical treatments. Common techniques for ablative treatment include curettage, cryotherapy, or the use of CO2 lasers. The choice of treatment regimen depends on factors such as the patient's age, the number and size of the lesions, their location, and, most importantly, the patient's preference (Reinehr, Bakos and al. 2019, Arenberger and Arenbergerova 2017).

### 1.2.2 Vulvar intraepithelial neoplasia

Vulvar intraepithelial neoplasia (VIN) is a precancerous lesion of the vulva with the potential to transform into vulvar carcinoma. Vulvar squamous cell carcinoma (SCC) constitutes approximately 4% of all genital carcinomas in women. Despite being a relatively rare condition, it is the most frequently occurring malignant tumour of the vulva, accounting for about 80-95% of all malignant vulvar cancers (Judson, et al. 2006, Stewart and Kleiheus 2003). It predominantly affects post-menopausal women over the age of 60. Of concern is not only the increased incidence of VIN in recent years, but also the shift towards younger women in their thirties (Joura, et al. 2000, Campion and Singer 1987, M. Campion 1987).

VINs can be classified in several ways. Squamous VINs can be categorized as VIN 1 to 3, representing mild, moderate, and severe dysplasia of the epithelium. An alternative and newer classification is provided by the International Society for the Study of Vulvovaginal Disease (ISSVD), which divides VIN into low-grade squamous intraepithelial lesions (LSIL) and high-grade squamous intraepithelial lesions (HSIL), both of which are HPV-associated, as well as a "differentiated type" that is not HPV-dependent. Additionally, there are rare non-squamous types such as Paget's disease of the vulva or melanoma in situ of the vulva. Figure 5 schematically illustrates the progression from normal epithelium to highly dysplastic lesions that ultimately transform into invasive carcinoma. It is noteworthy that dysplasia originates in the basal cell layer of the epithelium and progresses upwards as the grade of VIN increases. All precancerous lesions, including vulvar intraepithelial neoplasia, have, by definition, an intact basal membrane, which becomes invasive as carcinogenesis progresses.

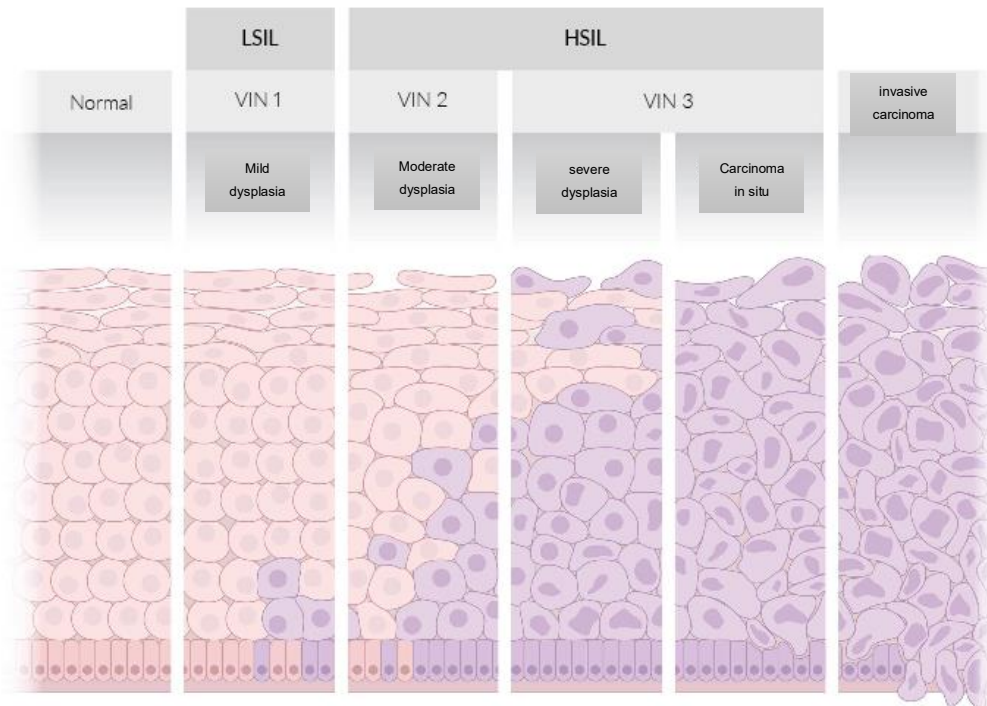


Figure 5: Schematic illustration of the development of normal tissue into an invasive vulvar carcinoma

Vulvar intraepithelial neoplasms (VINs) are precancerous lesion, possibly leading to the formation of invasive vulvar carcinomas. VINs can be categorized in VIN 1 to 3, representing mild, moderate, and severe dysplasia of the epithelium. Alternatively, the ISSVD-classification divides VINs into low-grade squamous intraepithelial lesions (LSIL) and high-grade squamous intraepithelial lesions (HSIL), both of which are associated with HPV infections. Not shown is the non-HPV-associated "differentiated type" (modified from AMBOSS GmbH 2021).

In the ISSVD classification, human papillomavirus appears to play a crucial role in the initiation and the progress of VINs. The oncogenic high-risk HPV types, such as HPV 16 and 18, are associated with the carcinogenesis of vulvar neoplasia (De Vuyst, et al. 2009). However, there are other risk factors linked to vulvar intraepithelial lesions, including the effects of oestrogen (such as nulliparity or few pregnancies), obesity, smoking, multiple sexual partners, immunosuppression, and genetic susceptibility.

The potential carcinogenic impact of human papillomaviruses was first introduced by zur Hausen in 1977. Since then, researchers have accumulated substantial evidence linking HPV and its biology to the aetiology of various tumours, including genital cancer. As HPV is a sexually transmitted virus, it has been found to be present in the genital tract of a significant number of sexually active women (Reid, Greenberg, et al. 1987). However, it is important to note that there are numerous HPV types, each causing different types of lesions with varying potential for malignant transformation, requiring separate

consideration. For instance, HPV types 6 and 11 are commonly associated with genital warts or VIN grade I, while types 16 and 18, among others, are predominantly found in high-grade VINs or invasive carcinoma (Campion and Singer 1987, M. Campion 1987). Macroscopically, VINs present as macules that can be erythematous, white, or pigmented. The skin appears rough, and hyperkeratotic plaques are frequently observed (Hoang, et al. 2016).

In terms of treatment, extended vulvectomy was the primary option in the past. However, this aggressive surgical approach is associated with significant physical and psychological constraints. Consequently, less invasive treatment options have been extensively discussed in recent years, including laser ablation, topical application of Imiquimod, or photodynamic therapy (ACOG 2011).

### 1.3 Photodynamic therapy

Photodynamic therapy (PDT) is a relatively straightforward treatment option that utilizes visible light to target dermatological lesions such as actinic keratosis. The underlying mechanism of PDT involves the generation of reactive oxygen species (ROS) within the target cells, leading to cellular damage and subsequent cell death. Importantly, this detrimental effect is relatively specific to the abnormal target cells while sparing the healthy surrounding tissue. The key component in PDT is the photosensitizer, which plays a crucial role in the process.

Currently, aminolevulinic acid (ALA) and methyl aminolevulinate (MAL) are the photosensitizers commonly employed in dermatology for PDT. These photosensitizers are classified as prodrugs that, upon topical application, are metabolized by cellular machinery into photoactivatable porphyrins. These porphyrins, particularly protoporphyrin IX, are naturally involved in the cellular heme synthesis pathway. As depicted in figure 6, when stimulated by specific light wavelengths (404-420nm and 635nm), these porphyrins transition to an excited state of higher energy. Upon returning to the ground state, they release this energy to the surrounding environment. The released energy can directly interact with substrates or react with tissue oxygen, inducing the formation of ROS. The resulting cellular damage ultimately triggers cell death in the target cells.

$\gamma$ -H2AX is a protein found in the nucleus of cells and is part of the histone octamer. When a cell experiences damage, this protein undergoes phosphorylation, initiating a cascade of reactions involved in cell and DNA damage repair. Therefore,  $\gamma$ -H2AX can serve as a

marker for cell damage, specifically DNA double-strand breaks, providing valuable insights into the effectiveness of PDT (Kuo and Yang 2008).

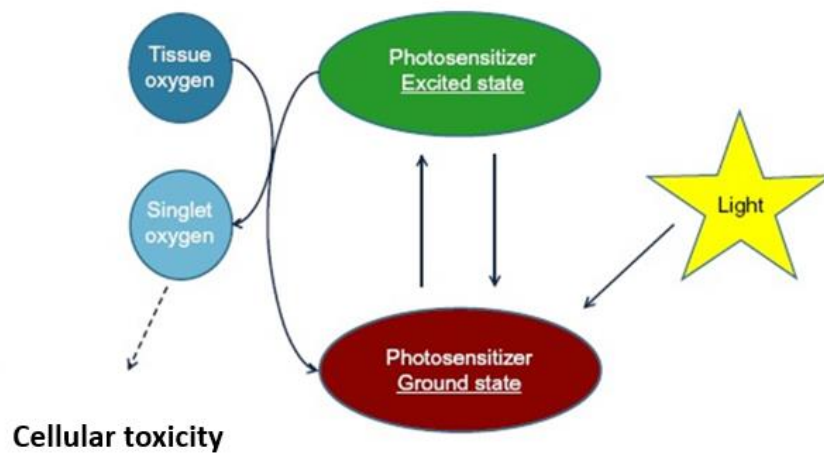


Figure 6: Illustration of the cell-damaging photochemical effect during photodynamic therapy

The applied light stimulates the photosensitizer to rise into an excited state. By returning to the ground state energy is released to tissue oxygen inducing reactive oxygen species (modified from Wan and Lin 2014).

The cellular damage induced by PDT exhibits a relatively high degree of specificity towards cancerous or precancerous cells while sparing the surrounding healthy tissue. This selectivity is attributed to the more effective accumulation of photosensitizers in tumour cells compared to normal cells (Van Hillegersberg, et al. 1992). The conversion of ALA, a prodrug, to protoporphyrin IX appears to occur more efficiently in tumour cells than in healthy tissue. This phenomenon can be attributed to the higher production of precursor metabolites of protoporphyrin IX or the altered enzymatic machinery involved in heme biosynthesis in tumour cells, leading to decreased elimination rates (Schoenfeld, et al. 1988, El-Sharabasy, et al. 1992).

During PDT, the exposure of photosensitizers to light triggers the production of ROS, causing cellular damage and subsequent activation of stress response pathways in the targeted cells. These pathways, in turn, activate specific enzymes and transcription factors, ultimately resulting in cell death. PDT has been associated with various forms of cell death, including apoptosis, necrosis, autophagy, and necroptosis, the programmed variation of necrosis (Buytaert, Dewaele and Agostinis 2007, Coupienne, et al. 2011). The specific type of cell death initiated by PDT depends on factors such as the type of tumour, the photosensitizer employed, and its concentration (Buytaert, Dewaele and Agostinis 2007).

During PDT treatment, the photosensitizer is topically applied to the lesion and left for a period of three to four hours for incubation. During this time, the photosensitizer can penetrate the cells and undergo metabolic conversion into photoactivatable porphyrins. The successful uptake of aminolevulinic acid (ALA) or methyl aminolevulinate (MAL) into the cells and their subsequent transformation into porphyrins can be visualized through fluorescence. By exposing the cells incubated with ALA/MAL to a light source, such as black light with a wavelength ranging from 345 to 380nm, the absorbed amount of photosensitizers can be assessed, and the potential therapeutic efficacy of PDT can be predicted. The fluorescence properties of ALA/MAL have also been utilized in fluorescence-guided surgery, particularly in neurosurgery for the resection of glioblastoma (Stummer, et al. 2006). Furthermore, an ALA-based fluorescence diagnostic approach has been described for the identification of cervical intraepithelial lesions (CIN) (Vansevičiūtė, et al. 2014).

PDT finds a broad range of indications primarily in the field of dermatology. It serves as a first-line treatment for actinic keratosis and is also employed for squamous cell carcinoma, basal cell carcinoma, cutaneous T-cell lymphoma, acne vulgaris, rosacea, and photoaging (Wan and Lin 2014). Moreover, PDT has been described for the therapy of oral cancers and precancers such as oral leucoplakia (Chen, et al. 2012) as well as for vulvar lesions, including for instance the therapy of vulvar lichen sclerosis (Prodromidou, et al. 2018) and of vulvar intraepithelial neoplasia (Tosti, et al. 2018).

PDT is a relatively simple yet versatile therapeutic approach, with applications extending from dermatology to gynaecology. In addition to its broad range of applications, PDT is associated with relatively few side effects. Common local reactions include erythema, itching, and exfoliation. Patients often experience pain during PDT (Gholam, Kroehl and Enk 2013). These local reactions and the accompanying pain are indicative of a PDT-induced local inflammatory response. The infiltration of immune cells into the targeted area appears to induce an adaptive anti-tumour immune response, which contributes to the therapeutic efficacy of this anti-tumour modality (Dougherty, et al. 1998).

## 1.4 Necroptosis and RIPK3

When a cell is so severely damaged that survival and further replication are no longer possible, cell death becomes inevitable. One form of cell death is apoptosis, a programmed process that occurs naturally during organism development and plays a role in morphological changes and structural differentiation. Apoptosis is initiated through a cascade of reactions, leading to a highly regulated and controlled destruction of the

cell. During this process, the cell undergoes shrinkage, nucleosome condensation, and DNA fragmentation. The resulting particles, known as apoptotic bodies, are subsequently engulfed and digested by phagocytes.

Necrosis, on the other hand, is a form of cell death that typically follows severe injury and acute damage. Unlike apoptosis, necrosis lacks a strictly regulated signalling pathway or controlled procedure. The cell loses its structural integrity, leading to the release of internal components into the extracellular environment. This cellular rupture triggers an inflammatory response, causing further damage to surrounding cells.

Necroptosis exhibits characteristics of both apoptosis and necrosis. Specific signalling pathways trigger programmed cell destruction, but at the same time, the release of multiple damage-associated molecular patterns (DAMPs) induces an inflammatory response, affecting the cellular environment. This relatively recent form of cell death has been the subject of intensive research in recent years. It has been demonstrated that various stimuli can initiate necroptotic signalling pathways, including Tumour Necrosis Factor alpha (TNF $\alpha$ ), FasL, Tumour Necrosis Factor-Related Apoptosis-Inducing Ligand (TRAIL), pathogen-associated molecular patterns, as well as viral and bacterial-induced signalling (Vanlangenakker, Vanden Berghe and Vandenabeele 2012). Given that the signalling pathways, particularly TNF $\alpha$ -induced necroptosis, have been well investigated and understood, the following outline will focus on TNF $\alpha$ -induced necroptosis as a model (figure 7).

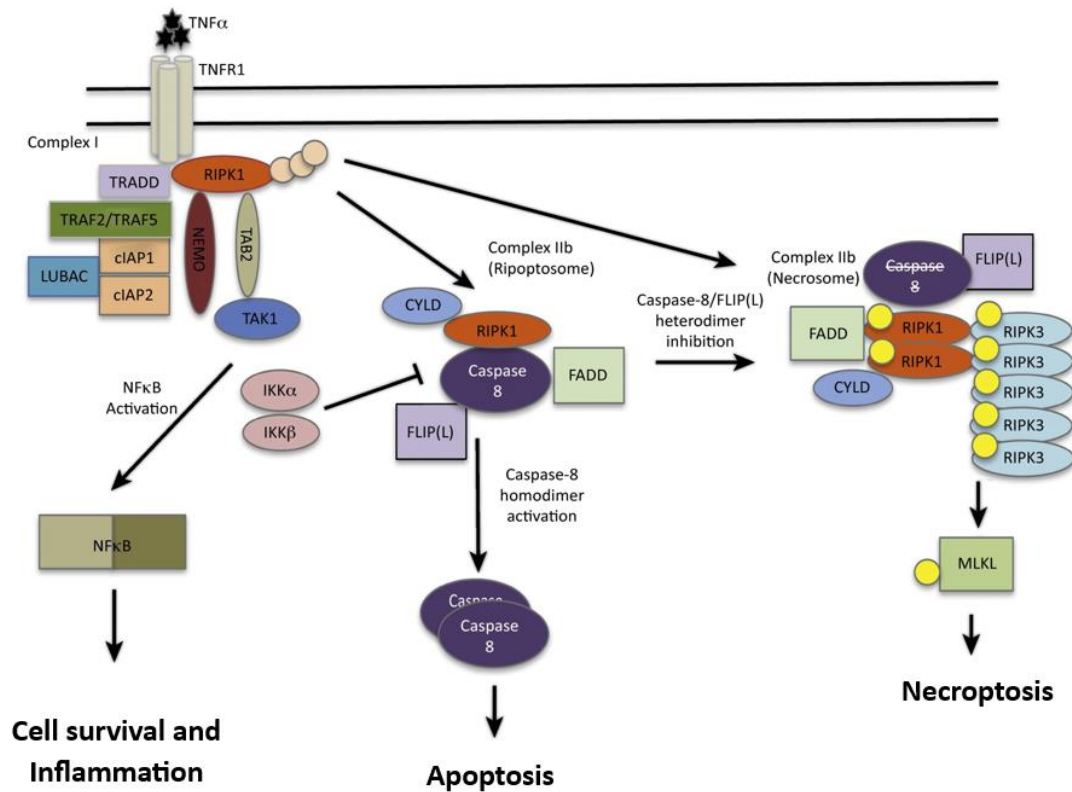


Figure 7: Simplified schematic illustration of TNF- $\alpha$  induced signaling pathways

The formation of distinct complexes involving Receptor-interacting serine/threonine-protein kinase 1 (RIPK1) relies on the specific signalling pathways triggered by TNF $\alpha$  activation. One potential interaction involves RIPK3, which leads to the induction of necroptosis. (modified from Wegner, Saleh and Degterev 2017).

Complex I and complex IIb (Ripoptosome) are formed in response to TNF $\alpha$  induction to promote cell survival and apoptosis, respectively. On the other hand, the macromolecular protein complex IIb, known as the necrosome, triggers necroptotic cell death. The activation of caspase 8 plays a central role in determining whether apoptosis or necroptosis is executed. Caspase 8 activation leads to apoptotic signalling pathways, while its inhibition initiates the pro-necroptotic machinery (Wegner, Saleh and Degterev 2017). The de-ubiquitination of RIPK1 by Cylindromatosis (CYLD) is crucial for the progression of necroptosis (Moquin, McQuade and Chan 2013). Following this, RIPK1 and RIPK3 are phosphorylated through autophosphorylation and cross-phosphorylation (Cho, et al. 2009). Once RIPK3 is phosphorylated and forms homodimers, the pro-necroptotic enzyme Mixed lineage kinase domain-like pseudokinase (MLKL) is recruited. Studies by Murphy et al. demonstrated that the recruitment of MLKL is a critical step in initiating necroptotic cell death, as cells lacking this protein are unable to undergo necroptosis (Murphy, et al. 2013). MLKL is responsible for the loss of cell membrane integrity, leading to the release of cellular content into the extracellular space and the

subsequent inflammatory response characteristic of necrosis (Wang, et al. 2014). Interestingly, it has been observed that RIPK3 activation is the key step in the formation of the necrosome. Even in the absence of RIPK1, RIPK3 activation and subsequent homodimerization are sufficient to induce necroptosis (Wu, et al. 2014). Although the regulation of necroptosis is complex and not fully understood, the pivotal role of RIPK3 in the necroptotic signalling network has led to the investigation of RIPK3 expression in cell cultures in this study.

RIPK3 is a serine/threonine kinase and belongs to the receptor-interacting protein (RIP) kinase family, which comprises seven members (Zhang, Lin and Han 2010). All members of this family are involved in cell death-inducing or pro-inflammatory signalling pathways. Structurally, RIPK3 consists of an N-terminal kinase domain, a RIP-homotypic interaction motif (RHIM), and a unique C-terminal domain. RIPK3 is predominantly localized in the cytoplasm, but it can shuttle between the cytoplasm and nucleus due to the presence of nuclear localization signals (Yang, et al. 2004).

In addition to necroptosis, the RIPK1/RIPK3 signalling pathway is implicated in various disease pathologies, including ischemic injury and acute and chronic inflammatory diseases (Wegner, Saleh and Degterev 2017). In mouse models, inhibition of RIPK1 significantly reduced the effects of ischemic brain injury (Degterev, et al. 2005). Furthermore, RIPK1/RIPK3-mediated necroptosis is associated with the development of systemic inflammatory response syndrome (SIRS), a life-threatening condition characterized by an excessive systemic immune response leading to severe end-organ damage (Duprez, et al. 2011). While RIPK1-dependent pro-inflammatory signalling appears to promote the development of autoimmune skin diseases such as neutrophilic dermatosis (Lukens, et al. 2013), RIPK3 is involved in the inflammatory cascade that promotes atherosclerotic plaque formation (Meng, et al. 2016). Conversely, studies have hypothesized that RIPK1, RIPK3, and their downstream signalling effectors, as well as apoptosis and necroptosis, play key roles in the prevention of autoimmune diseases (Alvarez-Diaz, et al. 2016).

The role of RIPK1/RIPK3 and necroptosis in cancer development and anti-tumor therapy is of great interest. It may play three different, partially opposing roles in carcinogenesis:

- “Induction of necroptosis can be made to eliminate cancer cells that show resistance to treatment”.
- “Promoting necroptosis can enhance surveillance and protective immunity against cancer”.
- “Inhibition of necroptosis can lead to a reduction in cancer-promoting inflammation” (Wegner, Saleh and Degterev 2017).



In cancer treatment, the selection pressure favours the development of apoptosis-resistant cells. Han et al. (2007) demonstrated that necroptosis could serve as an alternative pathway to eliminate apoptosis-resistant cancer cells (Han, et al. 2007). On the other hand, Seifert et al. (2016) showed that RIPK-mediated inflammation plays a key role in tumorigenesis by promoting the development of a highly immunogenic myeloid and T cell infiltrate in pancreatic ductal adenocarcinoma (Seifert, et al. 2016). In contrast, the inhibition of RIPK3 is associated with significantly reduced tumour progression. As RIPK-induced signalling and subsequent NFκB-dependent inflammatory response are involved in priming lymphocytes against necroptotic cells, RIPK1 and RIPK3 appear to play a crucial role in the body's defence against cancer cells (Yatim, et al. 2015). These findings clearly demonstrate the high involvement of RIPK1 and RIPK3, along with their downstream signalling effectors, in tumorigenesis. The exact underlying mechanisms are not fully understood and require further research. However, the modulation of RIPK-mediated signalling pathways has significant potential to revolutionize anti-tumour therapy.

## 1.5 Aim of the study

It is well-established that RIPK3 is involved in the signalling pathway that leads to the induction of necroptosis during photodynamic therapy (PDT). PDT is commonly employed for treating patients with actinic keratosis, and thus, the primary objective of this study was to investigate whether there are variations in RIPK3 expression among patients with actinic keratosis and whether there is any correlation between RIPK3 levels and the clinical response to PDT treatment. Currently, radical excision is the standard therapy for patients with vulvar intraepithelial neoplasia (VIN). Introducing PDT as a new standard therapy for VIN could revolutionize treatment approaches and substantially reduce physical and psychological side effects for patients. Therefore, the *in vivo* analyses were expanded to include patients with VIN to determine if there are differences in RIPK3 expression and whether RIPK3 levels correlate with the degree of differentiation. Numerous previous studies have demonstrated that the effectiveness of PDT is based on its ability to induce cell death, and RIPK3 plays a critical role in the signalling pathways involved in this induction. As a result, PDT holds promise as a minimally invasive therapy option for patients with vulvar intraepithelial lesions.

Using a cutaneous 3D cell culture model, we investigated the effects of HPV8 E6 on protein expression and the impact of photodynamic therapy (PDT) *in vitro*. This model allowed us to replicate the architecture of human skin *in vitro* and analyse protein expression using various staining techniques. We visualized the harmful effects of PDT *in vitro* by utilizing  $\gamma$ -H2AX as a marker for DNA double-strand breaks. Additionally, we examined the impact of PDT on the proliferation rate of keratinocytes using ki67 as a proliferation marker. By transducing keratinocytes with HPV8 E6, we simulated an HPV8 infection to analyse the effects of PDT, including DNA damage and cell proliferation rate.

In summary, the objective of this study was to further investigate the role of RIPK3 in precancerous lesions and its involvement in PDT treatment. Additionally, we aimed to determine the extent to which an HPV8 infection directly influences RIPK3 expression and the susceptibility to PDT *in vitro*.

## 2 Material

### 2.1 Cell lines

The cell lines used in this work are listed in table 1.

*Table 1: Cell lines used*

<b>Cell line</b>	<b>description</b>
EXFBU	Fibroblasts (Walch-Rückheim, et al. 2015)
HaCaT	Immortal human skin keratinocyte cell line, mutated in the p53 protein (Boukamp, et al. 1988), (Lehmann, et al. 1993)
pLXSN- HPV 8E6-transduced HaCaT	Immortal human skin keratinocytes transduced either with pLXSN-HPV 8E6 or pLXSN (Marthaler, et al. 2017).
pLXSN-transduced HaCaT	

### 2.2 Cell Culturing

#### 2.2.1 Media used for cell culture

The media used for cell culture are listed in table 2.

*Table 2: Media used for cell culture*

<b>media</b>	<b>company</b>
Dulbecco's Modified Eagle Medium (DMEM) High Glucose (4,5g/L) with L-Glutamine	Sigma-Aldrich, Steinheim
Dulbecco's Modified Eagle Medium Nutrient Mixture F-12 Ham (with L-Glutamine, 15 mM HEPES) (DMEM: F12)	Sigma-Aldrich, Steinheim
Dulbecco's Modified Eagle Medium 10X	Sigma-Aldrich, Steinheim

## 2.2.2 Reagents used for cell culture

Reagents used for cell culture in this thesis are shown in table 3.

Table 3: Reagents used for cell culture

Reagents	company
Cholera toxin	Sigma-Aldrich, Steinheim
Dulbecco's Phosphate Buffered Saline (DPBS)	PAN Biotech, Aidenbach
Epidermal growth factor (EGF)	Invitrogen, Karlsruhe
Fetal Calf Serum (FCS), heat-inactivated for 30 min at 56°C	Gibco™, Karlsruhe
Hydrocortison	Sigma-Aldrich, Steinheim
Penicillin/Streptomycin [10000 U/mL, 10 mg/mL]	Sigma-Aldrich, Steinheim
Sodium pyruvate [100 mM], sterile filtered	Sigma-Aldrich, Steinheim
Trypsin (0,05% Trypsin und 0,02% EDTA)	Sigma-Aldrich, Steinheim
Lipofectamine RNAiMAX Reagent	Thermo Fisher Scientific, Belgien
Non-coding-siRNA	Dharmacon
siRIPK3	Dharmacon

## 2.2.3 Complex medium used for cell culturing of keratinocytes and fibroblasts

The cells are cultured in a complex composed medium. 500 ml of DMEM High Glucose with L-Glutamine is supplemented with following ingredients:

- 10% FCS
- 1% Penicillin/Streptomycin
- 1 millimolar Sodium pyruvate

## 2.2.4 Complex medium used for cell culturing of siRNA transfected keratinocytes

For cells transfected with siRNA a cell culture medium without antibiotics is used: 500 ml of DMEM High Glucose with L-Glutamine is supplemented with following ingredients:

- 10% FCS
- 1 millimolar Sodium pyruvate

## 2.2.5 Complex medium used for 3D-cultures

The medium used for 3D cultures (FAD medium) is composed of 250ml Dulbecco's Modified Eagle Medium Nutrient Mixture F-12 Ham (DMEM: F12) and 250ml of DMEM High Glucose with L-Glutamine in a ratio of 1:1. Additionally following ingredients are added:

- 10% FCS
- 1% Penicillin/Streptomycin
- 1 mM Sodium pyruvate
- 10 ng/ml Cholera toxin
- 0,4 µg/ml Hydrocortisone
- 10 ng/ml Epidermal growth factor

## 2.3 Antibodies for immunohistochemical staining

The following antibodies are used in the indicated dilution for immunohistochemical staining of tissue (VINs, actinic keratosis) and 3D cultures (table 4 and table 5).

### 2.3.1 Primary antibodies

*Table 4: Primary antibodies used for immunohistochemical staining*

<b>Antigen</b>	<b>species</b>	<b>application</b>	<b>dilution</b>	<b>company</b>
RIPK3	rabbit	Actinic keratosis	1:20000	Thermo Fisher Scientific, Belgien
RIPK3	rabbit	VIN	1:30000	Thermo Fisher Scientific, Belgien
RIPK3	rabbit	3D-culture	1:500	Thermo Fisher Scientific, Belgien
Ki67	mouse	3D-culture	1:3000	Dako Pathology Solutions, Santa Clara, USA
γ-H2XA	mouse	3D-culture	1:50000	Millipore, JBW301

### 2.3.2 Secondary antibodies

*Table 5: Secondary antibodies used for immunohistochemical staining*

<b>Antibody target</b>	<b>Species</b>	<b>company</b>
Anti-mouse Peroxidase	Horse	Vector Laboratories, Burlingame, US
Anti-rabbit Peroxidase	Horse	Vector Laboratories, Burlingame, US

## 2.4 Chemicals and reagents

All chemicals and reagents utilized for the experimental work of this thesis are listed in table 6.

Table 6: Chemicals and reagents used

<b>Chemical/reagent</b>	<b>company</b>
Aminolaevulinic acid	Sigma-Aldrich, Steinheim
Bovines Serumalbumin (BSA)	Sigma-Aldrich, Steinheim
Ethanol absolut (C <sub>2</sub> H <sub>5</sub> OH)	Roth, Karlsruhe
Hematoxyline	Vector Laboratories, Burlingame, US
Hydrogen peroxide (H <sub>2</sub> O <sub>2</sub> )	Merck, Darmstadt
Natriumhydroxide (NaOH)	Merck, Darmstadt
o-Xylol 99% pure	Thermo Fischer Scientific, Belgien
Paraformaldehyde	Sigma-Aldrich, Steinheim
Potassium chloride (KCl)	Grüssing GmbH, Filsum
Potassium dihydrogen phosphate (KH <sub>2</sub> PO <sub>4</sub> )	Merck, Darmstadt
Sodium chloride (NaCl)	VWR, Darmstadt
Sodium dihydrogen phosphate (NaH <sub>2</sub> PO <sub>4</sub> )	J.T. Baker Chemicals B.V, Deventer, Netherland
Tris-(hydroxymethyl)-aminomethane (Tris)	Roth, Karlsruhe
Trisodium citrate dihydrate	Roth, Karlsruhe
Trypanblue	Sigma-Aldrich, Steinheim

## 2.5 Buffer and solutions

The compositions of buffers and solutions utilized in this thesis are shown below.

### 2.5.1 10x Phosphate buffered saline (PBS)

- 80g Sodium chloride
- 2g Potassium chloride
- 11,4g Sodium dihydrogen phosphate (NaH<sub>2</sub>PO<sub>4</sub>)
- 2g Potassium dihydrogen phosphate (KH<sub>2</sub>PO<sub>4</sub>)
- Ad 1000ml dH<sub>2</sub>O
- Regulate the pH to 7.2 using the pH-meter

### 2.5.2 1x PBS

- 100 ml 10x PBS
- 900 mL dH<sub>2</sub>O

### 2.5.3 0.25% trypan blue solution

- Trypan blue
- 1x PBS

- 0.25 g in 100 mL PBS
- The solution is sterile filtrated.

#### 2.5.4 10x Tris-buffered saline (TBS)

- 24,2 g Tris
- 80 g sodium chloride
- ad 1000 ml dH<sub>2</sub>O
- The solution is adjusted to a pH of 7,6 using 1molar hydrogel chloride

#### 2.5.5 1x TBS

- 100 ml 10x TBS
- ad 900ml dH<sub>2</sub>O

#### 2.5.6 Sodium-citrate-buffer

- 2,94g Trisodium citrate dihydrate
- Ad 1000ml dH<sub>2</sub>O

#### 2.5.7 2.5.7. 4% formaldehyde-solution

## 2.6 Equipment

Further laboratory equipment and consumables used are listed in table 7.

*Table 7: Equipment used*

<b>Equipment/expendables</b>	<b>company</b>
24 Well Cell Culture Plate	Greiner bio-one GmbH, Frickenhausen
6 Well Cell Culture plate	Greiner bio-one GmbH, Frickenhausen
Black-light lamp	Idealderm Wood-Lampe
Cooling plate Tissue TEK Cryo Console	Miles Scientific
Coverslips 24 x 24 mm	R. Langenbrinck GmbH, Emmendingen
forceps	Hartenstein Laborversand
Incubator Heracell 240i	Heraeus, Hanau
Leica DMI 6000 B	LeicaMicrosystems, Wetzlar
Leica DMi1 inverted microscope	LeicaMicrosystems, Wetzlar
Megafuge 1.0R	Hereaus, Hanau
Mikrotome RM2235	Leica, Nussloch
Neubauer counting chamber	Brand, Wertheim
Paraffine	Vogel Medizintechnik, Gießen

## Material

PDT-lamp	Medlight, Herford
pH-meter	WTW, Weilheim
Pipetboy acu	INTEGRA Biosciences GmbH, Bieberta
Pipettes	Gilson, Middleton, USA
Scale Denver Summit SI-2002	Denver Instruments, Göttingen
Sterile bench	Waldner, Wangen
SuperFrost Plus® glass slides	R. Langenbrinck GmbH, Emmendinge
Tubes (50/25/2/1.5 mL)	Sarstedt AG & Co. KG, Nümbrecht
Water bath	Memmert, Schwabach

## 2.7 Software

The software used to edit the data of this work is listed in table 8.

*Table 8: Software used*

<b>software</b>	<b>company</b>
GraphPad Prism 8.2.1	GraphPad Software, San Diego, US
Leica V3	LeicaMicrosystems, Wetzlar
Microsoft Office 365 2018	Microsoft, Redmond, USA



## 3 Methods

### 3.1 Ethical evaluation

Since human material is used in this experimental work, an approval by the ethics committee of the Medical Association of Saarland was required, which was granted to Prof. Dr. Sigrun Smola. Furthermore, the experimental work in this thesis has been performed under the ethical principles for medical research summarized in the declaration of Helsinki.

### 3.2 Sample collection

In cooperation with the institute of dermatology in Homburg, under the direction of Prof. Dr. Thomas Vogt, the paraffin blocks containing samples of patients diagnosed with actinic keratosis (22 samples) and vulvar intraepithelial lesions (18 samples) are generously provided by Dr. med. Cornelia S.L. Müller. The patients with vulvar intraepithelial lesions have been randomly selected in a period between the years 2008 and 2016, and patients with actinic keratosis between the years 2006 and 2017 respectively. In addition, the institute of dermatology provided information on the patients' date of birth, gender, and response to treatment with PDT.

### 3.3 Culturing of eukaryotic cells

Primary fibroblasts and HaCaT cells are incubated in a 175 cm<sup>2</sup> cell culture bottle with DMEM medium at 37°C and 5% CO<sub>2</sub>. As soon as the cells have reached confluency of 80-90%, the medium is removed, and the cells are washed with 10 ml PBS. Then 3 ml of Trypsin is added, and the cell culture bottle is placed back into the incubator until all cells have been detached. Trypsin is an enzyme which breaks down the connections of cells among each other and between the cells and the cell culture bottle. Whether all cells have been successfully detached can be verified under the microscope. Trypsin is neutralized with 7 ml medium, and the cell-trypsin-medium-suspension is filled into a 50 ml falcon for centrifugation (5 min, 1400 rpm, 25°C). The supernatant is discarded, and the cell pellet is resuspended in a 1 ml medium. After counting the cells in a Neubauer counting chamber with trypan blue, the required number of cells is seeded into the cell

culture bottle and again placed in the incubator. The medium is exchanged every second day.

### 3.4 Cell counting

For accurate cell number determination, the cells are counted with a Neubauer cell chamber system. Therefore, the cells are detached from the bottom of the cell culture bottle using trypsin as described before and then centrifuged for 5 minutes at 1400rpm. After that, the pellet is resuspended in 10 ml fresh medium. 10µl of this cell suspension is diluted with 10 µl of 0,5% trypan blue and again 10µl of this trypan blue-cell suspension is filled into the Neubauer counting chamber. The vital cells, appearing as white spots under the microscope, in all four quadrants are counted. The number of cells per ml can now be determined using the following formula:

$$cell\ number\ per\ ml = \frac{\text{Number of cell in all 4 quadrants}}{4} \times 2 \times 10^4$$

### 3.5 Production of 3D-Cultures

Generation of 3D cultures is based on a method described in Marthaler et al. (2017).

#### 3.5.1 Preparation of fibroblast-collagen-matrixes

First, the adherent growing fibroblasts are trypsinised from the cell culture bottle. After neutralising, the cell suspension is filled into a 50ml falcon and centrifuged for 5min at 25°C with 1400rpm. Subsequently, the supernatant is discarded, and the cell pellet is resuspended in 10 ml medium. The cells are counted as described above.  $5 \times 10^5$  cells per culture are necessary. The required number of cells are filled into a 50ml falcon and centrifuged (5min, 1400rpm, 25°C). After discarding the supernatant, the cell pellet is dissolved in 1ml of FCS.

For the collagen matrix, rat collagen and 10x DMEM are mixed on ice. The required quantity of rat collage and DMEM is listed in table 9.

## Methods

Table 9: Required quantity of components to produce 5 or 10 ml of collagen.

	<b>Rat collagen</b>	<b>DMEM</b>	<b>2M NaOH</b>	<b>fibroblasts</b>
5 ml collagen	3,95ml	0,55	500-550µl	10x 500000 cells in 0,5ml FCS
10 ml collagen	7,9 ml	1,1ml	1000µl	10x 500000 cells in 1ml FCS

The mixture is neutralized with 2M NaOH (500-550µl or 1000µl) until a change in colour from yellow to red becomes visible. The fibroblasts in FCS are added to the collagen, mixed and afterwards 1ml of this solution is pipetted into each well of a 24- well-plate. This working step should be carried out quickly as the neutralized collagen can already harden. The plate is placed in the incubator until the collagen became fully hardened. At that point, 1ml of cell medium (FAD medium) can be pipetted on top of the collagen-fibroblast matrixes. All working steps are performed under sterile conditions. The plate is placed into the incubator at 37°C and 5% CO<sub>2</sub> overnight.

### 3.5.2 Preparation of keratinocytes

The following day the adherent growing keratinocytes are trypsinised as described before. The cell suspension is filled into a 50ml falcon and centrifuged for 5min at 25°C with 1400rpm. After discarding the supernatant, the cell pellet is resuspended in 10 ml medium and counted. 700000 cells per 3D culture are centrifuged and dissolved in 1ml FAD medium per 700000 cells. After removing the medium on top of the collagen matrixes, 1ml of the keratinocytes dissolved in the FAD medium are pipetted on top of the collagen layer. The 24- well-plate is placed again in the incubator overnight.

### 3.5.3 Transfer of the 3D cell cultures onto the lattice work

The next day a sterile mesh platform is placed in each well of a 6-well-culture-plate and the wells are filled with FAD medium until the medium surface contacts the bottom side of the mesh. The medium under the latticework must be free from air bubbles as otherwise the 3D cultures might not be nourished sufficiently. Now the collagen matrixes with the keratinocytes on top are carefully lifted out of their wells with sterile forceps and placed in the centre on each latticework. All working steps are again performed under sterile conditions.

The 3D cultures are left growing in the incubator at 37°C and 5% CO<sub>2</sub>. How many days the cell cultures are in the incubator depends on the experiment planned. Keratinocytes transfected with siRNA and the corresponding control cultures without siRNA are left in the incubator for 4 days. As the effect of the transfected siRNA declines, gradually a shorter period for growth has been chosen. For the remaining experimental approaches, the 3D cultures are left growing for 6 days. Every second day the FAD medium under the latticework is exchanged.

The complete process of 3D cell culture production is illustrated schematically in figure 8.

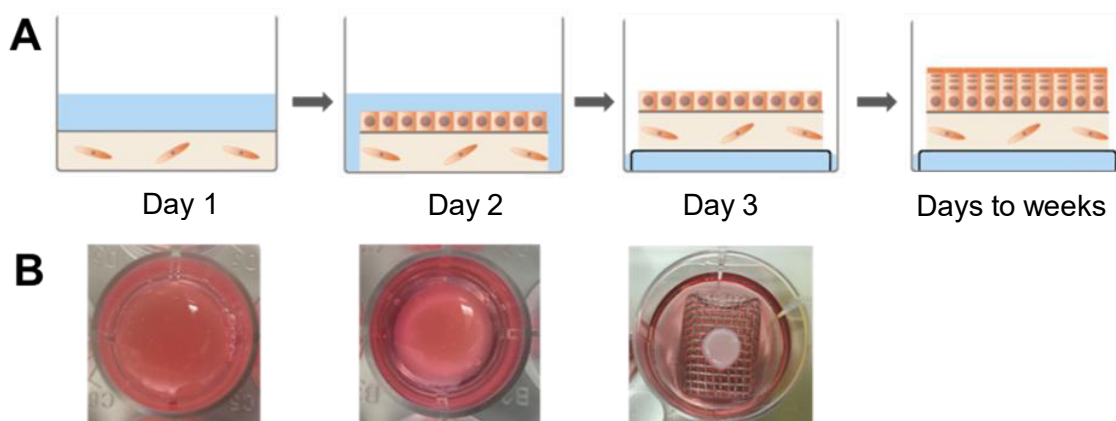


Figure 8: Schematic process of 3D cell culture production

**A:** On the first day, the fibroblasts are cultured in the collagen matrix for 24h with the medium. The next day keratinocytes are placed on top of the fibroblast-collagen matrix. On the third day, the whole cell culture is placed on a latticework and left there for several days for growing. **B:** The single working steps are illustrated as photographs (modified from Knerr-Rupp K., 2017)

## 3.6 Production of siRNA-transfected 3D cultures

### 3.6.1 Seeding

First, the adherent growing keratinocytes (HaCaTs) are detached from the cell culture bottle using trypsin as described before. 400000 cells per well are counted in the Neubauer counting chamber (see above) and seeded in wells of a 6-well- plate with the cell culture growth medium. Per approach (non-coding siRNA, siRIPK3, non-transfected control) two wells are seeded. The cells are incubated at 37°C and 5% CO<sub>2</sub> overnight.

### 3.6.2 Transfection

For transfection, a siRNA approach per well is prepared. The ingredients for the transfection of keratinocytes with siRNA with non-coding siRNA and the siRIPK3 are listed in table 10.

siRNAs are effectively delivered into the cell where the target gene can be knocked down using Lipofectamine RNAiMAX Reagent. In addition, a non-coding siRNA is used which is not addressing any gene in particular. Therefore, it serves as a control approach, examining whether the siRNA itself has any effect on the cell cultures. Furthermore, an approach without any siRNA added is used.

*Table 10: Ingredients for siRNA transfection of keratinocytes with non-coding siRNA or siRIPK3*

	<b>Non-coding siRNA</b>	<b>siRIPK3</b>
siRNA-mix	3µl non-coding-siRNA+250µl OptiMEM	3µl siRNA +250µl OptiMEM
LipoRNAiMax-mix	5 µl LipoRNAiMAX + 250µl OptiMEM	5 µl LipoRNAiMAX + 250µl OptiMEM

The siRNA-mix is added to the LipoRNAiMAX-mix and incubated at room temperature for 10 minutes. Meanwhile, the keratinocytes incubated overnight in the 6-well plate can be washed 3 times with 1xPBS. Afterwards, 1,5 ml of culturing medium is added. After 10 minutes of incubation, 500 µl of the LipoRNAiMAX -siRNA-mix can be added to each well. The plate can be placed back into the incubator for the next 24h.

### 3.6.3 Production of 3D cultures

The following day the keratinocytes are harvested and the same approaches (keratinocytes transfected with non-coding siRNA, transfected with RIPK3-siRNA and without siRNA-transfection) are pooled together. The cells are counted and 700000 transfected keratinocytes per well are seeded on top of the collagen-fibroblast matrix. The collagen matrixes are then incubated for another 24h at 37°C at 5% CO<sub>2</sub>.

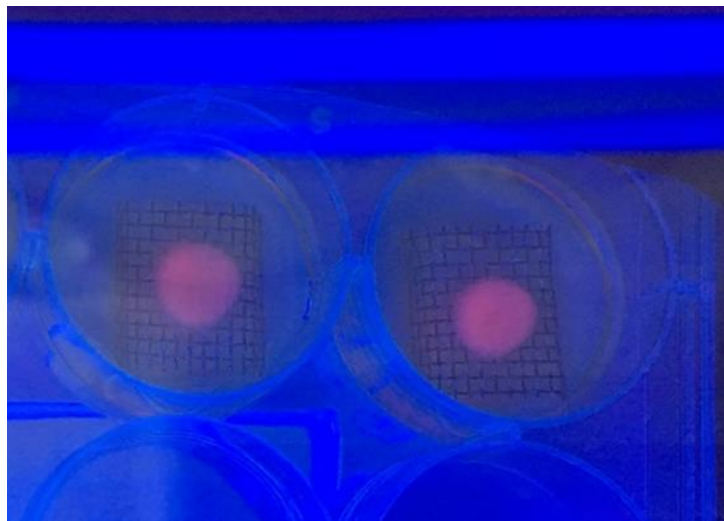
### 3.6.4 Transfer of the 3D-cell cultures onto the latticework

The next day the collagen matrixes are placed carefully on top of the sterile latticework in a 6-well-culture-plate with FAD medium as described before. All working steps are again performed under sterile conditions.

The 3D cultures are left growing in the incubator at 37°C and 5% CO<sub>2</sub> for 4 days as the siRNA is no longer stable and active, respectively. Every second day the FAD medium under the mesh platform is exchanged.

### 3.7 Photodynamic radiation of 3D-cultures

7 days later, 3D-cultures are treated with 4% aminolaevulinic acid (ALA). 200 µl ALA, dissolved in FAD medium, is pipetted on top of the 3D culture. After 4 hours incubation at 37°C, the absorption of ALA into the cells is checked under a black light lamp as illustrated in figure 9. Next, the 6-well-culture-plate with the 3D cultures is placed under the PDT-lamp at a 10 cm distance and radiated for 9 min with a red light of a wavelength of 630 nm. Generously, Mrs Claudia Schiekofer from the institute of dermatology provided the PDT-Lamp located in the operating room of the institute. The control 3D cultures are only incubated with ALA but not radiated. Afterwards, the medium under the cultures is exchanged and the plates are once again placed in the incubator.



*Figure 9: Absorption-check with the black-light-lamp*

When ALA is absorbed into the cells the 3D-culture fluoresced under the black-light lamp

### 3.8 Fixation and embedding

After 24 hours (2, 3, 4, 5, 6 days) the medium under the cultures is replaced by 4% paraformaldehyde-solution for fixation and the plate is left for 24 hours at 4°C. The next day, the cultures are fully covered in paraformaldehyde and incubated at 4°C. 24 hours later, the 3D cultures are carefully removed from the mesh platform with forceps and

placed in plastic embedding capsules which are then positioned in a fully automatic embedding machine. The machine conserved, dehydrated and embedded the 3D cultures in paraffin. These steps are performed at the institute of dermatology (thanks to Anne Kerber and Dr. med. Cornelia S. L. Müller). After the embedding, the cultures are placed into a metal mould, poured with hot paraffine (65°C) and covered with the lid of the embedding capsule. The metal form is now placed on a cooling plate for hardening the paraffin. Finally, the metal form is removed and the paraffin block is ready for cutting.

### 3.9 Production of paraffin sections

The paraffin blocks are placed on a - 5°C cold plate. Sections of 6 µm are made with a microtome. For unfolding, the sections are put into a 37°C warm water bath placed on microscope slides.

### 3.10 Immunohistochemical staining

Paraffin is removed by three-times incubation in Xylol for 10 minutes followed by a rehydration in descending alcohol series (99%, 90%, 80%, 70%, 50%) for 2 minutes each. After washing for 5 minutes in distilled water, the slides are placed in a microwaveable cuvette and boiled in citrate buffer in the microwave for 10 Minutes for antigen demasking. Therefore, the slides inside the cuvette with citrate buffer are heated until the citrate buffer begins to boil. Then the microwave is paused for a short cool down. The procedure is repeated for 10 minutes in total. Afterwards, slides are cooled down to room temperature and then covered with 3% H<sub>2</sub>O<sub>2</sub> in TBS for 15 minutes in the dark at room temperature to deactivate the endogen peroxidase. After that, the slides are washed again in 1x TBS buffer and incubated for 30 minutes with 2.5% normal horse serum in a humidified chamber at room temperature. After removing the excess serum, the primary antibody is applied, and the slides are incubated overnight in the humidified chamber at 4°C.

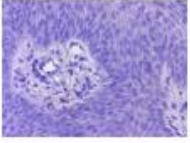
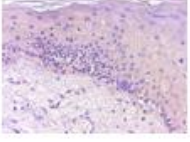
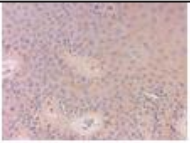

The next day the slides are washed in TBS buffer for 5 minutes and then incubated with the secondary antibody at room temperature in the humidified chamber for 30 minutes. After washing again two times for 5 minutes in TBS the peroxidase substrate is applied, and the slides are left for 1 minute in the dark. Afterwards, the reaction is stopped by washing the slides in distilled water for 2 minutes. The staining is counterstained with haematoxylin and blued under flowing water subsequently. Next, the slides are

dehydrated in ascending alcohol series (50%, 70%, 80%, 90%, 99%) for 2 minutes each and placed into xylol bevor covering with a coverslip.

### 3.11 Evaluation of immunohistochemical staining intensity

The pictures of three independent experiments are evaluated. The image sections analysed are selected as a representative part of the total picture. The immunohistochemical staining is evaluated regarding the staining intensity and the number of stained nuclei. The evaluation has been performed according to the immunoreactive score (IRS) by Remmele and Stegner. Table 11 shows the evaluation of immunohistochemical staining exemplary for RIPK3 staining of different actinic keratosis lesions. Staining intensity of “1= None” implies an IRS total of 0, “2= weak” an IRS total of 1, staining intensity of “3 = moderate” an IRS sum of 2-4 and staining intensity of “4 = strong” an IRS sum of 4-6. The maximum sum reached has been 6.

*Table 11: Evaluation of immunohistochemical staining shown for RIPK3 staining of actinic keratosis lesions*

Staining intensity	Pictorial example
1=None	
2=Weak	
3=Moderate	
4=strong	

### 3.12 Treatment response to photodynamic therapy

Along with the patient samples, information regarding the response of these patients to the PDT were provided by Dr. med. Cornelia S. L. Müller. The treatment outcome is categorized into four groups (excellent, good, moderate, bad). The therapy response is



determined solely clinically by considering the local skin reaction, inflammatory response, and reduction of the lesion after PDT at the side of irradiation with PDT. In terms of better lucidity, the four categories are summarized into 2 groups, a good and a bad response (table 12).

Table 12: Treatment response groups of patients with actinic keratosis to PDT

Original treatment response groups	Summarized treatment response groups
excellent	good=1
good	
moderate	poor=2
poor	

### 3.13 Testing of patient samples for HPV

The testing of the patients' samples for the presence of HPV was kindly performed by Mrs Barbara Best, Smola lab, using PCR (Bernhard, et al. 2021).

### 3.14 Statistical analysis

The statistical analysis was conducted using GraphPad Prism 8.0. Unpaired t-tests were employed to determine the statistical differences between two groups. The level of significance ( $\alpha$ ) was set at 0.05% for all conducted tests. P-values exceeding 0.05 were deemed insignificant.

To assess the correlation between the staining intensity of RIPK3 and the grade of VIN (VIN I- VINIII), an ordinary one-way ANOVA test was employed. Adjusted p-values were obtained using a post-hoc t-test, specifically Tukey's multiple comparison test, which was applied to all combinations.

For the analysis of the correlation between two or more variables (e.g.,  $\gamma$ -H2XA-positive nuclei/time (day 1 to day 6); ki67-positive nuclei/time (day 1 to day 6); Transduction (HPV8 E6, pLXSN)/treatment (Control, PDT)/ $\gamma$ -H2XA-positive nuclei; Transduction (HPV8 E6, pLXSN)/treatment (Control, PDT)/ki67-positive nuclei; siRNA (siRIPK3, non-coding siRNA, no siRNA)/treatment (Control, PDT)/ $\gamma$ -H2XA-positive nuclei; siRNA

(siRIPK3, non-coding siRNA, no siRNA)/treatment (Control, PDT)/ki67-positive nuclei), a two-way ANOVA test was performed. Once again, adjusted p-values were calculated using a post-hoc t-test, specifically Tukey's multiple comparison test, which was applied to all combinations.

The error bars in the graphs represent the standard deviation.

## 4 Results

### 4.1 RIPK3 expression varies in lesions of actinic keratosis and is correlated to PDT response

Samples from 22 patients with actinic keratosis were subjected to RIPK3 staining. Table 14 shows the notable variations in staining intensity observed among the individual samples. For instance, patient C exhibited higher RIPK3 expression compared to patient A, where minimal expression was detected. Positive staining for RIPK3 was primarily observed in the cytosol of keratinocytes across all samples. The staining was evenly distributed throughout the epidermis, with limited expression in the dermis. However, occasional stained nuclei were observed (patient D). These nuclei were predominantly located in the basal and suprabasal layers of the epidermis, while the upper layers exhibited cytosol staining. The frequency distribution of each staining pattern out of 22 samples is listed in table 13.

*Table 13: Frequency distribution of RIPK3 staining patterns in actinic keratosis samples*

Total number of each staining pattern (1-4) for RIPK3 out of a sample collection of 22 samples of patients with actinic keratosis.

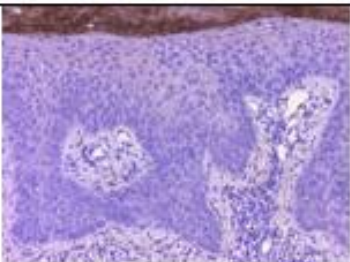
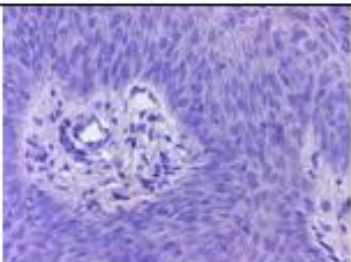
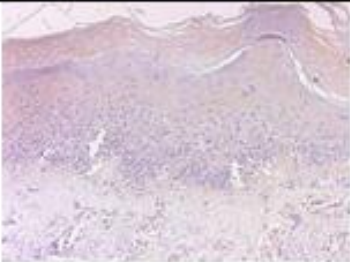
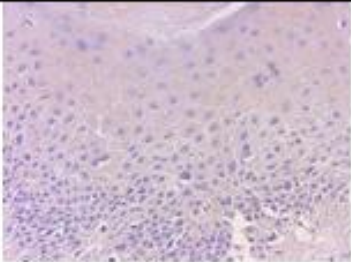
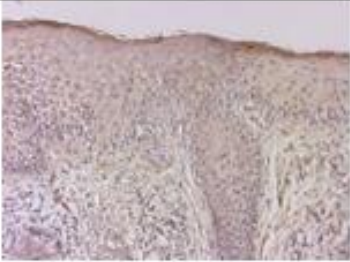
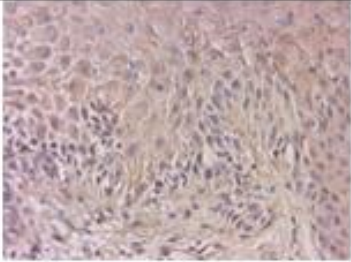
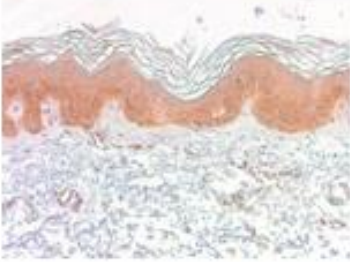
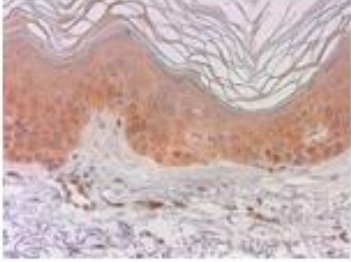
Staining intensity	Frequency distribution
1	1
2	7
3	7
4	7

The staining intensity was determined using the scoring system described before (chapter 3.11). Four representative examples are illustrated below (table 14).

## Results

*Table 14: Immunohistochemical RIPK3 staining of actinic keratosis lesions*

Samples of 22 patients were stained for the presence of RIPK3. Below, four representative histological sections from different patients with distinct staining patterns are presented. The tissue sections are depicted at magnifications of 10-fold and 20-fold.

Patient	Staining intensity	Actinic keratosis lesion Magnification: 10x	Actinic keratosis lesion Magnification: 20x
A	1		
B	2		
C	3		
D	4		

There were significant differences observed in the expression of RIPK3 among actinic keratosis lesions in this patient group. Further analysis was conducted to determine whether age or gender had any influence on the expression of RIPK3. Since actinic keratosis is more common in the elderly, the patient cohort was divided into two groups based on the age of 75 as the dividing point. Age group "1" consisted of patients younger than 75 years (n=10), while age group "2" included patients aged 75 years or older (n=12). No significant difference has been found between the two age groups ( $p=0.4377$ ) (figure 10a). Additionally, figure 10b demonstrates the correlation between the patient's

sex and the staining intensity of RIPK3 as detected by immunohistochemical staining. Once again, no significant difference was observed between the two genders. However, the majority of the analysed samples were obtained from male patients (n=15), while only 7 patients were female. All patients included in the study received photodynamic therapy at the clinic of dermatology. Figure 10c illustrates the correlation between the expression of RIPK3 in actinic keratosis samples and the treatment outcome. Patients with a poor treatment response exhibited significantly lower average levels of RIPK3, whereas those who responded well to photodynamic therapy showed higher expression of the protein (p=0.0108). Subsequently, the question was raised whether the response to PDT was dependent on the patient's age or sex. Figures 10d and 10e demonstrate that there was no correlation between the response to PDT and these parameters.

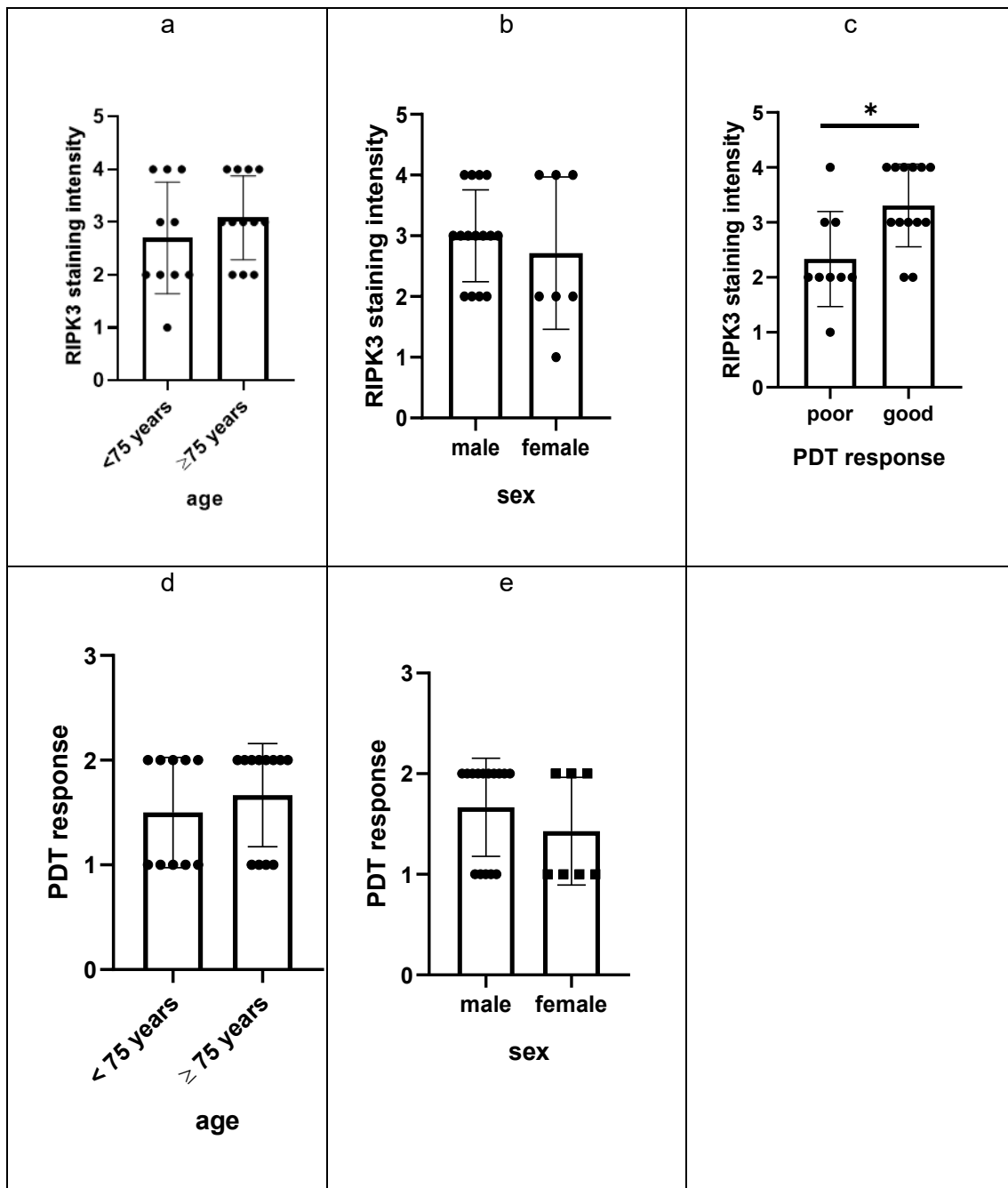


Figure 10: Correlation between RIPK3 staining intensity and PDT response to patients' age and sex

a: Correlation between RIPK3-staining intensity in actinic keratosis lesions and age of patients. Staining intensity: 1=none, 2=weak, 3=moderate, 4=strong,  $p=0.3433$ ;  $t=0.9706$ ,  $df=20$  (unpaired t-test). b: Correlation between RIPK3-staining intensity in actinic keratosis lesions and the patient's sex. Staining intensity: 1=none, 2=weak, 3=moderate, 4 =strong;  $p=0.5114$ ,  $t=0.6687$ ,  $df=20$  (unpaired t-test). c: Correlation between therapy response to PDT and RIPK3-staining. Staining intensity:1=none, 2=weak, 3=moderate, 4=strong;  $p=0.0108$ ,  $t=2.812$ ,  $df=20$  (unpaired t-test). d: Correlation between the age of patients with actinic keratosis lesions and their therapy response to PDT treatment. PDT response: 1=poor, 2=good;  $p=0.4527$ ,  $t=0.7658$ ,  $df=20$  (unpaired t-test). e: Correlation between the sex of patients with actinic

keratosis lesions and their therapy response to PDT treatment. PDT response: 1=poor, 2=good;  $p=0.3128$ ,  $t=1.035$ ,  $df=20$  (unpaired t-test). Error bars depict standard deviation.

## 4.2 Immunohistochemical RIPK3-staining of 3D cultures

### 4.2.1 RIPK3 expression *in vitro* does not change under PDT


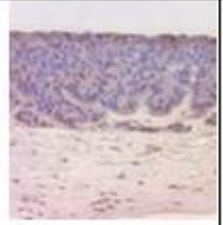
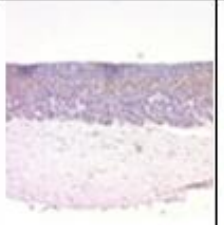
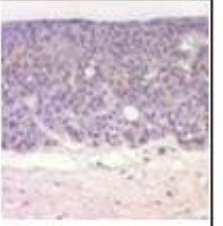

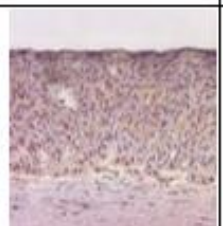

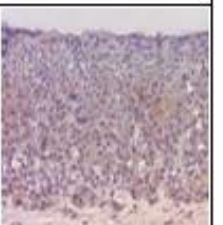
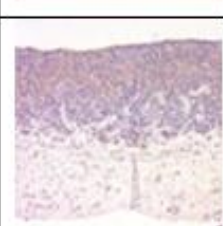
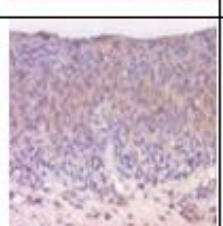

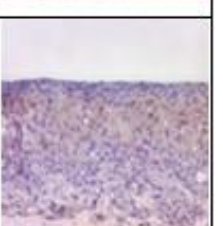
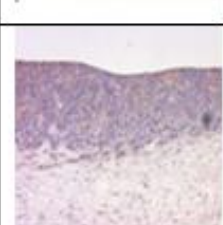
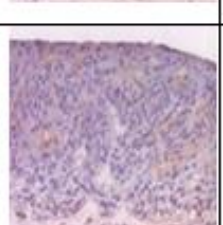

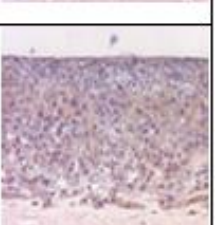
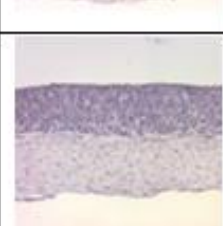
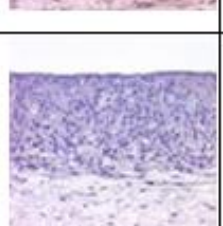

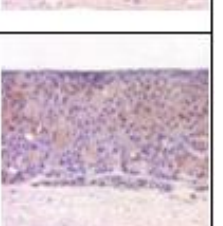
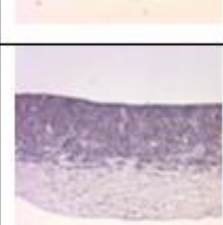
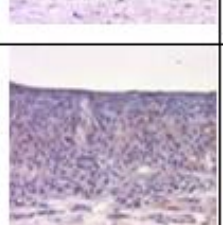
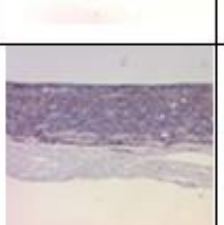
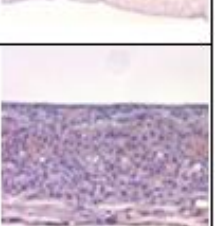
The expression profiles of RIPK3 showed significant variations among patients with actinic keratosis and vulvar intraepithelial neoplasia. Moreover, the presence of RIPK3 appeared to be correlated with the clinical outcome when actinic keratosis was treated with PDT. Hence, it was of interest to investigate the changes in RIPK3 expression *in vitro* upon the application of PDT.

HaCaT 3D cultures were treated with ALA and subsequently exposed to red light using the PDT-lamp, while control cultures were not radiated. At 1, 2, 3, 4, 5, and 6 days after treatment, the cultures were fixed, embedded and subjected to immunohistochemical staining to detect the presence of RIPK3 (table 15).

## Results

*Table 15: Immunohistochemical RIPK3 staining of 3D cultures*

HaCaT 3D cultures were treated with ALA and afterwards either radiated with red light under the PDT-lamp or not (control cultures). After 1, 2, 3, 4, 5, and 6 days the cultures were fixed and immunohistochemically stained for the presence of RIPK3. (n=2). The tissue sections are depicted at magnifications of 10-fold and 20-fold.

Time until fixation after treatment	Control: Not-PDT- treated 3D cell cultures		PDT- treated 3D cell cultures	
	Magnification: 10x	Magnification: 20x	Magnification: 10x	Magnification: 20x
1 d				
2 d				
3 d				
4 d				
5 d				
6 d				



Examining the expression profiles of RIPK3 in the 3D cell culture model, no apparent staining patterns could be observed. The level of RIPK3 expression appeared to be similar in the 3D cultures treated under the PDT lamp and the control cultures. However, in the PDT-treated cultures, RIPK3 expression was minimal or absent in the superficial layer, while it was clearly detectable in the intermediate and basal layers. In the control cultures, RIPK3 expression seemed to be evenly distributed throughout the cultures. There were no significant changes in RIPK3 expression over time.

### 4.2.2 HPV8 E6 alters RPK3 expression in 3D cultures

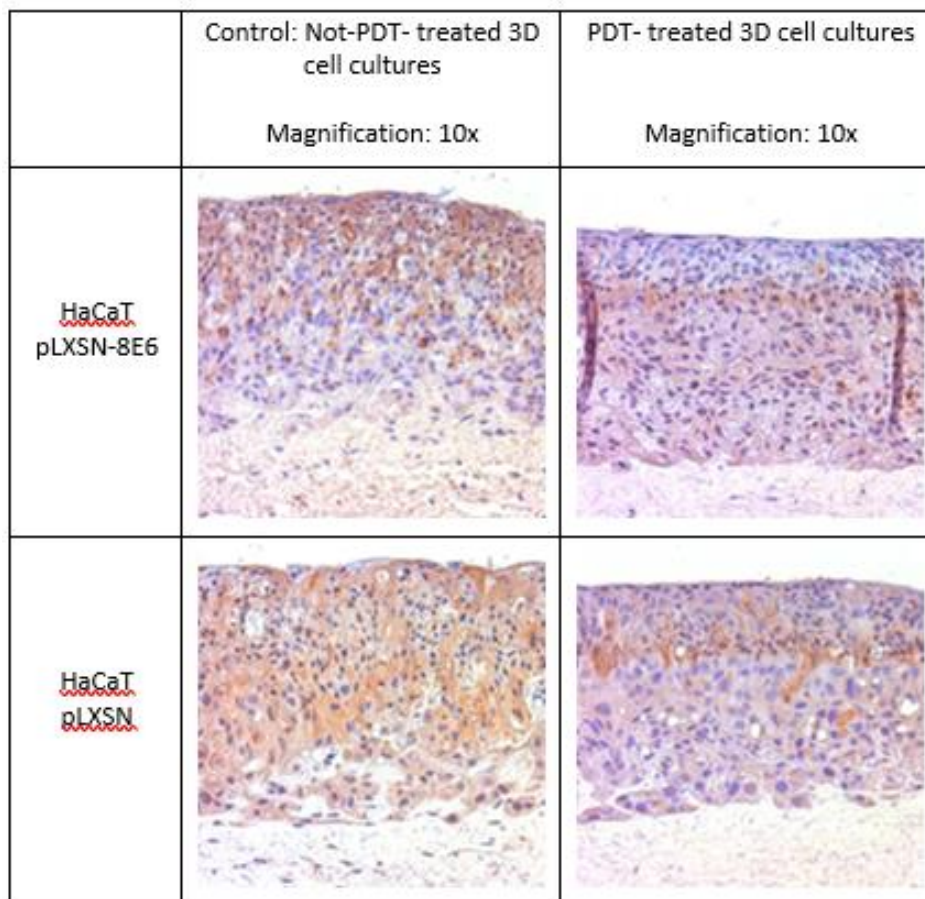
As mentioned in the introduction, cutaneous HPVs, such as HPV8, appear to play a critical role in the initiation of tumorigenesis, specifically in squamous skin cancer. These HPVs facilitate cell proliferation and unrestricted cell growth through interactions with various proteins. Some of these interactions indirectly modulate p53 signalling, impact the host immune system, or influence the cellular microenvironment. Notably, the key player in necroptosis induction, RIPK3, has been previously shown to exhibit expression differences (as discussed in Chapter 4.1) *in vivo* among patients with actinic keratosis, an HPV-associated precancerous lesion in the development of skin cancer. Interestingly, the intensity of RIPK3 staining was found to be correlated with the therapeutic outcome following photodynamic therapy (PDT) in these patients (see figure 10c). Consequently, it was of interest to investigate the potential impact of HPV8 on RIPK3 expression in transduced and PDT-treated cells in an *in vitro* 3D-cell culture model.

3D cultures were generated, consisting of a fibroblast-collagen matrix and keratinocytes transduced with an HPV8 E6-encoding vector or the empty vector pLXSN. The cultures were treated with ALA and subsequently exposed to red light using the PDT lamp (control cultures were only incubated with ALA but not exposed to light). 1, 2, 3, 4, 5, and 6 days after treatment the cell cultures were fixed, embedded and subjected to immunohistochemical staining to detect the presence of RIPK3 (table 16).

## Results

*Table 16: Immunohistochemical RIPK3 staining of 3D cultures transduced with HPV 8E6 and pLXSN*

HaCaT 3D cultures were transduced with HPV8 E6 or pLXSN by retroviral gene transfer. The cell cultures were treated with ALA and afterwards either radiated with red light under the PDT-lamp or not (control cultures). After 1, 2, 3, 4, 5, and 6 days the cultures were fixed and immunohistochemically stained for the presence of RIPK3. (n=2). The tissue sections are depicted at magnifications of 10-fold.



Notably, the expression of RIPK3 exhibited a significant increase in the control cultures as compared to the cell cultures treated under the PDT lamp. This trend was consistent in both the HPV 8E6-transduced and pLXSN-transduced cells. In the pLXSN-transduced control culture, RIPK3 expression was distributed throughout the entire culture, while in the HPV 8E6-transduced control culture, RIPK3 expression was limited to the upper and central layers, sparing the lower and basal layers. HPV 8E6 seemed to suppress RIPK3 in the basal and suprabasal layers while upper layers were not affected.

In the cell cultures subjected to PDT treatment, RIPK3 expression was predominantly observed in the central and lower layers. Conversely, the upper layer of the HPV 8E6-transduced cultures exhibited minimal RIPK3 expression. However, both the HPV 8E6-transduced cultures and the pLXSN-transduced cultures displayed reduced intensity of RIPK3 staining in the upper layer directly exposed to PDT, in comparison to the control cultures.

### 4.3 Impact of PDT on cell damage and proliferation

PDT represents a widely employed therapeutic approach for managing precancerous conditions such as actinic keratosis. *In vivo* investigations have provided evidence regarding the association between RIPK3 expression and the response to PDT (Chapter 4.1). Correspondingly, *in vitro* experiments employing the 3D cell culture model have also demonstrated variations in the RIPK3 expression profiles between the control group and the cell cultures subjected to PDT illumination (Table 16). Nevertheless, it remained pertinent to further examine the effects of PDT on cellular systems. In this research, two immunohistochemical markers, namely  $\gamma$ -H2AX and Ki67, were employed to evaluate cell damage and proliferation, respectively.

#### 4.3.1 Double strand breaks occur especially in superficial cell layers after PDT

HaCaT 3D cultures were subjected to ALA treatment followed by exposure to red light using the PDT lamp (control cultures were only treated with ALA and not exposed to light). After 1, 2, 3, 4, 5, and 6 days, the cultures were fixed, embedded and subjected to immunohistochemical staining to detect the presence of  $\gamma$ -H2AX. The cultures treated under the PDT lamp displayed intense staining of  $\gamma$ -H2AX, irrespective of the time until fixation.  $\gamma$ -H2AX-staining was particularly intense in the superficial layers of cultures directly exposed to PDT radiation. Conversely, the control cultures exhibited very low or negligible expression of  $\gamma$ -H2AX. Some sporadic staining was observed throughout the control culture with a minimal increase over time (table 17).

## Results

*Table 17: Immunohistochemical  $\gamma$ -H2AX staining of 3D cultures over time*

HaCaT 3D cultures were treated with ALA and afterwards either radiated with red light under the PDT-lamp or not (control cultures). After 1, 2, 3, 4, 5, and 6 days the cultures were fixed and immunohistochemically stained for the presence of  $\gamma$ -H2AX. (n=3). The tissue sections are depicted at magnifications of 10-fold and 20-fold.

Time until fixation after treatment	Control: Not-PDT- treated 3D cell cultures		PDT- treated 3D cell cultures	
	Magnification: 10x	Magnification: 20x	Magnification: 10x	Magnification: 20x
1 d				
2 d				
3 d				
4 d				
5 d				
6 d				

The nuclei exhibiting positive staining for  $\gamma$ -H2AX were quantified in each culture at various time points and depicted graphically in figure 11. Initially, the results demonstrated a significantly higher number of  $\gamma$ -H2AX-positive nuclei in the PDT group compared to the control cultures ( $p=0.0082$ ), regardless of the time. Across all time points, the number of  $\gamma$ -H2AX-positive nuclei was consistently greater in the cell cultures exposed to PDT compared to the control cultures that were not subjected to PDT treatment. However, a further analysis of the temporal sequence revealed fluctuations in the expression of  $\gamma$ -H2AX within the 3D cultures. For instance, when comparing the number of  $\gamma$ -H2AX-positive nuclei in the cultures fixed one day after treatment (PDT or Control) with those fixed six days later, an increase in the count was observed after six days. Thus, on average, 25 nuclei exhibited positive staining after one day after PDT treatment compared to only six positive nuclei in the control culture. However, after six days of PDT treatment, 33 detectable nuclei were observed on average after PDT, while the control culture exhibited only 17 positive nuclei. Nevertheless, the differences between the PDT and Control cultures at each time point were not statistically significant ( $p>0.05$ ).

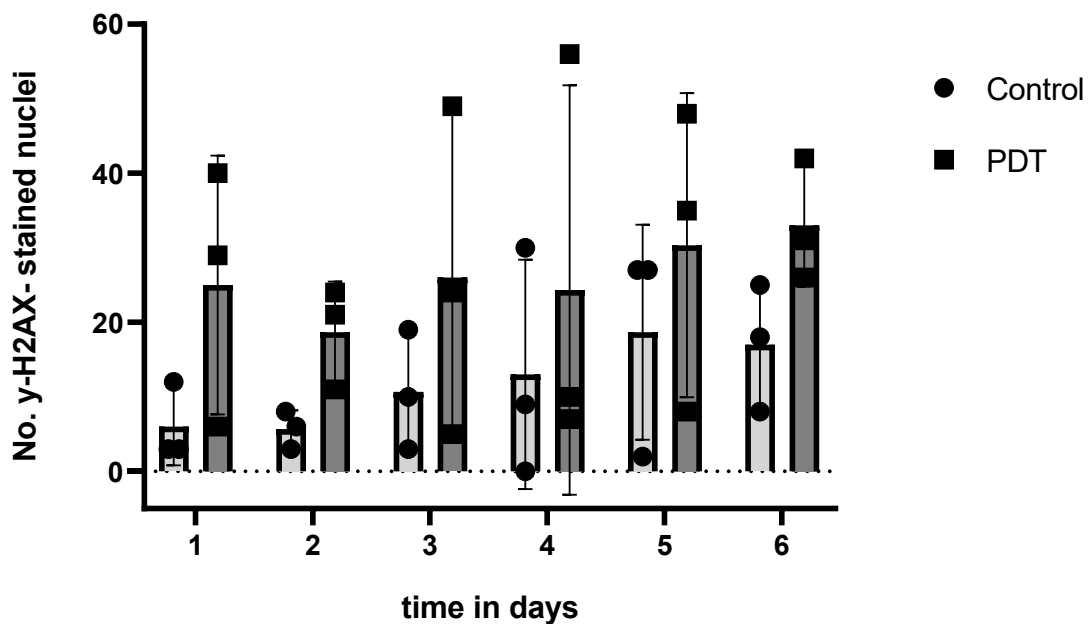


Figure 11:  $\gamma$ -H2AX-positive stained nuclei in PDT- and control cell cultures over time

HaCaT 3D cultures were treated with ALA and afterwards either radiated with red light under the PDT-lamp or not (control cultures). After 1, 2, 3, 4, 5, and 6 days the cultures were fixed and immunohistochemically stained for the presence of  $\gamma$ -H2AX. The number of  $\gamma$ -H2AX-positive nuclei in PDT-treated and control cultures from three independent replicates is illustrated over time. Error bars depict standard deviation ( $n=3$ ; time (day 1-6):  $p=0.6474$ ;  $F=0.6736$ ;  $DFn=5$ ;  $DFd=24$ ; Treatment (Control vs. PDT):  $p=0.0082$ ;  $F=8.319$ ;  $DFn=1$ ;  $DFd=24$ ; Interaction (time vs. treatment):  $p=0.9975$ ;  $F=0.05816$ ;  $DFn=5$ ;  $DFd=24$  (ordinary two-way

## Results

ANOVA). Adjusted p-values: day 1-Control vs- day 1-PDT:  $p=0.9090$ ; day 2-Control vs. day 2-PDT:  $p=0.9937$ ; day 3-Control vs. day 3-PDT:  $p=0.9776$ ; day 4-Control vs. day 4-PDT:  $p=0.9980$ ; day 5-Control vs. day 5-PDT:  $p=0.9974$ ; day 6-Control vs. day 6-PDT:  $p=0.9697$ ; day 1-Control vs. day 2-Control:  $p=>0.9999$ ; day 1-Control vs. day 3-Control:  $p=>0.9999$ ; day 1-Control vs. day 4-Control:  $p=>0.9999$ ; day 1-Control vs. day 5- Control:  $p=0.9949$ ; day 1-Control vs. day 6-Control:  $p=0.9985$ ; day 2-Control vs. day 3-Control:  $p=>0.9999$ ; day 2-Control vs. day 4-Control:  $p=>0.9999$ ; day 2-Control vs. day 5-Control:  $p=>0.9999$ ; day 2-Control vs. day 6-Control:  $p=>0.9999$ ; day 3-Control vs. day 4-Control: $p=>0.9999$ ; day 3-Control vs. day 5-Control:  $p=>0.9999$ ; day 3-Control vs. day 6-Control:  $p=>0.9999$ ; day 4-Control vs. day 5-Control: $p=>0.9999$ ; day 4-Control vs. day 6-Control:  $p=>0.9999$ ; day 5-Control vs. day 6-Control:  $p=>0.9999$ ; day 1-PDT vs. day 2-PDT:  $p=>0.9999$ ; day 1-PDT vs. day 3-PDT:  $p=>0.9999$ ; day 1-PDT vs. day 4-PDT:  $p=>0.9999$ ; day 1-PDT vs. day 5-PDT:  $p=>0.9999$ ; day 1-PDT vs. day 6-PDT:  $p=>0.9999$ ; day 2-PDT vs. day 3-PDT: $p=>0.9999$ ; day 2-PDT vs. day 4-PDT:  $p=>0.9999$ ; day 2-PDt vs. day 5-PDT:  $p=0.9974$ ; day 2-PDt vs. day 6-PDT:  $p=0.9864$ ; day 3-PDT vs. day 4-PDT:  $p=>0.9999$ ; day 3-PDT vs. day 5-PDT: $p=>0.9999$ ; day 3-PDT vs. day 6-PDT:  $p=>0.9999$ ; day 4-PDT vs. day 5-PDT:  $p=>0.9999$ ; day 4-PDT vs. day 6-PDT:  $p=0.9998$ ; day 5-PDT vs. day 6-PDT: $p=>0.9999$ ; remaining post-hoc tests not reported (Tukey's multiple comparison test)).

Interestingly, in cell cultures exposed to radiation under the PDT lamp, the expression of  $\gamma$ -H2AX was notably intense in the superficial layers of the cell culture. There appeared to be a distinct belt-like pattern of intense staining, spanning approximately the same width throughout the superficial third of the culture. This phenomenon is schematically depicted in figure 12 for better visualization and understanding.

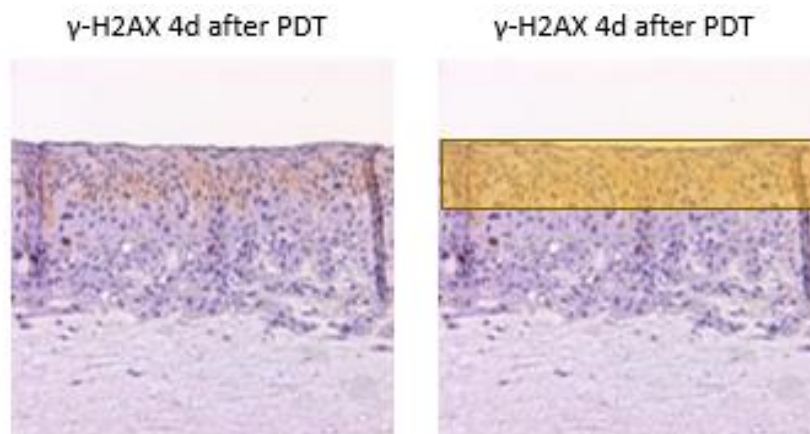


Figure 12: Schematic illustration of the  $\gamma$ -H2AX staining profile in PDT-treated cultures

In 3D cell cultures exposed to radiation under the PDT lamp, the expression of  $\gamma$ -H2AX is notably intense in the superficial layer of the cell culture. The amber bar in the right picture demonstrates the high expression of  $\gamma$ -H2AX in the upper layer of the cell cultures.

Notably, there were noticeable variations in epithelial growth among the different cultures during the incubation period. It appeared that certain conditions directly influence the proliferation of cells within the cultures. To investigate these effects more comprehensively, the proliferation marker Ki67 was stained and analyzed.

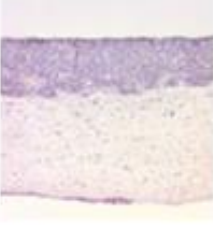
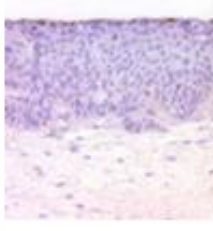
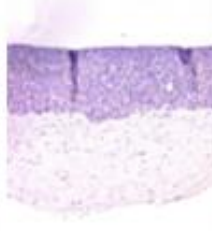
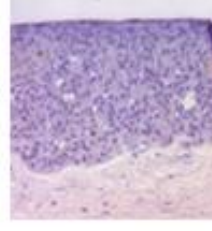
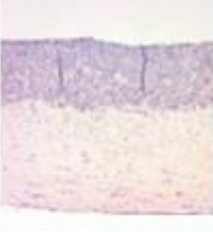
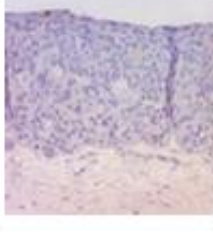

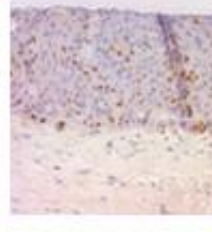
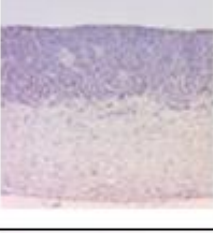
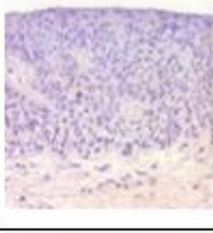
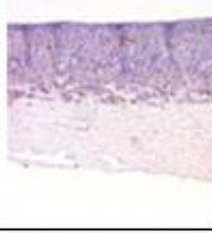
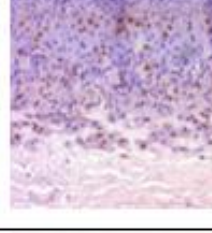

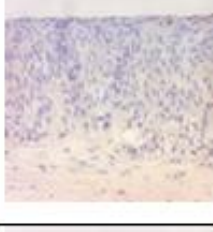

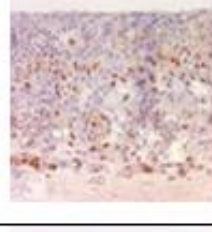
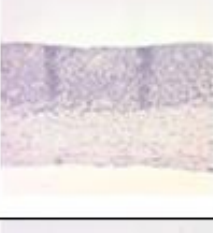
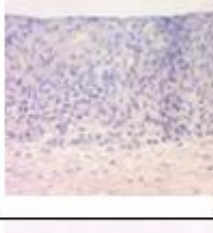
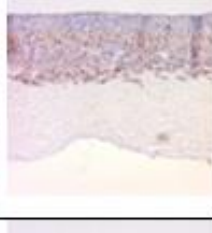
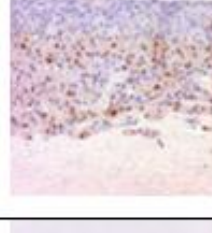
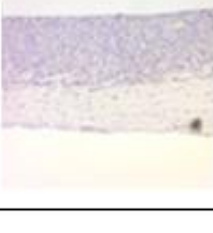
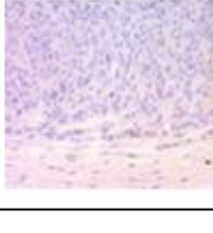
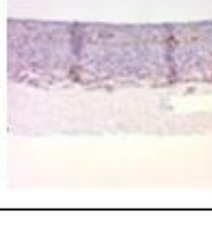
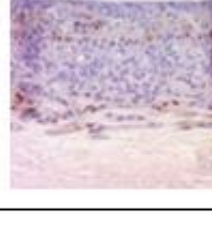
### 4.3.2 PDT leads to higher Ki67 expression in 3D cell cultures

HaCaT 3D cultures were subjected to ALA treatment and subsequently exposed to red light under the PDT lamp, while control cultures were not exposed to light. After 1, 2, 3, 4, 5, and 6 days, the cultures were fixed, embedded and subjected to immunohistochemical staining to detect the presence of Ki67. In the control cultures, there was minimal or no detectable expression of Ki67. However, in the PDT-treated cultures, Ki67 expression was much higher, particularly in the middle and lower layers of the culture. Conversely, the upper layers of the culture exhibited negligible expression of Ki67 (table 18).

## Results

*Table 18: Immunohistochemical Ki67 staining of 3D cultures over time*

HaCaT 3D cultures were treated with ALA and afterwards either radiated with red light under the PDT-lamp or not (control cultures). After 1, 2, 3, 4, 5, and 6 days the cultures were fixed and immunohistochemically stained for the presence of Ki67. (n=3). The tissue sections are depicted at magnifications of 10-fold and 20-fold.

Time until fixation after Treatment	Control: Not-PDT- treated 3D cell cultures		PDT- treated 3D cell cultures	
	Magnification: 10x	Magnification: 20x	Magnification: 10x	Magnification: 20x
1 d				
2 d				
3 d				
4 d				
5 d				
6 d				



Ki67 staining was markedly more prominent in the cell cultures subjected to PDT treatment compared to the untreated control cultures. This phenomenon was consistently observed across all time points, except for day one where minimal or no Ki67 staining could be detected in both the PDT and control approaches. In the control cultures, regardless of the time until fixation, Ki67 staining was minimal or absent. However, in the cell cultures exposed to PDT, Ki67 staining was observed primarily in the cell nuclei located in the basal and suprabasal cell layers, while the superficial layers exhibited less staining. This pattern was consistently observed at all time points, excluding day one as previously described.

For the quantitative analysis, the number of Ki67-positive stained nuclei was counted in each cell culture approach at each time point (figure 13). The analysis revealed a significant difference ( $p=0.0050$ ) in the number of stained nuclei between the PDT group and the control group, irrespective of the time. Across all time points the number of Ki67-positive nuclei was consistently higher in the cell cultures exposed to PDT compared to the control cultures. For instance, three days after PDT treatment, an average of 36 nuclei were stained Ki67-positive, whereas only six nuclei, on average, exhibited staining in the untreated control culture.

However, further analysis of the temporal sequence revealed minimal fluctuations in the expression of Ki67 within the 3D culture approaches. For example, when comparing the number of Ki67-positive nuclei in the cultures fixed two days after treatment with those fixed five days later, no increase in the count was observed after five days. Thus, on average, 34 nuclei exhibited positive staining two days after PDT treatment compared to 32 positive nuclei after five days. Consequently, the differences between the PDT and Control cultures at each time point were not statistically significant ( $p>0.05$ ).

## Results

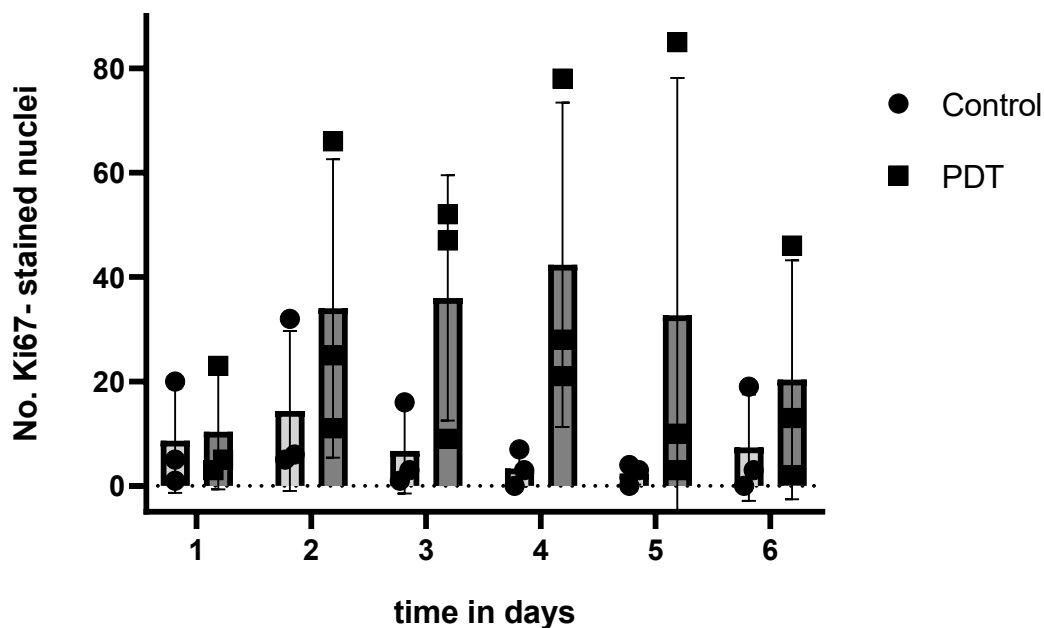


Figure 13: Ki67-positive stained nuclei in PDT- and control cell cultures over time

HaCaT 3D cultures were treated with ALA and afterwards either radiated with red light under the PDT-lamp or not (control cultures). After 1, 2, 3, 4, 5, and 6 days the cultures were fixed and immunohistochemically stained for the presence of Ki67. The number of Ki67- positive nuclei in PDT- treated and control cultures from three independent replicates is illustrated. Error bars depict standard deviation (n=3; time (day 1-6): p=0.8307; F=0.4191; DF<sub>n</sub>=5; DF<sub>d</sub>=24; Treatment (Control vs. PDT): p=0.0050; F=9.527; DF<sub>n</sub>=1; DF<sub>d</sub>=24; Interaction (time vs. treatment): p=0.7081; F=0.05894; DF<sub>n</sub>=5; DF<sub>d</sub>= 24 (ordinary two-way ANOVA). Adjusted p-values: day 1-Control vs- day 1-PDT: p=>0.9999; day 2-Control vs. day 2-PDT: p=0.9906; day 3-Control vs. day 3-PDT: p=0.8658; day 4-Control vs. day 4-PDT: p=0.5538; day 5-Control vs. day 5-PDT: p=0.8403; day 6-Control vs. day 6-PDT: p= 0.9997; day 1-Control vs. day 2-Control: p=>0.9999; day 1-Control vs. day 3-Control: p=>0.9999; day 1-Control vs. day 4-Control: p=>0.9999; day 1-Control vs. day 5-Control: p=>0.9999; day 1-Control vs. day 6-Control: p=>0.9999; day 2-Control vs. day 3-Control: p=>0.9999; day 2-Control vs. day 4-Control: p=>0.9999; day 2-Control vs. day 5-Control: p=>0.9999; day 2-Control vs. day 6-Control: p=>0.9999; day 3-Control vs. day 4-Control:p=>0.9999; day 3-Control vs. day 5-Control: p=>0.9999; day 3-Control vs. day 6-Control: p=>0.9999; day 4-Control vs. day 5-Control:p=>0.9999; day 4-Control vs. day 6-Control: p=>0.9999; day 5-Control vs. day 6-Control: p=>0.9999; day 1-PDT vs. day 2-PDT: p=>0.9635; day 1-PDT vs. day 3-PDT: p=0.9380; day 1-PDT vs. day 4-PDT: p=0.7930; day 1-PDT vs. day 5-PDT: p=0.9756; day 1-PDT vs. day 6-PDT: p=>0.9999; day 2-PDT vs. day 3-PDT:p=>0.9999; day 2-PDT vs. day 4-PDT: p=>0.9999; day 2-PDt vs. day 5-PDT: p=>0.9999; day 2-PDt vs. day 6-PDT: p=0.9996; day 3-PDT vs. day 4-PDT: p=>0.9999; day 3-PDT vs. day 5-PDT:p=>0.9999; day 3-PDT vs. day 6-PDT: p=0.9986; day 4-PDT vs. day 5-PDT: p=>0.9999; day 4-PDT vs. day 6-PDT: p=0.9781; day 5-PDT vs. day 6-PDT:p=0.9998; remaining post-hoc tests not reported (Tukey's multiple comparison test)).

The superficial layers of the culture directly affected by PDT exhibited high expression of  $\gamma$ -H2AX, indicating DNA damage, while Ki67, a marker of cell proliferation, was not expressed in this region. In contrast, in the underlying layers of the culture, Ki67 was

present, indicating active cell proliferation, while  $\gamma$ -H2AX expression was minimal. The protein profiles of Ki67 and  $\gamma$ -H2AX appeared to be complementary, showing distinct patterns in different layers of the culture. This phenomenon is depicted schematically in figure 14.

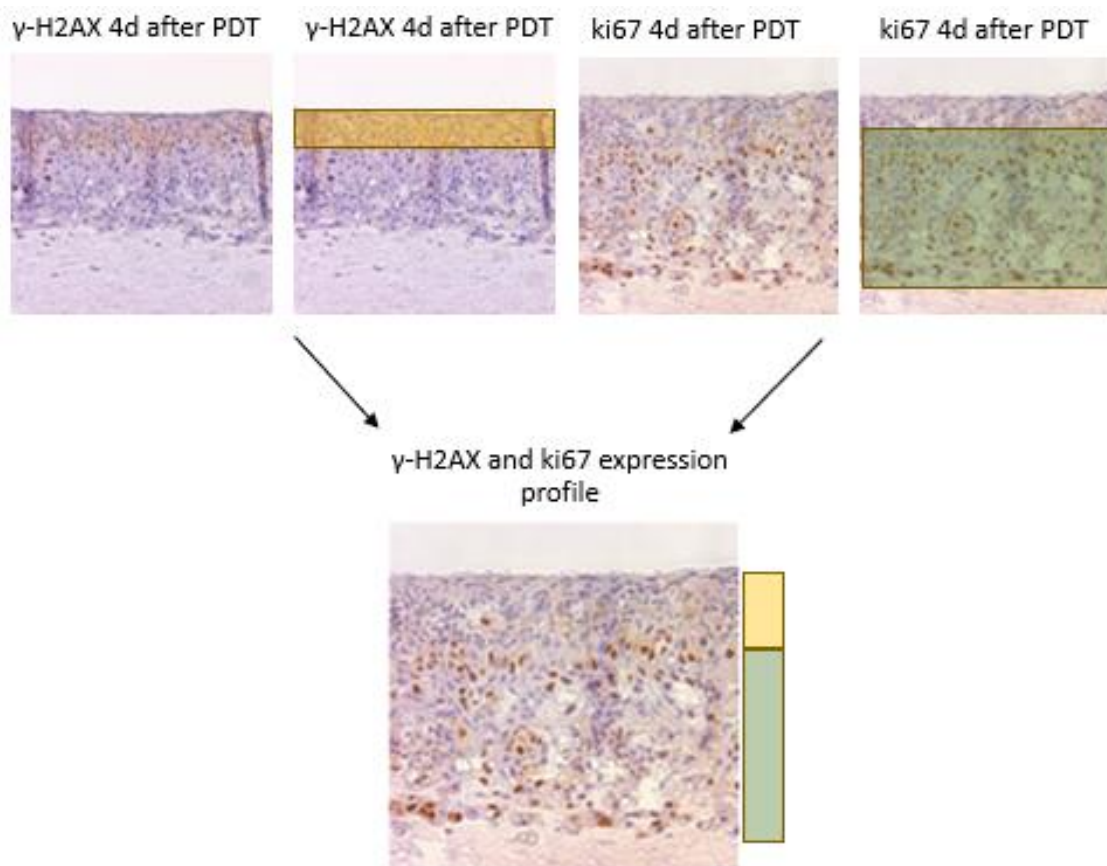


Figure 14: Schematic illustration of the expression profile of  $\gamma$ -H2AX and Ki67 in PDT-treated cultures

The superficial layers of the culture directly affected by PDT exhibited high expression of  $\gamma$ -H2AX (amber bar) while Ki67 was not expressed in this region. In contrast, in the underlying layers of the culture, Ki67 was present (green bar), indicating active cell proliferation, while  $\gamma$ -H2AX expression was minimal.

#### 4.4 Impact of the oncoprotein HPV 8E6 on the susceptibility to PDT

The influence of HPV8 E6 on the expression of RIPK3 in transduced cells has been previously examined in chapter 4.3.2. We now investigated whether HPV 8E6 affects the cellular response to PDT in terms of double-strand DNA-damage and cell proliferation.

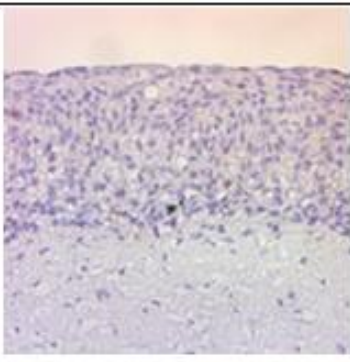
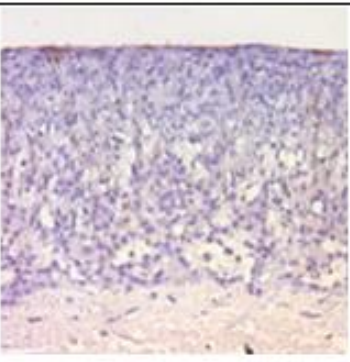
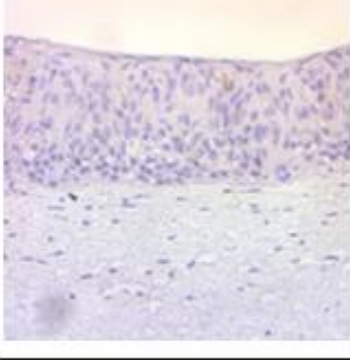
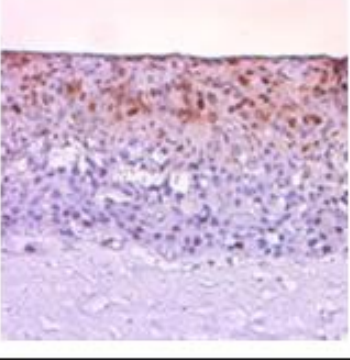
## Results

### 4.4.1 HPV 8E6-transduced keratinocytes express less $\gamma$ -H2AX when exposed to PDT

The 3D cultures, comprising a fibroblast-collagen matrix and keratinocytes transduced with either HPV 8E6 or pLXSN, were treated with aminolevulinic acid (ALA) and subsequently exposed to red light using the PDT lamp. Control cultures were solely incubated with ALA without light exposure. Following treatment, the cultures were stained to detect the presence of  $\gamma$ -H2AX. After 4 days, the culture medium was replaced with 4% paraformaldehyde for fixation. The 3D cultures were then embedded in paraffin and stained for  $\gamma$ -H2AX. The  $\gamma$ -H2AX-positive nuclei were counted in each culture and the mean value of the two experimental approaches was calculated and subjected to statistical analysis.

*Table 19: Immunohistochemical  $\gamma$ -H2AX-staining of 3D-cultures transduced with HPV 8E6 and pLXSN*

HaCaT 3D cultures were transduced with either HPV8 E6 or pLXSN by retroviral gene transfer, treated with ALA and afterwards either radiated with red light under the PDT-lamp or not (control cultures). After 4 days the cultures were fixed and immunohistochemically stained for the presence of  $\gamma$ -H2AX (n=2). The tissue sections are depicted at magnifications of 10-fold.

	Control: Not-PDT- treated 3D cell cultures  Magnification: 10x	PDT- treated 3D cell cultures  Magnification: 10x
<u>HaCaT pLXSN-8E6</u>		
<u>HaCaT pLXSN</u>		

## Results

The cell cultures, transduced with either pLXSN-8E6 or pLXSN vector, exhibited differential expressions of  $\gamma$ -H2AX depending on whether they were subjected to treatment with the PDT lamp or belonged to the untreated control group (table 19). Once again, the control cultures displayed minimal  $\gamma$ -H2AX expression, regardless of whether they were transduced with pLXSN-HPV 8E6 or pLXSN. As the pLXSN-transduced cell cultures served as the control group, their  $\gamma$ -H2AX expression profile aligned with that of the non-transduced 3D cultures described previously. Radiation with the PDT lamp seemed to induce DNA damage, which was detected through  $\gamma$ -H2AX staining. This damage was particularly pronounced in the superficial cell layers directly affected by the PDT treatment.

Upon comparing the cell cultures treated under the PDT lamp, it was essential to note that the pLXSN-transduced cultures exhibited higher levels of  $\gamma$ -H2AX compared to the pLXSN-HPV8 E6- transduced cultures. On average 46 cell nuclei were stained positive for  $\gamma$ -H2AX in the pLXSN-transduced cultures after PDT, whereas only 4 nuclei were detected in the pLXSN-HPV 8E6 cultures. In contrast to the pLXSN-control cultures, PDT treatment seemed to fail to induce a significant amount of double-strand damage and  $\gamma$ -H2AX expression, respectively, in HPV 8E6-transduced cells. No noticeable difference was observed between the HaCaT cells transduced with HPV 8E6 and subsequently radiated, and the HPV 8E6-transduced cultures that solely received ALA treatment without PDT radiation (Average number of staining nuclei in both groups was 1). However, the differences in the staining intensity described before between PDT-treated and control-cultures on the one hand and HPV 8E6-and pLXSN-transduced cell cultures on the other hand were statistically not significant (figure 15;  $p>0.05$ ).

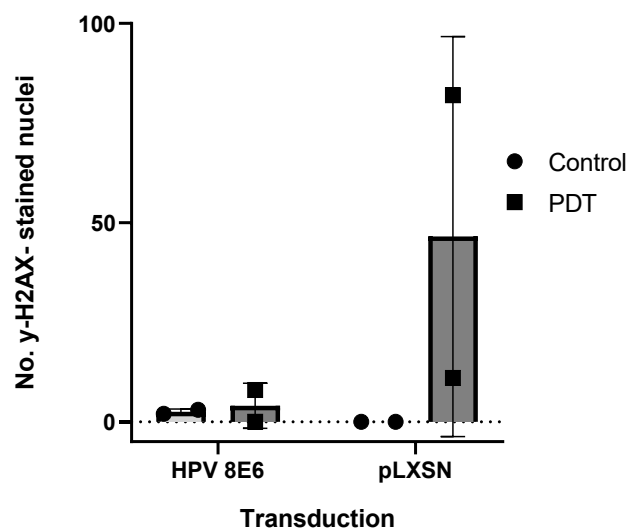


Figure 15:  $\gamma$ -H2AX-positive stained nuclei in PDT- and control cell cultures in HPV 8E6- and pLXSN-transduced cells

HaCaT 3D cultures were transduced with either HPV 8E6 or pLXSN by retroviral gene transfer, treated with ALA and afterwards either radiated with red light under the PDT-lamp or not (control cultures). After 4 days the cultures were fixed and immunohistochemically stained for the presence of  $\gamma$ -H2AX. The number of  $\gamma$ -H2AX- positive nuclei in PDT- treated and control cultures from two independent replicates is illustrated. Error bars depict standard deviation (n= 2; Transduction (HPV 8E6 vs. pLXSN): p=0.3256; F=1.253; DF<sub>n</sub>:1; DF<sub>d</sub>: 4; Treatment (Control vs. PDT): p=0.2503; F=1.805; DF<sub>n</sub>=1; DF<sub>d</sub>= 4; Interaction (Treatment vs. Transduction): p=0.2763; F=1.583; DF<sub>n</sub>:1; DF<sub>d</sub>:4 (ordinary two-way ANOVA). Adjusted p-values: HPV 8E6-Control vs. HPV 8E6-PDT: p=>0.9999; HPV 8E6-Control vs. pLXSN-Control: 0.9996; HPV 8E6-PDT vs. pLXSN-PDT: p=0.4350; pLXSN-Control vs. pLXSN-PDT: p=0.3749; remaining post-hoc tests not reported (Tukey's multiple comparison test)).

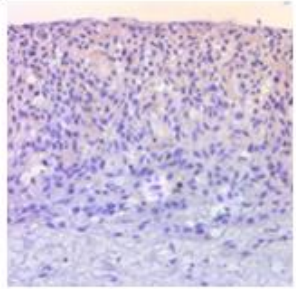
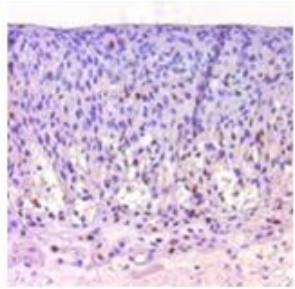
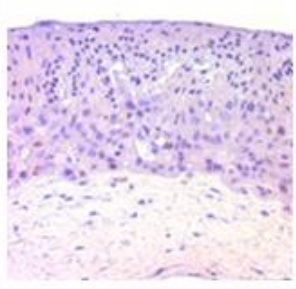
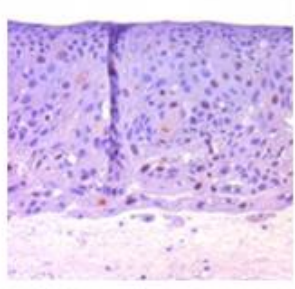
#### 4.4.2 HPV 8E6-transduced cells show higher Ki67 expression after PDT

The 3D cultures, composed of the fibroblast-collagen matrix and keratocytes transduced with either HPV 8E6 or pLXSN, were treated with aminolevulinic acid (ALA) and subsequently exposed to red light using the PDT lamp. In contrast, the control cultures were only incubated with ALA without receiving PDT radiation. The cultures were then subjected to staining to detect the presence of Ki67. After 4 days, the medium was replaced with 4% paraformaldehyde for fixation. The 3D cultures were embedded in paraffin using a fully automatic embedding machine and subsequently sectioned into 6  $\mu$ m slices with a microtome. For the numerical analysis, the nuclei positively stained for Ki67 were counted in each culture. The mean value of the two experimental approaches was calculated and analysed.

## Results

*Table 20: Immunohistochemical Ki67-staining of 3D cultures transduced with HPV 8E6 and pLXSN*

HaCaT 3D cultures were transduced with either HPV8 E6 or pLXSN by retroviral gene transfer, treated with ALA and afterwards either radiated with red light under the PDT-lamp or not (control cultures). After 4 days the cultures were fixed and immunohistochemically stained for the presence of Ki67 (n=2). The tissue sections are depicted at magnifications of 10-fold.

	Control: Not-PDT- treated 3D cell cultures Magnification: 10x	PDT- treated 3D cell cultures Magnification: 10x
<u>HaCaT pLXSN-8E6</u>		
<u>HaCaT pLXSN</u>		

In accordance with the previously described Ki67 expression pattern, control cell cultures, regardless of whether they were transduced with pLXSN-HPV 8E6 or pLXSN, exhibited minimal Ki67 expression. However, in the cell cultures treated under the PDT lamp, those transduced with HPV 8E6 displayed slightly higher Ki67 expression following PDT treatment compared to the pLXSN-transduced cells (table 20). The elevated expression was primarily observed in the basal and suprabasal layers of the cultures, while the superficial layers showed lower expression. These findings are consistent with the results observed in non-transduced cell cultures, indicating that PDT treatment stimulates cell proliferation. The statistical analysis (figure 16) further supports these observations, as the number of Ki67-positive nuclei was generally higher in PDT-treated cell cultures compared to control cultures. In the PDT-treated group the mean value of Ki67- positive nuclei was 25 (HPV8 E6-transduced cells) and 18 (pLXSN-transduced cells), respectively. On the other hand, the mean value of Ki67-positive nuclei in the control cultures was only 3 (HPV8 E6-transduced cells) and 5 (pLXSN-transduced cells), respectively. Additionally, in cells transduced with HPV 8E6, the number of Ki67-positive nuclei tended to be higher than in pLXSN-transduced cultures (25 vs.18). However, these differences in staining intensity were statistically not significant ( $p>0.05$ ).

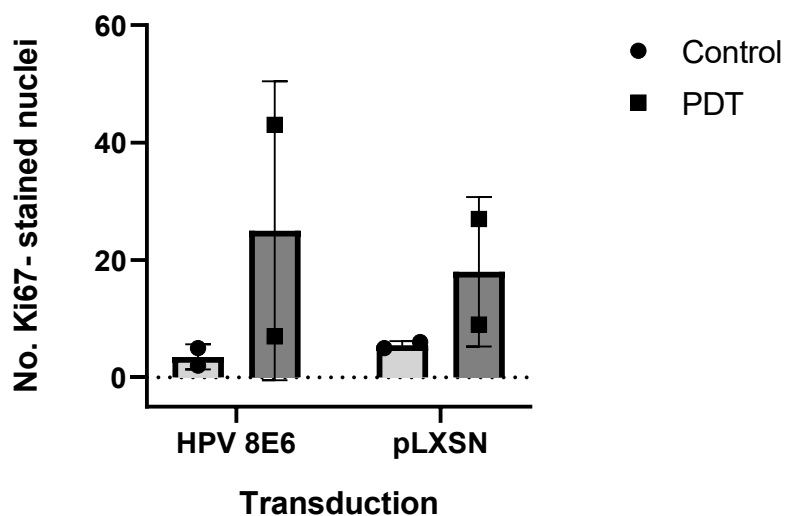


Figure 16: Ki67-positive stained nuclei in PDT- and control cell cultures in HPV 8E6- and pLXSN-transduced cells

HaCaT 3D cultures were transduced with either HPV8 E6 or pLXSN by retroviral gene transfer, treated with ALA and afterwards either radiated with red light under the PDT-lamp or not (control cultures). After 4 days the cultures were fixed and immunohistochemically stained for the presence of Ki67. The number of Ki67-positive nuclei in PDT- treated and control cultures from two independent replicates is illustrated. Error bars depict standard deviation. (n= 2; Transduction (HPV 8E6 vs. pLXSN):  $p=0.8166$ ;  $F=0.06135$ ;  $DFn:1$ ;  $DFd: 4$ ; Treatment (Control vs. PDT):  $p=0.1674$ ;  $F=2.837$ ;  $DFn=1$ ;  $DFd= 4$ ; Interaction (Treatment vs. Transduction):  $p=0.6788$ ;  $F=0.1988$ ;  $DFn:1$ ;  $DFd:4$  (ordinary two-way ANOVA). Adjusted p-values: HPV 8E6-Control vs. HPV 8E6-PDT:  $p>0.5103$ ; HPV 8E6-Control vs. pLXSN-Control: 0.9989; HPV 8E6-PDT vs. pLXSN-PDT:  $p=0.9572$ ; pLXSN-Control vs. pLXSN-PDT:  $p=0.8180$ ; remaining post-hoc tests not reported (Tukey's multiple comparison test)).

#### 4.5 Impact of the repression of RIPK3 on susceptibility to PDT in keratinocytes.

In line with previous experiments demonstrating the influence of the oncoprotein HPV 8E6 on PDT response, it is known that HPV 8E6, plays a critical role in the induction of tumorigenesis and the development of HPV-associated tumours such as squamous skin cancer. There is evidence to suggest that HPV may also regulate the expression of RIPK3 as a mechanism to evade cell death and promote viral replication (Ma, et al. 2016). To investigate the role of RIPK3 in the susceptibility of keratinocytes to PDT, RIPK3 was knocked-down by siRNA transfection. Cells were transfected with specific siRNA targeting RIPK3, and 3D cultures were harvested after four days to account for



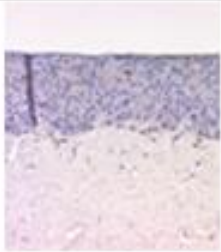
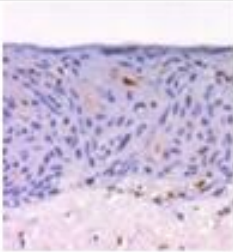
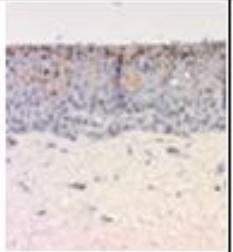
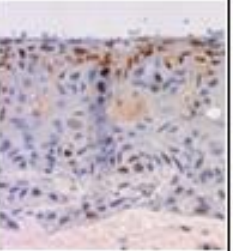
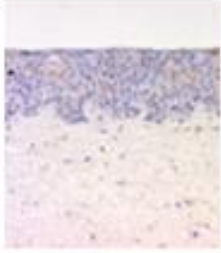
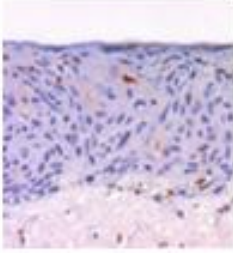
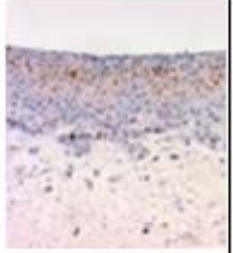
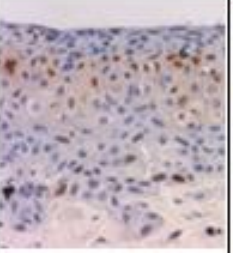
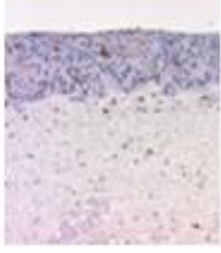
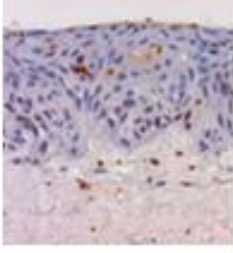
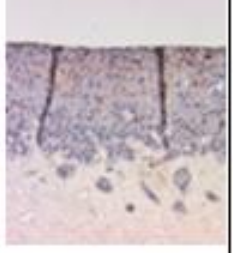
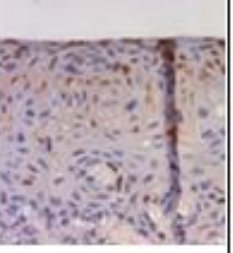
the transient effect of siRNA, as its stability and activity were limited. Non-coding siRNA transfection and cell cultures without any siRNA served as control approaches.

#### 4.5.1 $\gamma$ -H2AX-expression does not change after RIPK3 knock-down

The different siRNA approaches (no siRNA, non-coding siRNA, siRIPK3) were treated with ALA and then either radiated with red light under the PDT-lamp or incubated with ALA only (control cultures). After 4 days the cell cultures were fixed, embedded and immunohistochemically stained for the presence of  $\gamma$ -H2AX.

*Table 21: Immunohistochemical  $\gamma$ -H2AX-staining of 3D-cultures transfected with either siRIPK3, non-coding siRNA or no siRNA*

HaCaT 3D cultures were transfected with either siRIPK3, a non-coding siRNA or no siRNA, treated with ALA and afterwards either radiated with red light under the PDT-lamp or not (control cultures). After 4 days the cultures were fixed and immunohistochemically stained for the presence of  $\gamma$ -H2AX (n=2). The tissue sections are depicted at magnifications of 10-fold and 20-fold.

	Control: Not-PDT- treated 3D cell cultures		PDT- treated 3D cell cultures	
	Magnification: 10x	Magnification: 20x	Magnification: 10x	Magnification: 20x
HaCats without siRNA				
HaCats with non-coding siRNA				
HaCats with siRIPK3				

Consistent with the previously analysed protein profiles, the expression of  $\gamma$ -H2AX was higher in cell cultures exposed to PDT radiation compared to the control cultures, regardless of whether they were transfected with siRIPK3, non-coding siRNA, or not transfected with any siRNA (table 21). Once again, in the PDT-treated cell cultures, the superficial layers directly exposed to the radiation exhibited the highest level of  $\gamma$ -H2AX staining, while the basal layers showed minimal staining. In the control cultures,  $\gamma$ -H2AX staining appears sporadically without a specific pattern.

This observation is graphically illustrated in figure 17. The cell cultures treated with PDT displayed significantly higher  $\gamma$ -H2AX expressions ( $p= 0.0005$ ; mean value of  $\gamma$ -H2AX-positive nuclei: 50, 40, 43, respectively) compared to the non-radiated group (mean value of  $\gamma$ -H2AX-positive nuclei: 17, 9, 12, respectively). However, the number of cell nuclei exhibiting positive staining did not exhibit a statistically significant difference between the various siRNA approaches ( $p>0.05$ ), regardless of the treatment group (PDT or control).

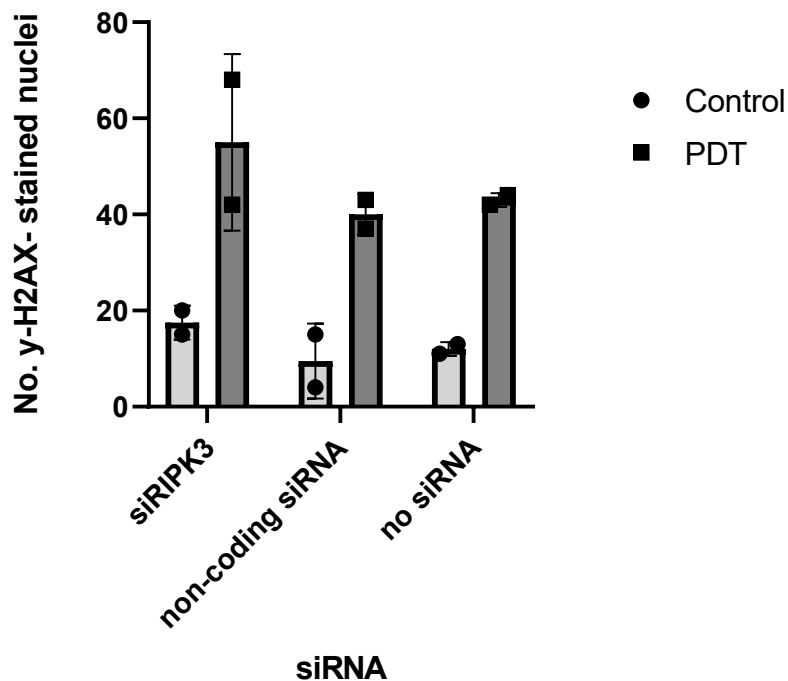


Figure 17:  $\gamma$ -H2AX-positive stained nuclei in PDT- and control cell cultures transfected with either siRIPK3, non-coding siRNA or no siRNA

HaCaT 3D cultures were transfected with either siRIPK3, a non-coding siRNA or no siRNA, treated with ALA and afterwards either radiated with red light under the PDT-lamp or not (control cultures). After 4 days the cultures were fixed and immunohistochemically stained for the presence of  $\gamma$ -H2AX. The number of  $\gamma$ -H2AX-positive nuclei in PDT- treated and control cultures from two independent replicates is illustrated. Error bars depict standard deviation ( $n=2$ , siRNA (siRIPK3 vs. non-coding siRNA vs. no siRNA):  $p=0.2161$ ;  $F=1.999$ ;  $DFn=2$ ;  $DFd=6$ ; Treatment (Control vs. PDT):  $p=0.0005$ ;  $F=45.27$ ;  $DFn=1$ ;  $DFd=6$ ; Interaction (siRNA vs. treatment):  $p=0.8153$ ;  $F=0.2113$ ;  $DFn=2$ ;  $DFd=6$  (ordinary two-way ANOVA). Adjusted p-values: siRIPK3-Control vs. siRIPK3-PDT:  $p=0.0319$ ; non-coding siRNA-Control vs. non-coding siRNA-PDT:  $p=0.0761$ ; no

## Results

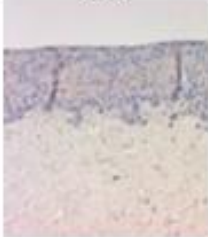
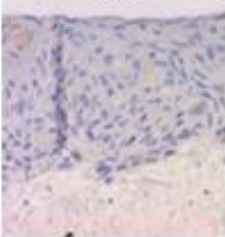
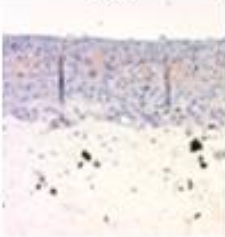
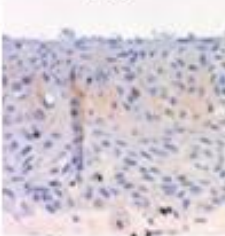
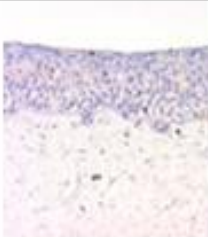
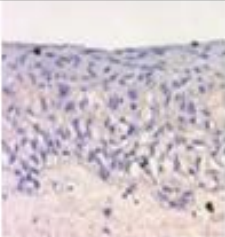

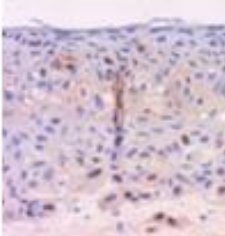
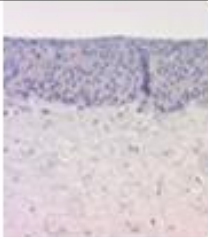
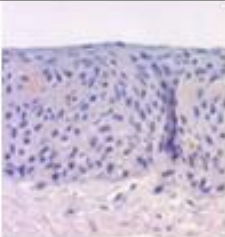
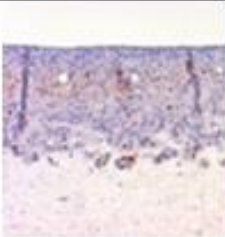
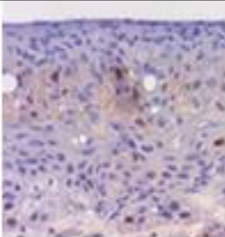
siRNA-Control vs. no siRNA-PDT:  $p = 0.0713$ ; siRIPK3-Control vs. non-coding siRNA-Control:  $p = 0.9211$ ; siRIPK3-Control vs. no siRNA-Control:  $p = 0.9821$ ; siRIPK3-PDT vs. non-coding siRNA-PDT:  $p = 0.5428$ ; siRIPK3-PDT vs. no siRNA-PDT:  $p = 0.7218$ ; non-coding siRNA-Control vs no siRNA-Control:  $p = 0.9995$ ; non-coding siRNA-PDT vs. no siRNA-PDT:  $p = 0.9989$ ; remaining post-hoc tests not reported (Tukey's multiple comparison test)).

### 4.5.2 Repression of RIPK3 reduces Ki67 expression in PDT-treated cells

The different siRNA approaches (no siRNA, non-coding siRNA, siRIPK3) were treated with ALA and then either radiated with red light under the PDT-lamp or incubated with ALA only (control cultures). After 4 days the cell cultures were fixed, embedded and immunohistochemically stained for the presence of Ki67.

*Table 22: Immunohistochemical Ki67-staining of 3D cultures transfected with either siRIPK3, non-coding siRNA or no siRNA*

HaCaT 3D cultures were transfected with either siRIPK3, a non-coding siRNA or no siRNA, treated with ALA and afterwards either radiated with red light under the PDT-lamp or not (control cultures). After 4 days the cultures were fixed and immunohistochemically stained for the presence of Ki67 ( $n = 2$ ). The tissue sections are depicted at magnifications of 10-fold and 20-fold.

	Control: Not-PDT- treated 3D cell cultures		PDT- treated 3D cell cultures	
	Magnification: 10x	Magnification: 20x	Magnification: 10X	Magnification: 20x
HaCats without siRNA				
HaCats with non-coding siRNA				
HaCats with siRIPK3				

Comparing the expression profiles of cell cultures exposed to PDT radiation with control cell cultures, it was evident that the expression of Ki67 was higher in the radiated cultures. Notably, in the radiated cultures, Ki67 expression was particularly high in the central layers of the culture. Again, the upper layer that was directly exposed to the radiation showed no detectable Ki67 expression. In contrast, Ki67 was rarely detectable in the control cultures, regardless of whether they were transfected with siRIPK3, non-coding siRNA, or not transfected with any siRNA (table 22). Additionally, Ki67 expression could also be observed in the lower layers of the culture.

This observation is graphically illustrated in figure 18. The statistical analysis revealed that the number of Ki67-positive nuclei in PDT-treated cell cultures was significantly higher ( $p=0.0278$ ; mean value of Ki67-positive nuclei: 11, 23, 26) compared to the number of Ki67-positive nuclei in the control cultures (mean value of Ki67-positive nuclei: 4, 5, 2), regardless of the siRNA approach. Furthermore, it seemed as if Ki67 was less detected in PDT-treated cultures after being transfected with siRIPK3 compared to transfection with a non-coding siRNA or no siRNA (mean value of Ki67-positive nuclei 11, compared to 23 and 26, respectively. However, this observation was statistically not significant ( $p>0.05$ ).

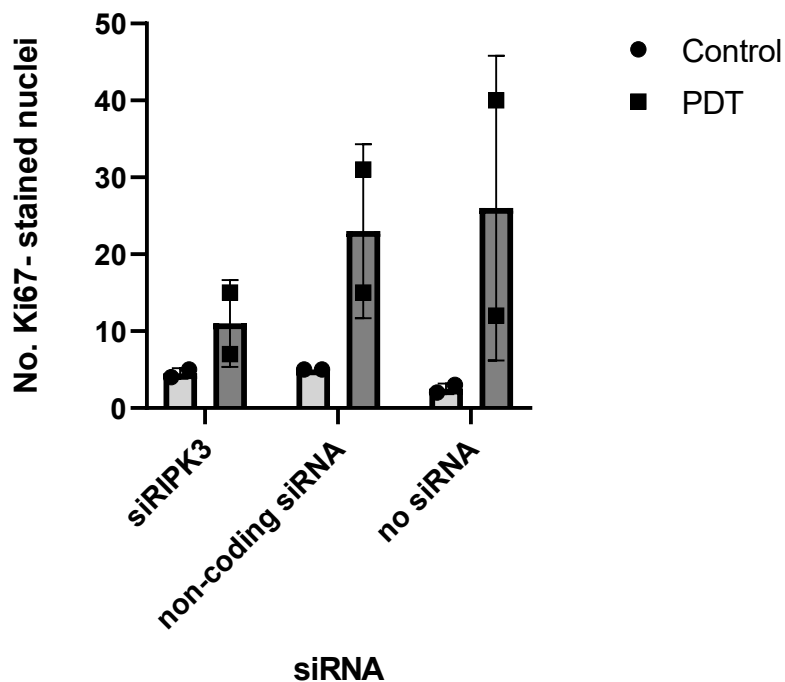


Figure 18: Ki67-positive stained nuclei in PDT- and control cell cultures transfected with either siRIPK3, non-coding siRNA or no siRNA

HaCaT 3D cultures were transfected with either siRIPK3, a non-coding siRNA or no siRNA, treated with ALA and afterwards either radiated with red light under the PDT-lamp or not (control cultures). After 4 days the cultures were fixed and immunohistochemically stained for the presence of Ki67. The number of Ki67-

## Results

positive nuclei in PDT- treated and control cultures from two independent replicates is illustrated. Error bar depict standard deviation (n=2, siRNA (siRIPK3 vs. non-coding siRNA vs. no siRNA):  $p=0.5843$ ;  $F=0.5886$ ;  $DFn=2$ ;  $DFd=6$ ; Treatment (Control vs. PDT):  $p=0.0278$ ;  $F=8.333$ ;  $DFn=1$ ;  $DFd=6$ ; Interaction (siRNA vs. treatment):  $p=0.4857$ ;  $F=0.8165$ ;  $DFn=2$ ;  $DFd=6$  (ordinary two-way ANOVA). Adjusted p-values: siRIPK3-Control vs. siRIPK3-PDT:  $p=0.9783$ ; non-coding siRNA-Control vs. non-coding siRNA-PDT:  $p=0.4905$ ; no siRNA-Control vs. no siRNA-PDT:  $p=0.2712$ ; siRIPK3-Control vs. non-coding siRNA-Control:  $p=>0.9999$ ; siRIPK3-Control vs. no siRNA-Control:  $p=>0.9999$ ; siRIPK3-PDT vs. non-coding siRNA-PDT:  $p=0.8008$ ; siRIPK3-PDT vs. no siRNA-PDT:  $p=0.6453$ ; non-coding siRNA-Control vs no siRNA-Control:  $p=0.9997$ ; non-coding siRNA-PDT vs. no siRNA-PDT:  $p=0.9994$ ; remaining post-hoc tests not reported (Tukey's multiple comparison test)).

### 4.6 RIPK3 expression negatively correlates with grade of VIN lesion

HPV has been implicated in the pathogenesis of vulvar cancer development and is involved, among other factors, in the induction of vulvar neoplasia. Furthermore, there is evidence of an interaction between high-risk HPV and RIPK3, an inducer of the necroptosis pathway, that plays a role in the specific cell death mechanism during PDT treatment (Ma, et al. 2016). PDT represents a potentially promising non-invasive treatment option for patients with vulvar neoplasia, and the presence of RIPK3 may influence patient selection or serve as a predictor of the clinical response to PDT. To investigate the expression of RIPK3 in samples of vulvar intraepithelial lesions and determine if there are any differences in expression profiles, immunohistochemical staining with an anti-RIPK3 antibody was performed on samples obtained from 18 patients diagnosed with VIN at various stages. Table 23 illustrates the frequency distribution of each staining pattern for RIPK3, table 16 shows RIPK3 staining exemplary for three patients with vulvar intraepithelial neoplasia I, II, and III.

*Table 23: Frequency distribution of RIPK3 staining patterns in vulva intraepithelial neoplasia samples*

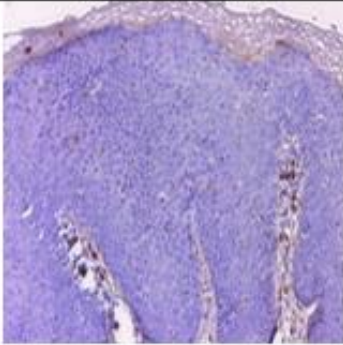
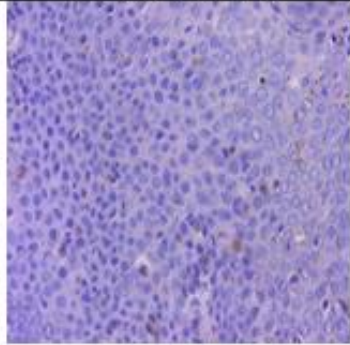
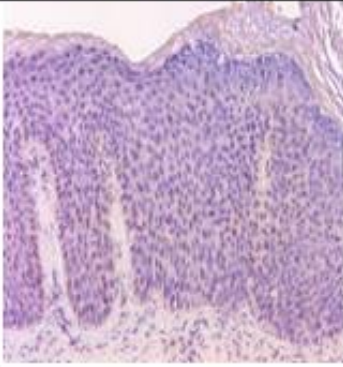
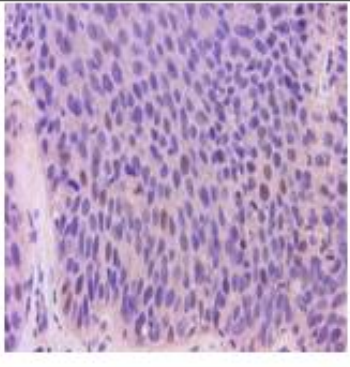
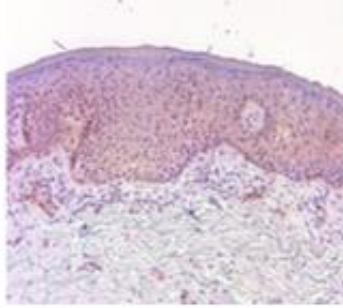
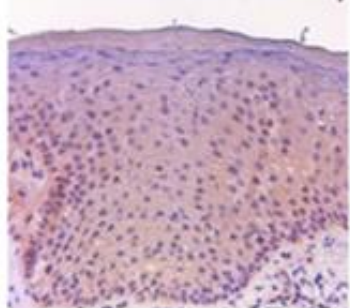
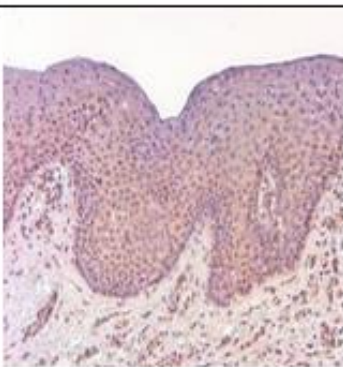
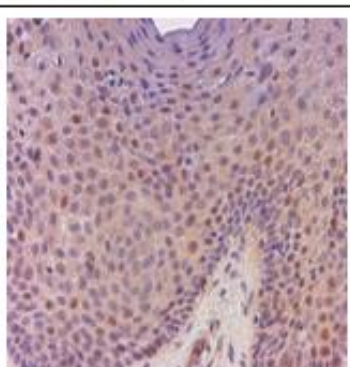
Total number of each staining pattern (1-4) for RIPK3 out of a sample collection of 18 samples of patients with vulvar intraepithelial neoplasia in different stages.

Staining intensity	Frequency distribution
1	8
2	2
3	4
4	4

## Results

*Table 24: Immunohistochemical RIPK3 staining of VIN lesions*

Samples of 18 patients with vulvar intraepithelial neoplasia in various stages were stained for the presence of RIPK3. Below, four representative histological sections from different patients with distinct staining patterns and varying grades of VIN differentiation are presented. The tissue sections are depicted at magnifications of 10-fold and 20-fold.

Staining intensity	VIN grade	Vulvar intraepithelial lesion	
		Magnification: 10x	Magnification: 20x
1	VIN 3		
2	VIN 2		
3	VIN 2		
4	VIN 1		

There were variations in the staining intensity of RIPK3 observed among patients with vulvar intraepithelial neoplasia. In the first row, the staining intensity for RIPK3 in the VIN 1 lesion was notably higher compared to the VIN 2 lesions in the second and third rows, where RIPK3 expression was almost absent. Moreover, the distribution of RIPK3 differed between patients, with localization observed in both the cytosol and the nucleus. To investigate the potential correlation between staining intensity and the grade of the vulvar intraepithelial lesion, the data were represented in a column chart (figure 19). The chart suggests a negative correlation between the grade of the vulvar lesion (VIN I/II/III) and the expression level of RIPK3. Higher-grade intraepithelial lesions exhibited lower levels of RIPK3 expression.

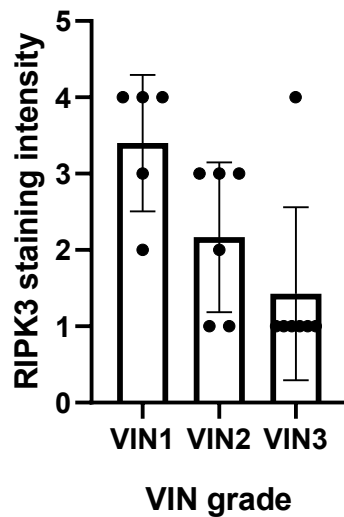


Figure 19: Correlation between VIN grade and RIPK3- staining intensity

Samples of 18 patients with vulvar intraepithelial neoplasia in various stages were stained for the presence of RIPK3. The RIPK3 staining intensity was correlated with the grade of VIN differentiation (Staining intensity: 1=none, 2=weak, 3=moderate, 4 =strong;  $p=0.0170$ ,  $F=5,412$ ,  $DFn=2$ ,  $DFd=15$  (ordinary one-way ANOVA). Error bars depict standard deviation. Adjusted p values: VIN 1 vs. VIN 2:  $p= 0.1494$ ; VIN 1 vs. VIN 3:  $p= 0.0131$ ; VIN 2 vs. VIN 3:  $p= 0.4195$  (Turkey's multiple comparison test)).

The patients' samples were subjected to HPV testing using PCR, which was carried out by Mrs. Barbara Best. Out of the 5 VIN 1 samples, 3 were found to be negative for HPV, while 2 were positive. Similarly, all 5 samples in the VIN 2 and VIN 3 groups tested negative for HPV, except for one sample in the VIN 2 group and two samples in the VIN 3 group, which were found to be positive for HPV. Overall, there was no correlation observed between the presence of HPV and the grade of the vulvar intraepithelial lesion.

## Results

The distribution of HPV-positive and HPV-negative samples among the VIN groups was approximately equal. In other words, the presence of HPV did not necessarily indicate a higher grade of vulvar lesion, nor did the absence of HPV indicate a lower grade. Furthermore, no significant correlation was found between the staining intensity of RIPK3 and the presence of HPV in the samples of vulvar intraepithelial lesions (figure 20).

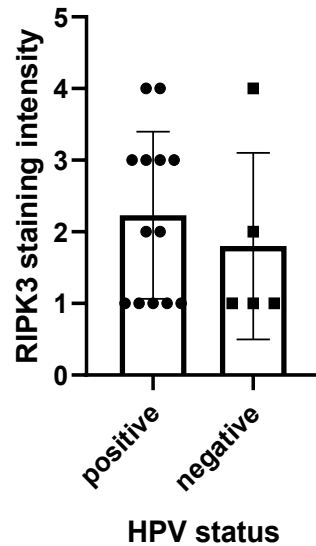


Figure 20: Difference in RIPK3 staining intensity depending on HPV status in VINs

Samples of 18 patients with vulvar intraepithelial neoplasia in various stages were stained for the presence of RIPK3. Additionally, PCR was performed to test for the presence of HPV in these samples. The staining intensity of RIPK3 was then compared with the HPV status ( $p=0.5055$ ,  $t=0.6812$ ,  $df=16$  (unpaired t-test). Error bars depict standard deviation).



## 5 Discussion

### 5.1 RIPK3 correlates with PDT susceptibility of actinic keratosis

RIPK3 staining of the patient samples with actinic keratosis revealed significant variations among individual patients. Correlating the intensity of RIPK3 staining with the response to PDT (figure 10c), the data indicated that patients with higher levels of RIPK3 expression appeared to be more responsive to this therapy. Interestingly, age and sex did not demonstrate any influence on therapy outcomes or RIPK3 expression (figure 10a, 10b, 10d, 10e).

Given that PDT induces necroptosis (Buytaert, Dewaele and Agostinis 2007; Coupienne, et al. 2011) and RIPK3 is involved in this signalling pathway (Cho, et al. 2009; Wu, et al. 2014), it is reasonable to assume that the therapy outcome is directly influenced by the level of RIPK3 expression in patients. Those with higher levels of RIPK3 protein appeared to be more susceptible to PDT. These findings are consistent with the findings of Coupienne et al. (2011), wherein the induction of RIPK3-dependent necroptosis following 5-ALA-PDT treatment was elucidated in patients afflicted with glioblastoma. However, the authors posited that in addition to RIPK3, other proteins may exert a pivotal influence on necrosome assembly, thereby necessitating further investigations. Paradoxically, they also demonstrated in a separate study that elevated RIPK3 expression in osteosarcoma cells conferred heightened cellular viability subsequent to PDT treatment, and alternative modes of cell demise such as apoptosis and autophagy potentially exhibited a PDT-protective capacity (Coupienne, Fettweis and Piette, 2011). Additionally, it should be noted that Koo et al. (2015) demonstrated that RIPK3 is often downregulated in cancer cells due to genomic hypermethylation. Consequently, the RIPK-dependent cell signalling and induced cell death are minimized, promoting cell survival. They propose combining established anti-tumour therapies with hypomethylating agents to increase RIPK3 expression and enhance cancer cell susceptibility to necroptosis (Koo, et al. 2015).

Hence, it is plausible that the assessment of RIPK3 expression before initiating therapy could serve as a predictive parameter for susceptibility to PDT treatment. However, these findings should be interpreted cautiously, given the limited sample size of the patient cohort, which comprised only 22 individuals. To further investigate the predictive role of RIPK3, larger sample sizes and prospective studies are imperative.

The correlation between RIPK3 expression and therapy response, as well as the patient's sex and age, did not reveal any significant associations (figure 10a, 10b, 10d, 10e). It should be noted that the patient cohort was limited in size and predominantly consisted of male individuals of advanced age (with an average age of 71.36 years). This imbalance in the distribution of the compared groups (male vs. female and age >75 years vs. <75 years) necessitates a critical interpretation of the data. Actinic keratosis is a dermatological condition that primarily affects elderly individuals, particularly in sun-exposed areas of the skin. Therefore, to obtain more meaningful insights regarding RIPK3 expression and patient data, a larger number of patients with well-matched age and gender controls would be required.

RIPK3 is a protein that is present in both the nucleus and cytoplasm. The immunoreactive score (IRS) developed by Remmele and Stegner has been employed to quantify the level of RIPK3 in the samples. However, the assessment of RIPK3 expression in samples from patients with actinic keratosis using IRS is inherently subjective, as it requires comparing individual staining intensities and subjective biases cannot be completely eliminated. An alternative approach would involve quantifying the staining intensity using specific software that automatically scans the slides and counts the positive nuclei if present. Nevertheless, even in this case, the determination of cut-off values and user parameters must be decided upon by an individual.

## 5.2 PDT does not alter RIPK3 expression in 3D cultures

To investigate the potential influence of PDT on *in vitro* RIPK3 expression, 3D cell cultures were utilized. However, the staining of RIPK3 in 3D cell cultures did not exhibit any evident differences, irrespective of whether the cultures were exposed to irradiation or not (table 15). These findings suggest that PDT treatment did not appear to affect the expression profile of RIPK3. Nevertheless, there might be a trend indicating that the superficial layers, which were directly exposed to PDT, exhibited lower levels of RIPK3 expression compared to the underlying cells and the control cultures where RIPK3 expression was more evenly distributed. As mentioned earlier, cancer cells can downregulate RIPK3 to diminish RIPK-dependent cell signalling and subsequently reduce cell death, thereby promoting cell survival (Koo, et al. 2015). This phenomenon was observable in the PDT-treated cell cultures, where keratinocytes directly impacted by PDT responded to induced cellular damage by downregulating RIPK3 to prevent subsequent cell death. As of the present moment, there exists a limited understanding

regarding the interrelation of RIPK3 expression and photodynamic therapy. Moreover, inquiries into RIPK3 expression concerning alternative therapeutic approaches like PUVA or radiotherapy remain notably absent. Consequently, the imperative for additional investigations becomes evident.

### 5.3 HPV 8E6 negatively influences the expression of RIPK3 in PDT-treated 3D cultures

The oncoproteins of HPV possess varying oncogenic potentials depending on the low- and high-risk variants (Doorbar, et al. 2012). HPV 8E6 promotes cell proliferation and tumorigenesis by inhibiting transcription of 53-induced proapoptotic genes (Giampieri and Storey 2004) or by altering p53-phosphorylation (Muschik, et al. 2011). Investigation of HPV 8E6-transduced cells and the impact of PDT revealed intriguing alterations in the expression of RIPK3. RIPK3 expression was higher in the control cultures compared to the cell cultures treated under the PDT lamp. Notably, cells transduced with HPV 8E6 exhibited almost complete absence of RIPK3 in the superficial layers when treated under the PDT lamp. A similar effect, though less pronounced, was observed in pLXSN-transduced cells treated with PDT (table 16). It appears that HPV 8 infection promotes the downregulation of RIPK3, particularly in cells directly affected by the treatment and exhibiting severe DNA damage. This mechanism may prevent RIPK3-induced cell death in HPV-infected keratinocytes and ensure viral replication. These findings align with the observations of Ma et al. (2016) suggesting that RIPK3 is influenced by high-risk HPV infection, although this hypothesis could not be confirmed in the analysis of HPV-positive VINs conducted previously (figure 20). Given that only the presence of HPV, and not its activity state, was tested, it is possible that RIPK3 expression is indeed influenced by active HPV. Therefore, further investigation is warranted.

However, it is noteworthy that the non-irradiated control cultures generally exhibited higher levels of RIPK3 expression compared to the therapy group, regardless of whether the keratinocytes were transduced with HPV 8E6 or pLXSN. This suggests that the PDT treatment itself may induce a certain degree of RIPK3 downregulation. However, the findings should be cautiously interpreted in terms of their significance and reproducibility as only two independent experimental approaches had been performed.

Another very important fact to discuss is that in the in vitro experimental approaches HaCaT-cells were used, an immortalized skin keratinocyte cell line, exhibiting various mutations, besides others, a mutation on the p53-gene (Lehman, et al. 1993). In contrast to primary keratinocytes, HaCaT-cells therefore display distinct differences in cellular

signalling in terms of cell cycle progression, apoptosis and tumorigenesis, consequently. To get a faithful simulation of skin tissue to examine the impact of PDT and HPV 8E6 *in vitro* it would be reasonable to perform the experiments with primary keratinocytes, representing the molecular status of tissue the best.

Another crucial point of discussion is the utilization of HaCaT cells in the *in vitro* experimental approaches. HaCaT cells are an immortalized skin keratinocyte cell line known to harbour various mutations, including a mutation in the p53 gene (Lehman et al., 1993). In contrast to primary keratinocytes. Even though RIPK3 is primarily involved in the necroptosis signalling pathway rather than the apoptotic signalling pathway, there is evidence suggesting potential interactions between these pathways. Several studies have indicated that RIPK3 can have crosstalk with apoptotic proteins and signalling molecules, leading to the modulation of apoptotic processes. For example, it has been shown that RIPK3 can interact with caspases, key players in the apoptotic pathway, and influence their activation or inhibition (Moriwaki, et al. 2015). These findings suggest that there could be intricate connections and regulatory mechanisms between necroptosis and apoptosis, potentially involving RIPK3. Therefore, the use of HaCaT cells may not faithfully demonstrate the molecular status of skin tissue. To accurately simulate the skin tissue and investigate the impact of PDT and HPV 8E6 *in vitro*, it would be advisable to conduct the experiments using primary keratinocytes, which better represent the molecular characteristics of the tissue.

## 5.4 PDT has opposite effects in 3D cultures dependent on the epithelial layer

### 5.4.1 PDT induces DNA damage in the superficial but favours cell growth in the lower cell layers of the 3D cultures

The analysis of  $\gamma$ -H2AX staining in the 3D cultures revealed that  $\gamma$ -H2AX intensity was notably higher in the superficial layers of the cultures that were irradiated compared to the control cultures incubated with ALA but not treated under the PDT lamp (table 17).  $\gamma$ -H2AX serves as a robust marker for DNA damage, particularly double-strand breaks in cells. Therefore, it can be inferred that the cell cultures treated under the PDT lamp experience a greater level of damage due to radiation. Thereby, the number of nuclei exhibiting positive  $\gamma$ -H2AX- staining was significantly higher in the PDT-exposed cultures compared to the control cultures ( $p=0.0082$ , figure 11). In other words, PDT treatment induced considerable cellular stress in the cultures, resulting in DNA damage and subsequent staining for  $\gamma$ -H2AX as a molecular damage marker.

The control cultures, which were also treated with ALA but not irradiated under the PDT lamp, sporadically exhibited diffuse  $\gamma$ -H2AX expression that appeared to increase over time. It is possible that the general handling of the cell cultures induced a basal level of damage, as evidenced by minimal  $\gamma$ -H2AX staining.

Furthermore, the superficial layers of the cell cultures directly exposed to radiation displayed the highest intensity of  $\gamma$ -H2AX staining, suggesting that the effectiveness of PDT in inducing DNA damage may depend on the penetration of radiation. In the schematic illustration in figure 12, the amber bar clearly indicated that  $\gamma$ -H2AX expression and DNA damage are limited to the upper third of the culture. The depth of penetration appeared to be a limiting factor in the efficacy of PDT treatment and the extent of DNA damage experienced. It has been demonstrated that ALA, with its low lipid solubility, has limited ability to penetrate the skin and cell membranes. Therefore, PDT with ALA as a photosensitizer is only suitable for superficial lesions, as the damaging effect of PDT is restricted to a few millimetres below the surface (Di Venosa, et al. 2008). Attempts have been made to overcome this limitation by utilizing nanoscale vesicle formation to enhance penetration capacity (Dirschka, et al. 2011), (Passos, et al. 2013). Other approaches suggest improving penetration through physical methods such as micro-needling or ultrasound, or by adding chemical enhancers, such as dimethyl sulfoxide (Zhang, Fang and Fang 2011). Nonetheless, the limited cell-damaging effect of PDT treatment must be carefully considered when selecting lesions and patients.

Analysis of the Ki67 expression profile in the 3D cell culture model suggested that PDT treatment stimulates cell proliferation, as evidenced by the increased staining intensity of Ki67 (table 18). Similarly, figure 13 demonstrated a significantly higher number of Ki67-positive stained nuclei in cell cultures exposed to PDT compared to non-treated cultures ( $P=0.0050$ ). Based on these findings, it can be suggested that the treatment of tumorous lesions such as actinic keratosis or vulvar intraepithelial neoplasia with PDT could potentially lead to disease progression and accelerated transformation into highly malignant cell growth. This outcome is highly undesirable, dangerous, and contrary to the intended therapeutic goal. Bhowmick and Girotti (2014) demonstrated similar effects of PDT in a prostate cancer cell model, where PDT-induced NOS2 and NO promoted cell survival and growth. Additionally, it has been shown that photogenerated reactive oxygen species are responsible for cell cycle progression and proliferation, confirming the findings of this study (Blázquez-Castro, et al. 2012). Furthermore, several studies have reported a significant increase in the incidence of squamous cell carcinoma of the male genitalia after using Psoralens and Ultraviolet A photochemotherapy (PUVA) to treat psoriasis. These studies described a dose-dependent increase in the risk of squamous cell carcinoma, which was up to 300 times higher compared to the general

population (Stern 1990). Therefore, the indication for using PUVA must be critically evaluated. Further investigations are necessary to determine whether PDT therapy might have a similarly dangerous long-term effect on neoplastic progression.

As previously mentioned, it is important to interpret all findings cautiously regarding their significance and reproducibility, primarily due to the limited number of experimental replicates and the utilization of an immortalized cell culture model.

## 5.5 HPV 8E6-transduced 3D cultures show an altered response to PDT

### 5.5.1 HPV 8E6-transduced cells show less DNA damage and higher proliferation rates in response to PDT

Cell cultures transduced with either HPV 8E6 or pLXSN vector exhibited different  $\gamma$ -H2AX expressions. The control cultures, regardless of whether they were transduced with HPV 8E6 or pLXSN vectors, showed minimal  $\gamma$ -H2AX expression and induced DNA damage, consequently. However, the pLXSN-transduced cell cultures treated under the PDT lamp displayed notably higher  $\gamma$ -H2AX expressions compared to the HPV 8E6-transduced and radiated cells. The  $\gamma$ -H2AX expression profile in the pLXSN-transduced cell cultures, which represents the control group, was consistent with the profile observed in non-transduced 3D cultures described earlier (table 17). In contrast, the PDT-treated cell cultures transduced with HPV 8E6, representing an infection with the human papillomavirus, exhibited minimal  $\gamma$ -H2AX expression (table 19, figure 15). This observation suggests that transfection with HPV 8E6 leads to reduced DNA damage or at least reduced DNA damage response induced by PDT treatment. It might be hypothesized that a viral infection somehow confers higher resistance to oxidative stress and creates a greater tolerance for cell death, such as RIPK3-induced necroptosis. Indeed, it has been demonstrated that HPV infection promotes the development of various mechanisms to evade host cells' attempts at immunological clearance and cell death induction. For example, downregulation of RIPK3 and its downstream effectors, such as MLKL, reduces necroptosis of infected keratinocytes (Ma, et al. 2016). Downregulating RIPK3 not only diminishes necroptosis of infected cells but also inhibits the release of interleukin 1 $\alpha$ , which stimulates dendritic cells to produce interleukin-12, crucial for an effective anti-tumour response (Schmidt, et al. 2015).

Furthermore, previous studies have demonstrated that HPV 16 induces a compromised response to radiation-induced DNA damage, despite the observed increase in  $\gamma$ -H2AX expression (Park et al., 2014). As a result, it was postulated that this impaired DNA damage repair response may contribute to heightened radiation sensitivity. However, contrasting these findings, HPV 16 E7 has been associated with increased resistance to radiation rather than heightened sensitivity. Conversely, several studies have suggested that HPVs, particularly  $\alpha$ -type HPVs, exploit host cells' DNA damage response to promote viral replication, rather than inhibiting the DNA damage response (Moody, 2017).

It is worth noting that these observations were made using mucosal HPV types, such as HPV 16. However, in the present study, the oncoprotein of a cutaneous HPV type, specifically HPV 8, was utilized. Therefore, further investigations are warranted to explore how both mucosal and cutaneous HPV types might impact double-strand damage induced by PDT and how these interactions influence susceptibility to PDT.

Furthermore, our findings again revealed a notable disparity in Ki67 expression between the cell cultures subjected to PDT and the control cultures. However, a statistically significant distinction between the cultures transfected with HPV 8E6 and those transfected with pLXSN could not be discerned (figure 16).

In general, these results offer preliminary insights into the alteration of radiation-induced DNA damage by cutaneous, although they must be cautiously interpreted due to the limited number of experimental approaches employed (n=2). Moreover, it is important to highlight that immortalized cell cultures were utilized in this study. To better mimic normal skin tissue, it is recommended to employ primary cell culture lines.

## 5.6 Repression of RIPK3 has no significant impact on PDT-induced DNA damage or post-PDT-proliferation in 3D cultures

The expression of  $\gamma$ -H2AX was significantly elevated in the cell cultures exposed to photodynamic therapy (PDT) radiation in comparison to the control cultures, irrespective of whether they were transfected with siRIPK3, non-coding siRNA, or no siRNA (p=0.0005, figure 17). In the PDT-treated cell cultures, the superficial layers directly exposed to the radiation demonstrated the highest levels of  $\gamma$ -H2AX staining, while the basal layers exhibited minimal staining (table 21). These findings substantiate the notion that PDT treatment elicits substantial DNA damage, specifically DNA double-strand breaks, as indicated by  $\gamma$ -H2AX staining. Importantly, this genetic damage appears to be independent of siRNA transfection, as all approaches exhibited similar susceptibility to

PDT treatment (figure 17). Once again, the depth of damage caused by the red light emitted from the PDT lamp seemed to be limited, resulting in restricted damage to the superficial keratinocytes. To augment the therapeutic efficacy of PDT irradiation, strategies such as micro-needling or ultrasound, as previously demonstrated (Zhang, Fang, & Fang, 2011), can be employed to enhance the depth of penetration. Furthermore, sporadic  $\gamma$ -H2AX staining observed in the control cultures can be attributed to routine cell culture handling, which may induce a certain degree of DNA damage.

The expression profile of Ki67 in the siRNA experiment aligns with the findings described earlier. Ki67, as a marker for cell proliferation, exhibited strong positivity in PDT-treated cultures compared to the control cultures ( $p=0.0278$ , figure 18). Again, in the cell cultures treated under the PDT lamp, Ki67 expression was particularly prominent in the intermediate and basal layers of the culture. These intermediate layers directly interact with the superficial cells that were directly exposed to radiation, where no Ki67 expression was detected. These observations held true regardless of siRIPK3 transfection, non-coding siRNA transfection, or no siRNA (table 22). As previously illustrated, the higher overall expression of Ki67, indicative of cell proliferation, in the treatment group compared to the control group supports the notion that PDT may stimulate cell proliferation. Given that PDT is commonly used in the therapy of various tumorous lesions, a growth-promoting effect on cells is highly undesirable and alarming in terms of tumour progression and expansion. Nevertheless, the cell-stimulating effects of PDT have been previously reported. Bhowmick and Girotti demonstrated that PDT-induced NOS2 and NO promote cell survival and growth in a prostate cell culture model, while Blázquez-Castro et al. revealed that photogenerated reactive oxygen species were responsible for cell cycle progression and proliferation (Bhowmick and Girotti 2014; Blázquez-Castro, et al. 2012).

Additionally, the findings from this experimental approach suggested that the post-therapeutic cell proliferative effect might depend on the presence of RIPK3 as Ki67 expression was lower in siRIPK3-transfected cultures compared to the cultures that were transfected with a non-coding siRNA or no siRNA, respectively. However, this correlation was not significant and further studies are necessary to investigate the role of RIPK3 in PDT-induced cell proliferation.

As already outlined before, these results must be cautiously interpreted due to the limited number of experimental approaches employed ( $n=2$ ) and usage of immortalized cell cultures. To better mimic normal skin tissue, it is recommended to employ primary cell culture lines. Furthermore, it is crucial to consider that siRNAs have a limited period of



activity. The production of the 3D cell cultures used in this experimental work took three days, and the cultures were incubated for only one day to minimize the time lag. Nonetheless, it is possible that by the time of cell culture irradiation and subsequent fixation (day 4), the activity of the used siRNAs was already declining, potentially compromising their effectiveness. Further tests are required to confirm the efficacy of the siRNAs and assess the corresponding reduction in protein presence. Alternatives for targeted gene suppression could also be tested for their practicability, such as ribozymes, RNA interference, or antisense oligonucleotides.

## 5.7 RIPK3 expression correlates with VIN grade

Significant variations in the expression of RIPK3 were observed among patients with actinic keratosis, and the levels of RIPK3 appeared to be directly correlated with the therapeutic response following photodynamic therapy (Chapter 4.1). It is noteworthy that not only skin precancerous lesions such as actinic keratosis are associated with HPV infections, but mucosal HPV also plays a critical role in the initiation of tumorigenesis, particularly in the oropharyngeal and anogenital regions (citation). To investigate the role of RIPK3 in lesions associated with mucosal HPV, samples from patients with VIN were examined.

RIPK3 expression profiles exhibited variations among the tested vulvar intraepithelial lesions. Consistent with the findings from RIPK3 staining in actinic keratosis samples, patients with vulvar lesions displayed diverse levels of RIPK3 expression (table 24). There was a negative correlation between the grade of vulvar intraepithelial lesions (VIN I/II/III) and RIPK3 expression (figure 19). The VIN grade reflects the stage of carcinogenic progression, ranging from VIN I (mildest form) to VIN grade III (severe dysplasia with minimal epithelial differentiation). The downregulation of RIPK3 in cancer cells impedes cell death and promotes cell survival, suggesting that RIPK3 is a critical component of the signalling pathway inducing necroptosis. This downregulation of RIPK3 in cancer cells has been previously documented (Koo, et al. 2015), which is further supported by our findings. As tumorigenesis advances, there is a pronounced decrease in RIPK3 expression. Heterogeneous RIPK3 expression profiles have also been observed in cervical squamous cell carcinomas and adenocarcinomas. Moreover, our group has previously demonstrated the significant impact of RIPK3 on the outcome of anti-tumour immunotherapy using Poly-IC. Therefore, it is recommended to assess the pre-therapeutic RIPK3 expression level. Loss of RIPK1/RIPK3 has been associated

with tumour progression and poorer overall outcomes in patients with head and neck squamous cell carcinoma (McCormick, et al. 2016), (Shi, Zhou, et al. 2019).

Considering the negative correlation between RIPK3 expression and VIN lesion grade, as well as the crucial role of high-risk HPV in altering RIPK3 expression (Ma, et al. 2016), it was of interest to investigate the relationship between HPV infection status and VIN lesion grade. However, the analysis of vulvar intraepithelial samples for the presence of HPV DNA did not reveal a significant correlation between HPV status and VIN grade. Among the tested VIN samples, the proportion of HPV-positive and HPV-negative samples was approximately equal.

This result could potentially be attributed to the limited sample size, as it is well-established that the prevalence of HPV in VINs is generally high. For instance, a meta-analysis conducted in 2017 by Faber et al. reported an overall prevalence of HPV in VINs exceeding 76%. Specifically, the pooled prevalence of HPV was found to be 75.8% in VIN I lesions and 82.7% in VIN II/III lesions. Examining the specific HPV types, De Vuyst et al. (2009) revealed that in VIN I lesions, HPV 6, 11, and 16 exhibited the highest prevalence, while in VIN II/III lesions, HPV 16 was found to be the most prevalent type by a significant margin.

Furthermore, when correlating RIPK3 staining intensity with HPV infection status in patients with vulvar intraepithelial neoplasia (figure 20), it was observed that HPV had no discernible impact on the expression of RIPK3. Samples that tested positive for HPV exhibited similar levels of RIPK3 expression compared to HPV-negative samples. It is imperative to note that no additional HPV typification has been executed; nonetheless, this aspect should be explored in subsequent investigations. Although RIPK3 expression was found to be directly associated with the grade of VIN, HPV does not seem to play a crucial role in this correlation. However, the sample size investigated was insufficient, rendering meaningful interpretation unfeasible. Moreover, as mentioned earlier, the state of HPV activity may hold more significance than the mere presence of the virus. These findings contradict those of Ma et al. (Ma, et al. 2016), which suggest that high-risk HPV infection directly alters gene expression, including that of RIPK3, in keratinocytes.

In addition to HPV, there have been findings indicating that other viruses involved in carcinogenesis, such as EBV, interact with the RIPK3 signalling pathway to evade RIPK3-dependent necroptosis. EBV appears to promote hypermethylation of the RIPK3 promoter, resulting in the downregulation of RIPK3 expression. This downregulation is directly associated with poorer disease-free survival and overall survival in HNSCC patients, respectively (Shi, Zhou, et al. 2019).

The utilization of PDT as a therapeutic approach for VINs and vulvar cancer has been increasingly prominent. This minimally invasive treatment modality offers significant reduction in physical and psychological distress for patients compared to radical extinctions. In order to delve deeper into the role of RIPK3 in mucosal lesions such as VINs or vulvar cancer, as well as its association with PDT response, it is imperative to conduct *in vitro* experiments using, for instance, HPV 16 transduced keratinocytes.

## 6 Acknowledgments

First and foremost, I would like to extend my sincere gratitude to Prof. Dr. Sigrun Smola for granting me the opportunity to conduct my experimental work for this dissertation at the Institute of Virology, Saarland University. I am deeply grateful for her support, guidance, and evaluation of this thesis.

I would like to express my heartfelt thanks to Dr. Katrin Knerr-Rupp and Dr. Stefan Lohse for their invaluable support throughout my time in the laboratory. Their patience, motivation, and guidance were instrumental in the completion of this dissertation. I am truly grateful for their unwavering assistance. I would also like to thank Dr. Lohse and Dr. Sternjakob for their corrections and suggestions on the thesis.

I would like to extend my appreciation to all the members of the research group who made my time in the laboratory joyful and enriching. Special thanks to Katharina Bastuck, Julia Treitz, Markus Vogelgesang, Michael Döring, Luca Vella and Ariane Wiegand for their continuous support, problem-solving, and valuable advice. I am immensely grateful for the opportunity to be part of such an amazing team. Working with you all has been a pleasure. I would also like to thank Mark Porter and his daughter Bailey for proofreading the grammar and language of the thesis.

I am indebted to my parents, grandparents, and my beloved brothers, Christian and Oliver, and my love Alexander for their unwavering support. Their encouragement and belief in me during challenging times have been crucial in keeping me focused and motivated to persevere. I would also like to express my gratitude to my friend Sarah for her support throughout this journey. Your presence and encouragement have been invaluable. I could not have completed this work without all of you.

## 7 Declaration

I hereby declare that I have written this thesis “Investigation of the association between receptor-interacting serine/threonine protein kinase 3 expression and the outcome of photodynamic therapy in vivo and in an HPV8-positive organotypic 3D cell culture model” on my own and that I have not used any other media or materials than the ones referred to in this thesis.

Place and date      Juliane Kütten

## 8 Curriculum Vitae

Aus datenschutzrechtlichen Gründen wird der Lebenslauf in der elektronischen Fassung der Dissertation nicht veröffentlicht.

## 9 References

- ACOG, Committee. "Opinion No. 509. Management of vulvar intraepithelial neoplasia." *Obstetrics and gynecology*, November 2011: 1192-1194.
- Alvarez-Diaz, S., P. C. Dillon, N. Lalaoui, M. C. Tanzer, and al. "The Pseudokinase MLKL and the Kinase RIPK3 Have Distinct Roles in Autoimmune Disease Caused by Loss of Death-Receptor-Induced Apoptosis." *Immunity*, 20 September 2016: 513-526.
- AMBOSS GmbH, Berlin und Köln, Germany. "Amboss." *Klassifikation vulvärer intraepithelialer Neoplasien (VIN)*. May 11, 2021. <https://next.amboss.com/de/article/b00HIT?q=vulvakarzinom#Zcf4750dea78d5e983986388bd13d63e0>.
- Antonsson, A., S. Karanfilovska, P. G. Lindqvist, and B. G. Hansson. "General acquisition of human papillomavirus infections of skin occurs in early infancy." *Journal of clinical microbiology*, June 2003.
- Arenberger, P., and M. Arenbergerova. "New and current preventive treatment options in actinic keratosis." *Wiley Online Library*. 14 August 2017. <https://doi.org/10.1111/jdv.14375>.
- Arron, S.T., J. G. Ruby, E. Dybbro, D. Ganem, and al. "Transcriptome sequencing demonstrates that human papillomavirus is not active in cutaneous squamous cell carcinoma." *The Journal of investigative dermatology*, August 2011.
- Aslan, F., C. Demirkesen, P. Cağatay, N. Tüzüner, and al. "Expression of cytokeratin subtypes in intraepidermal malignancies: a guide for differentiation." *J. Cutan Pathology*, August 2006.
- Berman, B., C.J. Cockerell, and al. "Pathobiology of actinic keratosis: ultraviolet-dependent keratinocyte proliferation." *Journal of the American Academy of Dermatology*, January 2013.
- Bernard, H.-U., R.D. Burk, Z. Chen, K. van Doorslaer, and al. "Classification of papillomaviruses (PVs) based on 189 PV types and proposal of taxonomic amendments." *Virology*, May 2010: 70-79.
- Bernhard, M. C., A. Zwick, T. Morh, G. Gasparoni, and at al. "The HPV and p63 Status in Penile Cancer Are Linked with the Infiltration and Therapeutic Availability of Neutrophils. ." *Molecular Cancer Therapeutics*, February 2021.



## References

---

- Bhowmick, R., and A. W. Girotti. "Pro-survival and pro-growth effects of stress-induced nitric oxide in a prostate cancer photodynamic therapy model." *Cancer Letters*, February 2014: 115-122.
- Blázquez-Castro, A., E. Carrasco, M. I. Calvo, P. Jaén, and al. "Protoporphyrin IX-dependent photodynamic production of endogenous ROS stimulates cell proliferation." *European Journal of Cell Biology*, March 2012: 216-223.
- Boukamp, P., R.T. Petrussevska, D. Breitkreutz, J. Hornung, and al. "Normal keratinization in a spontaneously immortalized aneuploid human keratinocyte cell line." *The Journal of Cell Biology*, March 1988: 761-771.
- Bouvard, V., R. Baan, K. Straif, Y. Grosse, and al. "A review of human carcinogenesis- Part B: biological agents." *The Lancet Oncology*, April 2009.
- Buytaert, E., M. Dewaele, and P. al. Agostinis. "Molecular effectors of multiple cell death pathways initiated by photodynamic therapy." *Biochimica et Biophysica Acta*, September 2007: 86-107.
- Bzhalava, D., C. Eklund, and J. Dillner. "International standardization and classification of human papillomavirus types." *Virology*, February 2015: 341-344.
- Campion, M. J., and A. Singer. "Vulvar intraepithelial neoplasia: A clinical review." *Genitourinary medicine*, June 1987: 147-52.
- Campion, M.J. "Clinical manifestations and natural history of genital human papillomavirus infection. ." *Obstetrics and Gynecology Clinics of North America*, June 1987: 363-388.
- Ceilley, R., and J. L. Jorizzo. "Current issues in the management of actinic keratosis." *Journal of the American Academy of Dermatology*, January 2013: 28-38.
- Chegg. *Biology/ Human Anatomy & Physiology*. November 2021. <https://www.chegg.com/flashcards/histology-slides-biol-150-human-anatomy>.
- Chen, H.-M., C.-H. Yu, H.-P. Lin, S.-J. Cheng, and al. "5-Aminolevulinic acid-mediated photodynamic therapy for oral cancers and precancers." *Journal of Dental Science*, December 2012: 307-315.
- Cho, Y., S. Challa, D. Moguin, R. Genga, and al. "Phosphorylation-Driven Assembly of RIP1-RIP3 Complex Regulates Programmed Necrosis and Virus-Induced Inflammation." *Cell*, June 2009: 1112-1123.

## References

---

- Cockerell, C. J. "Histopathology of incipient intraepidermal squamous cell carcinoma ("actinic keratosis")." *Journal of the American Academy of Dermatology*, January 2000.
- Coupienne, I., G. Fettweis, N. Rubio, P. Agostinis, and al. "5-ALA-PDT induces RIP3-dependent necrosis in glioblastoma." *Photochemical and Photobiological Science*, December 2011: 1868-1878.
- Cunliffe, Dr. Tim. "Primary care dermatology society." May 11, 2021. [http://www.pcds.org.uk/ee/images/made/ee/images/uploads/clinical/VIN\\_main\\_300\\_300\\_70\\_http:www.pcds.org.uk/ee/assets/img/watermark.gif\\_0\\_0\\_80\\_r\\_b\\_-5\\_-5\\_.jpg](http://www.pcds.org.uk/ee/images/made/ee/images/uploads/clinical/VIN_main_300_300_70_http:www.pcds.org.uk/ee/assets/img/watermark.gif_0_0_80_r_b_-5_-5_.jpg).
- Curado, M.P., B. Edwards, H.R. Shin, H. Storm, and al. "Cancer Incidence in Five Continents, Vol. IX." *Issues Oncology*, 2008: 1-837.
- De Vuyst, H., G. M. Clifford, M. C. Nascimento, M. M. Madeleine, and al. "Prevalence and type distribution of human papillomavirus in carcinoma and intraepithelial neoplasia of the vulva, vagina and anus: a meta-analysis." *International Journal of cancer*, April 2009: 1626-36.
- De Vuyst, H., G. M. Clifford, M. C. Nascimento, M. M. Madeleine, and S. Franceschi. "Prevalence and type distribution of human papillomavirus in carcinoma and intraepithelial neoplasia of the vulva, vagina and anus: A meta-analysis." *International Journal of Cancer*, January 2009.
- Degterev, Alexei, Zhihong Huang, Michael Boyce, Yaqiao Li, and & all. "Chemical inhibitor of nonapoptotic cell death with therapeutic potential for ischemic brain injury." *nature chemical biology*, 29 May 2005: 112-119.
- DGUV. Mai 25, 2023. [https://www.dguv.de/bk-info/icd-10-kapitel/kapitel\\_12/bk5103/index.jsp](https://www.dguv.de/bk-info/icd-10-kapitel/kapitel_12/bk5103/index.jsp).
- Di Venosa, Gabriela, , Laura Hermida, Alcira Batlle, Haydée Fukuda, and & al. "Characterisation of liposomes containing aminolevulinic acid and derived esters." *Journal of Photochemistry and Photobiology B: Biology*, July 24, 2008.
- Dirschka, T., P. Radny, R. Dominicus, H. Mensing, and & al. "Photodynamic therapy with BF-200 ALA for the treatment of actinic keratosis: results of a multicentre, randomized, observer-blind phase III study in comparison with a registered methyl-5-aminolaevulinate cream and placebo." *British Journal of Dermatology*, September 12, 2011: 137-146.

## References

---

- Doorbar, J., W. Quint, L. Bank, I.G. Bravo, and al. "The biology and life-cycle of human papillomaviruses." *Vaccine*, November 2012.
- Dougherty, T.J., C J Gomer, B W Henderson, G Jori, and & all. "Photodynamic therapy." *Journal of the National Cancer Institute*, June 17, 1998: 889-905.
- Duprez, Linde, Nozomi Takahshi, Filip Van Hauwermeiren, Benjamin Vandendriessche, and & all. "RIP kinase-dependent necrosis drives lethal systemic inflammatory response syndrome." *Immunity*, December 23, 2011: 908-918.
- Elbel, M., S. Carl, S. Spadema, and T. Iftner. "A comparative analysis of the interactions of the E6 proteins from cutaneous and genital papillomaviruses with p53 and E6AP in correlation to their transforming potential." *Virology*, December 1997.
- El-Sharabasy, M. M., A. M. el-Waseef, M. M. Hafez, and S. A. Salim. "Porphyrin metabolism in some malignant diseases." *British Journal of Cancer*, March 1992: 409-412.
- Faber, M. T., F. L. Sand, V. Albieri, B. Norrild, and al. "Prevalence and type distribution of human papillomavirus in squamous cell carcinoma and intraepithelial neoplasia of the vulva." *International Journal of Cancer*, June 2017.
- Gheit, T. "Mucosal and Cutaneous Human Papillomavirus Infections and Cancer Biology." *Frontiers in Oncology*, May 2019.
- Gholam, P., V. Kroehl, and AH Enk. "Dermatology life quality index and side effects after topical photodynamic therapy of actinic keratosis." *Dermatology*, 18 June 2013.
- Giampieri, S., and A. Storey. "Repair of UV-induced thymine dimers is compromised in cells expressing the E6 protein from human papillomaviruses types 5 and 18." *British Journal of Cancer*, June 2004.
- Green, A., G. Beardmore, V. Hart, D. Leslie, and al. "Skin cancer in a Queensland population." *Journal of the American Academy of Dermatology*, December 1988: 1045-1052.
- Gupta, J., S. Pilotti, F. Rilke, and R. Shah. "Association of human papillomavirus type 16 with neoplastic lesions of the vulva and other genital sites by in situ hybridization." *The American journal of pathology*, May 1987: 206-15.
- Han, W., L. Li, S. Qui, Q. Lu, and al. "Shikonin circumvents cancer drug resistance by induction of a necroptotic death." *Molecular Cancer Therapy*, Mai 2007: 1641-9.

## References

---

- Hasche, D., S.E. Vinzón, and F. Rösl. "Cutaneous Papillomaviruses and Non-melanoma Skin Cancer: Causal Agents or Innocent Bystanders?" *Frontiers in microbiology*, May 2018.
- Hoang, L. N., K. J. Park, R. A. Soslow, and R. Murali. "Squamous precursor lesions of the vulva: Current classification and diagnostic challenges." *Pathology*, June 2016: 291-302.
- "Infection and Immunity." May 11, 2021. <https://iai.asm.org/content/iai/78/12/4977/F2.large.jpg>, Fig. 2, *Infection and Immunity* Dec 1969.
- Jackson, S., C. Harwood, M. Thomas, L. Banks, and al. "Role of Bak in UV-induced apoptosis in skin cancer and abrogation by HPV E6 proteins." *Genes Dev.*, December 2000.
- James Heilman, MD. "Wikipedia." May 11, 2021. <https://commons.wikimedia.org/wiki/File:SolarAcanthosis.jpg>, <https://creativecommons.org/licenses/by-sa/4.0/legalcode>.
- Joura, E. A., A. Lösch, M.-G. Haider-Angeler, G. Breitenecker, and al. "Trends in vulvar neoplasia. Increasing incidence of vulvar intraepithelial neoplasia and squamous cell carcinoma of the vulva in young women." *The Journal of reproductive medicine*, August 2000: 613-5.
- Judson, P. L., E. B. Habermann, N. N. Baxter, S. B. Durham, and al. "Trends in the incidence of invasive and in situ vulvar carcinoma." *Obstetrics and gynecology*, May 2006: 1018-22.
- Knerr-Rupp, K. "Untersuchung der Rolle des Serin-Protease-Inhibitors SerpinB3 in der zervikalen Karzinogenese unter Zuhilfenahme des 3D-Zellkulturmodells." 2017.
- Knerr-Rupp, Katrin. "Untersuchung der Rolle des Serin-Protease-Inhibitors Serpin B3 in der zervikalen Karzinogene unter Zuhilfenahme des 3D-Zellkulturmodells." Homburg, n.d.
- Koo, G.-B., M. J. Morgan, D.-G. Lee, W.-J. Kim, and al. "Methylation-dependent loss of RIP3 expression in cancer represses programmed necrosis in response to chemotherapeutics." *Cell Research*, June 2015: 707-725.
- Kuo, L.J., and L. Yang. "Gamma-H2AX - a novel biomarker for DNA double-strand breaks." *In Vivo*, May-June 2008: 305-9.

## References

---

- Lehman, T. A., R. Modali, P. Boukamp, J. Stanek, W. P. Bennett, and al. "p53 mutations in human immortalized epithelial cell lines." *Carcinogenesis*, May 1993.
- Lehmann, T. A., R. Modali, P. Boukamp, J. Stanek, and al. "p53 Mutations in human immortalized epithelial cell lines." *Carcinogenesis*, May 1993: 833-839.
- Lukens, J. R., P. Vogel, G. R. Johnson, M. A. Kelliher, and al. "RIP1-driven autoinflammation targets IL-1 $\alpha$  independently of inflammasomes and RIP3." *Nature*, May 2013: 224-227.
- Ma, W., B. Tummers, E. M. G. van Esch, R. Goedemans, and al. "Human Papillomavirus Downregulates the Expression of IFITM1 and RIPK3 to Escape from IFN $\gamma$ - and TNF $\alpha$ -Mediated Antiproliferative Effects and Necroptosis." *Frontiers in Immunology*, November 2016.
- Marcuzzi, G. P., M. Hufbauer, H. U. Kasper, S. J. Weißenborn, and al. "Spontaneous tumour development in human papillomavirus type 8 E6 transgenic mice and rapid induction by UV-light exposure and wounding." *The Journal of general virology*, December 2009.
- Marthaler, A. M., M. Podgorska, P. Feld, A. Fingerle, K. Knerr-Rupp, and al. "Identification of C/EBP $\alpha$  as a novel target of the HPV8 E6 protein regulating miR-203 in human keratinocytes." *PLoS Pathogens*, June 2017.
- Marthaler, A. M., M. Podgorska, P. Feld, A. Fingerle, K. Knerr-Rupp, and al. "Identification of C/EBP $\alpha$  as a novel target of the HPV8 E6 protein regulating miR-203 in human keratinocytes." *PLoS Pathogens*, 22 June 2017.
- Marthaler, A. M., Podgorska M., P. Feld, A. Fingerle, and al. "Identification of C/EBP $\alpha$  as a novel target of the HPV8 E6 protein regulating miR-203 in human keratinocytes." *PLoS Pathogens*, June 22, 2017.
- McCormick, K. D., A. Ghosh, S. Trivedi, L. Wang, and al. "Innate immune signalling through differential RIPK1 expression promotes tumor progression in head and neck squamous cell carcinoma." *Carcinogenesis*, May 2016: 522-9.
- Meng, L., W. Jin, Y. Wang, and H. Huang. "RIP3-dependent necrosis induced inflammation exacerbates atherosclerosis." *Biochemical and Biophysical Research Communications*, April 2016: 497-502.
- Moody, C. A. "Mechanisms by which HPV Induces a Replication Competent Environment in Differentiating Keratinocytes." *Viruses*, September 2017.

## References

---

- Moquin, D. M., T. McQuade, and F.-K.-M. Chan. "CYLD Deubiquitinates RIP1 in the TNF $\alpha$ -Induced Necrosome to Facilitate Kinase Activation and Programmed Necrosis." *Plos one*, October 2013.
- Moriwaki, K., J. Bertin, P. J. Gough, and F. Ka-Ming Chan. "A RIPK3–Caspase 8 Complex Mediates Atypical Pro–IL-1 $\beta$  Processing." *The Journal of Immunology*, February 2015.
- Murphy, J. M., P. E. Czabotar, J.M. Hildebrand, Lucet, I. S., and al. "The pseudokinase MLKL mediates necroptosis via a molecular switch mechanism." *Immunity*, September 2013: 443-453.
- Muschik, D., I. Braspenning-Wesch, E. Stockfleth, F. Rösl, and al. "Cutaneous HPV23 E6 prevents p53 phosphorylation through interaction with HIPK2." *PLoS One*, 2011.
- Neale, R. E., S. Weissenborn, D. Abeni, J. N. B. Bavinck, and al. "Human papillomavirus load in eyebrow hair follicles and risk of cutaneous squamous cell carcinoma." *Cancer epidemiology, biomarkers & prevention*, April 2013.
- Orth, G. "Genetics of epidermodysplasia verruciformis: Insights into host defense against papillomaviruses." *Seminars in Immunology*, December 2006.
- Park, J. W., K. P. Nickel, A. D. Torres, D. Lee, and al.: "Human Papillomavirus Type 16 E7 Oncoprotein Causes a Delay in Repair of DNA Damage." *Radiotherapy and oncology*, December 2014.
- Passos, S.K., de Souza, P.E., Soares P.K., D.R. Eid, and al. "Quantitative approach to skin field cancerization using a nanoencapsulated photodynamic therapy agent: a pilot study." *Clinical, cosmetic and investigational dermatology*, February 2013: 51-59.
- Pfister, H. "Chapter 8: Human papillomavirus and skin cancer." *Journal of the National Cancer Institute. Monographs*, 2003.
- Prodromidou, A., E. Chatziioannou, G. Daskalakis, K. Stergios, and al. "Photodynamic Therapy for Vulvar Lichen Sclerosus-A Systematic Review." *Journal of lower genital tract diseases*, January 2018.
- Reid, R., and M. J. Campion. "The Biology and Significance of Human Papillomavirus Infections in the Genital Tract." *The Yale Journal of Biology and Medicine*, July 1988: 307-325.

## References

---

- Reid, R., M. Greenberg, A. B. Jenson, M. Husain, and al. "Sexually transmitted papillomaviral infection. I. The anatomic distribution and pathologic grade of neoplastic lesions associated with different viral types." *American Journal of Obstetrics and Gynecology*, January 1987: 212-22.
- Reinehr, C. P. H., R.M. Bakos, and al. "Actinic keratoses: review of clinical, dermoscopic, and therapeutic aspects." *Anais brasileiros de dermatologia*, November 2019: 637-657.
- Robert Koch Institut. Mai 11, 2021. [https://www.rki.de/DE/Content/Infekt/EpidBull/Merkblaetter/Ratgeber\\_HPV.html](https://www.rki.de/DE/Content/Infekt/EpidBull/Merkblaetter/Ratgeber_HPV.html).
- Roewert-Huber, J., E. Stockfleth, H. Kerl, and al. "Pathology and pathobiology of actinic (solar) keratosis - an update." *British Journal of Dermatology*, December 2007.
- Saraiya, M., E. R. Unger, T. D. Thompson, C. F. Lynch, and et al. "US Assessment of HPV Types in Cancers: Implications for Current and 9-Valent HPV Vaccines." *Journal of the national cancer institute*, 2015.
- Schaper, I. D., G., P. Marcuzzi, S. J. Weissenborn, H. U. Kasper, and al. "Development of skin tumors in mice transgenic for early genes of human papillomavirus type 8." *Cancer research*, February 2005.
- Schmidt, S. V., S. Seibert, B. Walch-Rückheim, B. Vicinus, and al. "RIPK3 expression in cervical cancer cells is required for PolyIC-induced necroptosis, IL-1 $\alpha$  release, and efficient paracrine dendritic cell activation." *Oncotarget*, April 2015.
- Schmitt, A., J. B. Harry, B. Rapp, F.O. Wettstein, and T. Iftner. "Comparison of the properties of the E6 and E7 genes of low- and high-risk cutaneous papillomaviruses reveals strongly transforming and high Rb-binding activity for the E7 protein of the low-risk human papillomavirus type 1." *Journal of Virology*, November 1994.
- Schoenfeld, N., O. Epstein, M. Lahav, R. Mamet, and al. "The heme biosynthetic pathway in lymphocytes of patients with malignant lymphoproliferative disorders." *Cancer Letters*, December 1988: 43-48.
- Scholzen, T., and J. Gerdes. "The Ki-67 protein: From the known and the unknown." *JournL Of cellular Physiology*, 31 January 2000.
- Seifert, L., G. Werba, S. Tiwari, N. N. G. Ly, and al. "The necrosome promotes pancreatic oncogenesis via CXCL1 and Mincle-induced immune suppression." *Nature*, April 2016: 245-249.

- Shanmugasundaram, S., and J. You. "Targeting Persistent Human Papillomavirus Infection." *Viruses*, August 2017.
- Shi, F., M. Zhou, L. Shang, Du, Q., and al. "EBV(LMP1)-induced metabolic reprogramming inhibits necroptosis through the hypermethylation of the RIP3 promoter." *Theranostics*, April 2019: 2424-2438.
- Shi, F., M. Zhou, L. Shang, Q. Du, and al. "EBV(LMP1)-induced metabolic reprogramming inhibits necroptosis through the hypermethylation of the RIP3 promoter." *Theranostics*, April 2019: 2424-2438.
- Smola-Hess, S., J. Pahne, C. Mauch, P. Zigrino, and al. "Expression of membrane type 1 matrix metalloproteinase in papillomavirus-positive cells: role of the human papillomavirus (HPV) 16 and HPV8 E7 gene products." *The Journal of general virology*, May 2005.
- Sperling, T., M. Oldak, B. Walch-Rückheim, C. Wickenhauser, J. Doorbar, and al. "Human papillomavirus type 8 interferes with a novel C/EBP $\beta$ -mediated mechanism of keratinocyte CCL20 chemokine expression and Langerhans cell migration." *PLoS Pathogens*, 2018.
- Steger, G., and H. Pfister. "In vitro expressed HPV 8 E6 protein does not bind p53." *Archives of virology*, 1992.
- Stern, R.S. "Genital Tumors among Men with Psoriasis Exposed to Psoralens and Ultraviolet A Radiation (PUVA) and Ultraviolet B Radiation." *The New England Journal of Medicine*, April 19, 1990: 1093-1097.
- Sternlicht, M. D., and W. Werb. "How matrix metalloproteinases regulate cell behavior." *Annual review of cell and developmental biology*, 2001.
- Stewart, B.W., and P. Kleiheus. *World cancer Report*. Lyon: IARC Press, 2003.
- Stummer, Walter, Uwe Pichlmeier, Thomas Meinel, Otmar Dieter Wiestler, and & all. "Fluorescence-guided surgery with 5-aminolevulinic acid for resection of malignant glioma: a randomised controlled multicentre phase III trial." *The Lancet*, April 13, 2006.
- Summer, W., U. Pichlmeier, T. Meinel, O. D. Wiestler, and al. "Fluorescence-guided surgery with 5-aminolevulinic acid for resection of malignant glioma: a randomised controlled multicentre phase III trial." *The Lancet Oncology*, May 2006: 392-401.



- Tan, M. J. A., E. A. White, Sowa, M. E., J. W. Harper, and al. "Cutaneous  $\beta$ -human papillomavirus E6 proteins bind Mastermind-like coactivators and repress Notch signaling." *Proceedings of the National Academy of Science of the United States of America*, June 2012.
- Taute, S., H. J. Pfister, and G. Steger. "Induction of Tyrosine Phosphorylation of UV-Activated EGFR by the Beta-Human Papillomavirus Type 8 E6 Leads to Papillomatosis." *Frontiers in microbiology*, November 2017.
- Tosti, G., A. D. Iacobone, Petri, E. P., S. Vaccarie, and al. "The Role of Photodynamic Therapy in the Treatment of Vulvar Intraepithelial Neoplasia." *Biomedicines*, February 2018.
- Ulrich, C., J. S. Jürgensen, A. Degen, M. Hackethal, and al. "Prevention of non-melanoma skin cancer in organ transplant patients by regular use of a sunscreen: a 24 months, prospective, case-control study." *The British journal of dermatology*, November 2009: 78-84.
- Underbrink, M. P., H. L. Howie, K. M. Bedard, J. I. Koop, and al. "E6 proteins from multiple human betapapillomavirus types degrade Bak and protect keratinocytes from apoptosis after UVB irradiation." *Journal of Virology*, November 2008.
- Van Hillegersberg, R., J.W. Van der Berg, W.J. Kort, Terpstra O.T., and al. "Selective accumulation of endogenously produced porphyrins in a liver metastasis model in rats." *Gastroenterology*, August 1992: 647-51.
- Vanlangenakker, N., T. Vanden Berghe, and P. Vandenabeele. "Many stimuli pull the necrotic trigger, an overview." *Cell death and differentiation*, January 2012: 75-86.
- Vansevičiūtė, R., J. Venius, S. Letautienė, and al. "5-Aminolevulinic acid-based fluorescence diagnostics of cervical preinvasive changes." *Medicina*, 2014: 137-143.
- Walboomers, J. M., M. V. Jacobs, M. M. Manos, F. X. Bosch, and al. "Human papillomavirus is a necessary cause of invasive cervical cancer worldwide,." *The Journal of pathology*, September 1999.
- Walch-Rückheim, B., R. Mavrova, M. Henning, B. Vicinus, and et al. "Stromal Fibroblasts Induce CCL20 through IL6/C/EBP $\beta$  to Support the Recruitment of Th17 Cells during Cervical Cancer Progression." *Cancer Research*, December 15, 2015.

## References

---

- Wallace, N. A., K. Robinson, H. L. Howie, D. A. Galloway, and al. "HPV 5 and 8 E6 abrogate ATR activity resulting in increased persistence of UVB induced DNA damage." *PLoS Pathogens*, July 2012.
- Wan, M.T., and J.Y. Lin. "Current evidence and applications of photodynamic therapy in dermatology." *Clinical, Cosmetic and Investigational Dermatology*, May 2014: 145-163.
- Wang, H., L. Sun, L. Su, J. Rizo, and al. "Mixed lineage kinase domain-like protein MLKL causes necrotic membrane disruption upon phosphorylation by RIP3." *Molecular Cell*, April 2014: 133-146.
- Wegner, K.W., D. Saleh, and A. Degterev. "Complex Pathologic Roles of RIPK1 and RIPK3: Moving Beyond Necroptosis." *Trends in pharmacological science*, March 2017: 202-225.
- Weissenborn, S. J., I. Nidl, K. Purdie, C. Harwood, and al. "Human papillomavirus-DNA loads in actinic keratoses exceed those in non-melanoma skin cancers." *The journal of investigative dermatology*, July 2005.
- White, E.A., R.E. Kramer, M. J. A. Tan, S. D. Hayes, and al. "Comprehensive analysis of host cellular interactions with human papillomavirus E6 proteins identifies new E6 binding partners and reflects viral diversity." *Journal of virology*, December 2012.
- WHO. "Human papillomavirus (HPV) and cervical cancer." November 2021.
- Wozniak, L., and K., W. & Zielinski. "Wikipedia." May 11, 2021. <https://commons.wikimedia.org/wiki/File:SkinTumors-P5280056.JPG>, „SkinTumors-P5280056“, <https://creativecommons.org/licenses/by-sa/3.0/legalcode>.
- Wu, X.-N., Z.-H. Yang, X.-K. Wang, Y. Zhang, and al. "Distinct roles of RIP1-RIP3 hetero- and RIP3-RIP3 homo-interaction in mediating necroptosis." *Cell death and differentiation*, June 2014: 1709-1720.
- Yang, Y., J. Ma, Y. Chen, and M. Wu. "Nucleocytoplasmic shuttling of receptor-interacting protein 3 (RIP3): identification of novel nuclear export and import signals in RIP3." *Journal of Biological Chemistry*, September 2004: 38820-38829.
- Yatim, N., H. Jusforgues-Saklani, S. Orozco, O. Schulz, and al. "RIPK1 and NF-kappaB signaling in dying cells determines cross-priming of CD8(+) T cells." *Science*, October 2015: 328-334.

## References

---

- Yim, E.-K., and J.-S. Park. "The Role of HPV E6 and E7 Oncoproteins in HPV-associated Cervical Carcinogenesis." *Cancer research and treatment*, December 2005: 319-24.
- Zhang, Duanwu, Juan Lin, and Jiahuai Han. "Receptor-interacting protein (RIP) kinase family,." *Cellular & Molecular Immunology*, 12 April 2010: 243-249.
- Zhang, J., Y. Zhang, and Z. Zhang. "Prevalence of human papillomavirus and its prognostic value in vulvar cancer: A systematic review and meta-analysis." *PLoS ONE*, September 2018.
- Zhang, L.-W., Y.-P. Fang, and J.-Y. Fang. "Enhancement techniques for improving 5-aminolevulinic acid delivery through the skin." *Dermatologica Sinica*, March 2011: 1-7.
- zur Hausen, H. "Human papillomaviruses and their possible role in squamous cell carcinomas." *Current topics in microbiology and immunology*, 1977: 1-30.